NIWA
Taihoro Nukurangi

Land Drainage Recovery Programme: Tsunami Study

Prepared for
Christchurch City Council

June 2019

Prepared by:
Cyprien Bosserelle
Jade Arnold
Emily Lane

For any information regarding this report please contact:

Emily Lane
Hydrodynamics Scientist
Hydrodynamics
emily.lane@niwa.co.nz

National Institute of Water & Atmospheric Research Ltd
PO Box 8602
Riccarton
Christchurch 8011

Phone +64 3 348 8987

NIWA CLIENT REPORT No: 2018039CH
Report date: June 2019
NIWA Project: CCC18504

Quality Assurance Statement		
	Reviewed by:	Graeme Smart
	Formatting checked by:	Fenella Falconer
	Approved for release by:	Charles Pearson

Contents

Tables

Figures

Executive summary

NIWA was commissioned by Christchurch City Council (CCC) to carry out a numerical modelling study of tsunami inundation in Christchurch caused by two tsunamis originating from distant sources. This study aims to aid the understanding of the tsunami hazard in the greater Christchurch area so that Christchurch City Council has a better understanding of the influence of tsunamis on flooding risk. The results of this project will feed into the multi-hazard analysis being undertaken by the LDRP97 project team in preparing the floodplain management plan.

The selected tsunami sources were a 1:500-year return period event cause by a magnitude 9.28 earthquake and a 1:2500-year return period event caused by a magnitude 9.49 earthquake both at the Peru subduction zone. The simulations were completed for different sea-level rise scenarios (present day, 0.19 m, 0.41 m and 1.06 m) taking into account predicted shoreline changes predicted for 2065 and 2120. Note that the magnitude 9.49 scenario at current sea-level was produced in a previous study and not replicated here.

Both tsunami scenarios result in major inundation in Christchurch which, as expected, worsens with the higher sea-level scenarios. The inundation extent was similar for both tsunami scenarios but the inundation depth and flow velocities along the coastal strip were much larger for the worst-case tsunami (1:2,500-year scenario). The total inundation extent for the higher sea level rise scenario (1.06 m above present sea level) was 70 km^2 for the 1:500-year return period tsunami event, 79 per cent more than for the same tsunami occurring at present day sea level.

Such large tsunami events are expected to cause severe erosion of the coastal strip and at the mouth of the Waimakariri River and the Avon-Heathcote Estuary. Severe erosion can also be expected at the Avon Bridge Street bridge and the Heathcote Ferry Road bridge. This erosion could cause increased inundation by removing dunes and opening river and estuary mouths which is not taken into account in this modelling.

The results for areas specifically modelled in this study are considered more robust and should supersede previous interpretations.

1 Introduction

Christchurch is subject to a range of natural hazards and one of these is tsunami. Since the Canterbury Earthquake Sequence (CES), the direct effects of the earthquakes have caused changes that may exacerbate future natural hazards. The Land Drainage Recovery Programme seeks to understand the post-earthquake flood risk in the greater Christchurch area, including multi-hazards in the form of co-location, coincident or cascading hazards. Christchurch City Council (CCC) engaged a project team to investigate these multi-hazard risks and develop a floodplain management plan encompassing these. The project is split into three parts. Firstly, a gap analysis; secondly, studies aiming to fill those gaps; and finally, the development of the floodplain management plan. Tsunamis were identified as one of the areas where future research is need. Consequently, NIWA was commissioned by Christchurch City Council to model tsunami inundation in Christchurch City from two earthquake scenarios and consider various sea level rise scenarios.

This study aims to aid the understanding of the tsunami hazard in the greater Christchurch area so that Christchurch City Council has a better understanding of the influence of tsunamis on flooding risk. The results of this project will feed into the multi-hazard analysis being undertaken by the LDRP97 project team in preparing the floodplain management plan.

The first tsunami source scenario used was the same as that used by Lane et al. (2014, 2017) and involves a tsunami originating from a moment magnitude (M_w) 9.485 earthquake at the South Peru / North Chile Subduction Zone. This scenario was based on the findings of Power (2013) and represents a 1:2,500-year return period event; this is considered an extreme scenario. A less-extreme scenario was also considered based on previous work from Power (2013). The 1:500-year return period earthquake scenario was selected as the most likely magnitude for the most likely source (50th percentile in Power 2013). The most realistic rupture mechanism was selected from two scenarios of fault rupture mechanism presented in a progress report (Lane and Bosserrelle 2017).

Kohout et al. (2015) have previously simulated various scenario of earthquake from the Hikurangi faults. These Hikurangi scenario are not used here because they produce smaller wave height at coast than the far-field scenarios.

A local tsunami source was initially considered based on multiple ruptures with recurrence interval of 12,500 – 35,000 years. However, tsunami propagation simulation showed that the tsunami wave height at the coast was significantly smaller than for far-field scenarios (and with return period that far exceeds the return period of the far field events). Results for local source scenarios were presented in a progress report (Lane and Bosserrelle 2017). For convenience these results are included as an appendix to this report. Subsequently, CCC decided that local source scenarios were not a priority, and to focus on the distant source tsunami scenarios.

This report presents the results for modelled tsunami inundation caused by these tsunami scenarios at different sea-level. Four sea-level scenarios were considered: current conditions, sea level rise for 2040 (0.19 m), 2065 (0.41 m) and 2120 (1.06 m) all based on the analysis of Tonkin & Taylor Ltd (2017). The modelling assumes the tsunami coincides with Mean High Water Spring tide (MHWS), which was taken to be 1.2 m above Lyttelton Vertical Datum 1937 (LVD37) as calculated in Bell (2011) (this corresponds to 10.24 m in Christchurch Drainage Datum); consistent with the MHWS value used in previous modelling Lane et al. (2014, 2017). MHWS was set as the baseline water level for the modelling and represents the case where the largest wave arrives in conjunction with high tide for an average spring tide. Flow from the Avon, Heathcote and Waimakariri Rivers were included in the simulation to account for the tsunami wave propagation in the rivers.

Outputs of maximum inundation depth, maximum flow velocity and maximum shear-stress maps are presented as well as time series of water level, speed and shear-stress. Areas of interest include Avon-Heathcote Estuary, the Waimakariri River Mouth, Brookland Lagoon and bridges in the lower reaches of the rivers.

1.1 Use of this report

The distant source scenarios modelled have long estimated return periods (2,500 years and 500 years) and represent extreme scenarios. Information provided in this report may also be useful for strategic development and infrastructure planning as it may, when used with other hazard and risk information, highlight areas of higher vulnerability that are potentially unsuitable for future development. Maps of the inundation extents should not be used at scales finer than 1:25,000. The overview maps are intended as a guide only and should not be used for interpreting inundation.

The main purpose of this report is to provide the Council with a clearer understanding of the potential tsunami inundation extent and the effects of sea level rise on the Christchurch City region (from the Waimakariri River Mouth to Sumner Head). The information provided is intended to aid understanding of the tsunami for current conditions and sea level rise scenarios up to 2120 (1.06 m) including how tsunamis could impact the local estuaries and lagoons in terms of geomorphic changes, scouring and deposition and resulting long-term effects. Results are intended to inform the Land drainage recovery program (LDRP97).

1.2 Caveat

This report is based on state-of-the-art knowledge and modelling capabilities of tsunamis and tsunami inundation at the time of writing. While every effort was made to provide accurate information, there are many uncertainties involved including knowledge of potential tsunami sources, source characteristics, bathymetry and topography (see Section 2.5 of this report for details). In addition, while the hydrodynamic models capture much of the physics involved in tsunami propagation and inundation, they also include some simplifying assumptions, as with all models.

This report also provides a qualitative assessment of the potential erosion caused by the tsunami. This assessment is based on the model prediction of maximum shear stress which is only a proxy for sediment transport potential. As a result, no estimates can be made of the amount of erosion or the depth of scouring of stop banks.

The information provided in this report is of a technical nature and should be considered with the above limitations in mind.

2 Tsunami Inundation Modelling

2.1 Source model and initial conditions

Power (2013) provides a wave height at the Christchurch coast of 12.63 m for the 2,500-year return period tsunami at the 84th percentile confidence level[1]. The de-aggregation of this wave height identified South Peru / North Chile as a major source of the hazard and that an earthquake of M_w 9.485 was required to produce that wave height at the Christchurch coast (Power 2014). For consistency with previous work by Lane et al. (2014, 2017), this source and corresponding modelling approach is used to model the tsunami in this study. The overarching scenario was guided by the GNS Science tsunami database and uses source segments from Tang et al. (2010). In Lane et al. (2014) four earthquake rupture scenarios were modelled. All had the same moment magnitude (M_w) but differed in configurations of rupturing segments and corresponding displacements. For this report we model the largest of those four scenarios as was done in Lane et al. (2017).

This study also analyses the inundation from a 1:500-year return period tsunami at the 84th percentile confidence level also from the South Peru / North Chile region. Two tsunami waves were initially simulated both originating from a magnitude of M_w 9.28 earthquake occurring in the South Peru area. The fault segment involved in the earthquake were selected to produce the largest tsunami waves for Christchurch using a sensitivity analysis of the SIFT (Short-term Inundation Forecast for Tsunamis) database Gica et al. (2008). Both tsunamis produced similar waves in Pegasus Bay offshore of Christchurch. Scenario B (Lane and Bosserelle 2017) was selected for inundation simulation as it was produced by the most realistic fault rupture mechanism.

The two tsunami scenarios show very dissimilar waves with the 1:500-year return period scenario showing only large long period waves whereas the 1:2500-year return period scenario is showing large short period wave riding on top of large long period waves. The scenarios are expected to produce different waves at the coast because the initial tsunami sources were produced using different faults (i.e., the larger earthquake is produced on a longer fault segment) and because the wave interacted differently with the continental shelf when approaching the coast. In addition, the method for propagating the tsunami waves across the Pacific was completed using different models (Gerris for the 1:2500-year return period scenario and ComMIT for the 1:500-year return period scenario) and using different resolutions. However, the models are fundamentally similar (i.e., both are solving the shallow water equations) and are not expected to produce significant differences.

2.2 Progress report - Decisions

In the progress report, initial tsunami propagation simulations (typically completed at a coarser resolution than inundation simulation) were used to decide which scenarios and parameters to focus on in this study.

Far-field tsunami were modelled from sources across the Pacific Ocean to the edge of the inundation grid. De-aggregation results from the New Zealand Probabilistic Tsunami Hazard Assessment (Power 2013, Power 2014) were used to identify a representative source fault rupture, and (Okada 1985)

[1] In probabilistic tsunami hazard assessment, the 84th percentile confidence level refers to the confidence level (or uncertainty) regarding the water level due to the contributions of different fault sources and uncertainty in the parameters of those sources (see Power 2013 for further details).

was used to create the initial surface deformation. Higher resolution modelling of two of these scenarios was approved for further investigation.

Digital elevation models were developed for the new representative beach topography (in 6) under the two most extreme sea level rise scenarios for 2065 (0.41 m) and 2120 (1.06 m) using the results from the Christchurch Coastal Hazards Assessment ((Tonkin & Taylor Ltd 2017).

Four local tsunamis caused by fault rupture in Pegasus Bay and North Canterbury (two single faults and two multi-faults where one fault rupture triggers rupture in a neighbouring fault) were modelled (although the land deformation and potential effect of liquefaction were not taken into account). Faults were taken from an update of the National Seismic Hazard Model and used to create the initial surface deformation. CCC subsequently decided these scenarios were not a priority for this study. These results are reproduced in Appendix B for convenience.

2.3 Inundation modelling and grid

The tsunami modelling is undertaken using the Basilisk model, a partial differential equation solver based on adaptive grids that has been used for tsunami modelling in a range of situations (Popinet 2011, Popinet 2012, Lee et al. 2015).

The Basilisk model (Popinet 2015), a successor to Gerris (Popinet 2011, Popinet 2012), was used to model the inundation together with the river flow. Both Gerris and Basilisk have been used for tsunamis (Popinet 2011, Popinet 2012) and flood inundation (Bind and Smart 2010, Smart 2017) which is why Basilisk, the more recent of the two, was chosen for this modelling. A feature of Basilisk and Gerris is that these models use an adaptive grid where the spatial resolution varies throughout the duration of the simulation, with the grid resolution automatically increasing in areas of interest as defined by Popinet (2012), while lower resolution is maintained elsewhere, improving computational efficiency.

The model grid was confined to Christchurch and Kaiapoi, extending from Taylors Mistake in the south to The Pines in the north. The model grid was rotated by 13.8˚ counter-clockwise so that the edge of the grid was approximately parallel with the shoreline (Figure 2-1). The model was forced with the incoming wave height at its outer edge taken from the previous modelling. The grid is square in shape with the length of a side of the grid being 27 km. The resolution of the model was adapted to optimise the number of model cells while maintaining high accuracy for the water level, flow speed and river channels with the finest resolution of the grid at 13.2 m. The adaptive resolution of the model is illustrated with a snapshot of the final resolution used for the 1:500-year return period tsunami simulation for present day mean sea level in Figure 2-2.

The inundation model for the Christchurch region (between the Waimakariri River and Sumner Head) was developed using topography from Environment Canterbury LiDAR and bathymetry of the rivers, estuary and ocean developed by NIWA. Although results are only required for the south of the Waimakariri River, the modelling extended further north ensuring that the results were not affected by the boundary. Flow was included in the Avon, Heathcote and Waimakariri rivers. Stop-banks along the Waimakariri and Avon rivers and the Sumner sea-wall were resolved.

The same LiDAR data obtained from Environment Canterbury as used for the previous modelling (Lane et al. 2017) was used for the land area. For the Avon and Heathcote rivers bathymetry developed post-earthquake for Environment Canterbury (Measures and Bind 2013) was used. Environment Canterbury provided bathymetry for the lower reaches of the Waimakariri River (the lowest 3 km) but this was not comprehensive enough for the purposes of this modelling. We were also able to obtain cross-sections that were used to reconstruct river bathymetry further upstream. Details of this reconstruction technique are provided in Lane et al. (2017). For the more extreme sea level rise scenarios (2065 SLR 0.41, 20100 SLR 1.06m) we used the revised dune topographies documented in Appendix A.

Stop-bank crest levels were provided for the Waimakariri and Avon stop-banks and the Sumner seawall for previous projects (Lane and Arnold 2013, Lane et al. 2014, Kohout et al. 2015, Lane et al. 2017). In order to ensure that these features were resolved within Basilisk's adaptive refinement, the cells containing these features were refined to the highest level while other regions were allowed to adaptively refine according to details of the flow and whether they were inundated or not.

Following Lane et al. (2017) the rivers were initialised with mean river flows of 1.0, 1.7, and 60 m^3/s for the Heathcote, Avon (Cameron 1992, Orchard and Measures 2016) and Waimakariri rivers respectively. The black diamonds in Figure 2-1 indicate where this flow entered the rivers. The model was allowed to run for 1 day of model time to allow the rivers to fill up with water and reach a steady state. During this time the outer boundary was also gradually raised from LVD37 up to 1.2 m above LVD37. This gave us a baseline height of 1.2 m above LVD37 (i.e., MHWS) without resulting in ponding of low-lying regions of Christchurch that are below 1.2 m above LVD37 but are not connected to the sea. After 24 hours simulation time, a steady state river flow and sea level was reached and the tsunami forcing was initiated.

The model boundary forcing for the 1:2,500-year return period tsunami was extracted from far-field propagation of the tsunami across the Pacific Ocean, modelled using Gerris (Popinet 2003, Popinet 2011) in Lane et al. (2014). We did not repeat this modelling but used the same input conditions taken from it for ocean boundary conditions (the height and timing of the approaching tsunami waves) driving the inundation modelling in this report. The boundary forcing for the 1:500-year return period tsunami was extracted from far-field simulations produced using the ComMIT interface (Titov et al. 2011). The model offshore boundary is located 5,000m off the coast in the south and 6,000m in the north. The model was forced only on the offshore boundary with velocity and water level. Any wave reflected off the Banks Peninsula seaward of the offshore boundary is considered small and not accurately taken into account in the model.

The inundation model was used to simulate a 1:500-year tsunami under current sea level and sea level rise scenarios for 2040 (0.19 m), 2065 (0.41 m) and 2120 (1.06 m) and a 1:2,500-year tsunami (i.e., the maximum credible tsunami) under sea level rise scenarios for 2040 (0.19m), 2065 (0.41m) and 2120 (1.06 m). Results from these simulations (maps of maximum and integrated values of shear stress and time series at selected locations (see Figure 2-3 and Figure 2-4)) were used in a qualitative assessment of potential tsunami-induced changes to the geomorphology of the Avon-Heathcote Estuary and Waimakariri River mouths, as well as likely locations of scour and deposition by the tsunami in the Estuary, Brookland Lagoon and the lower river reaches.

While the model outputs are reported for the locations of the main bridges, the structures were not taken into account in the model because the model is too coarse (relative to bridge dimensions) and too little information about bridge dimension was available. Hence the model simulates the flow at the location of the bridge but ignores how bridge piles, and soffit height may affect the flow.

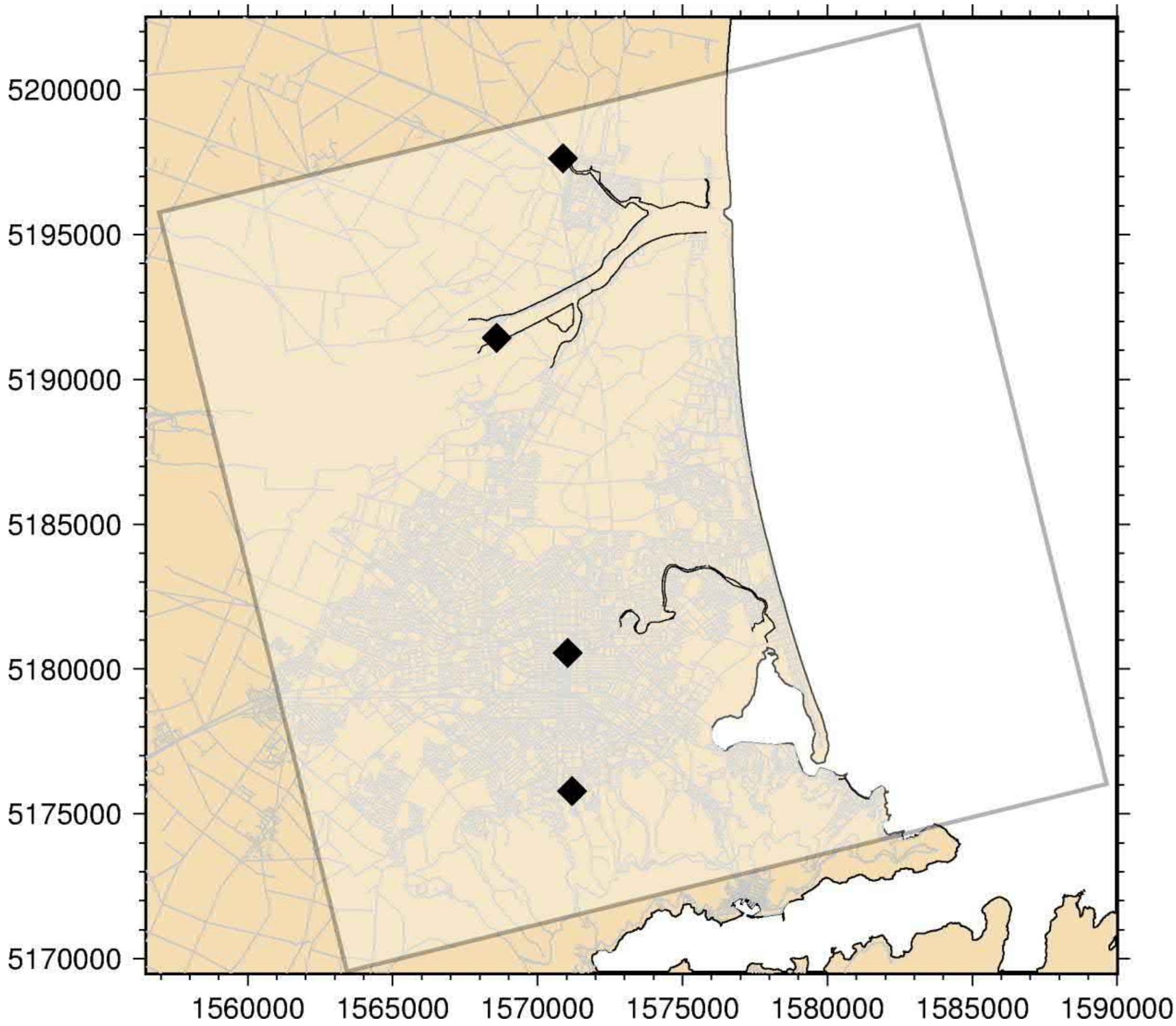

Figure 2-1: Model extent (white box) and location. The model uses an adaptive mesh that is 27 km wide and is rotated by 13.8 degrees (counter clockwise from the east) to be approximately parallel with the shore. The black lines show where stop-banks for the Waimakariri, Kaiapoi and Avon rivers are specified as well as the Sumner seawall. Black diamonds indicate where water was added to create flow down the rivers.

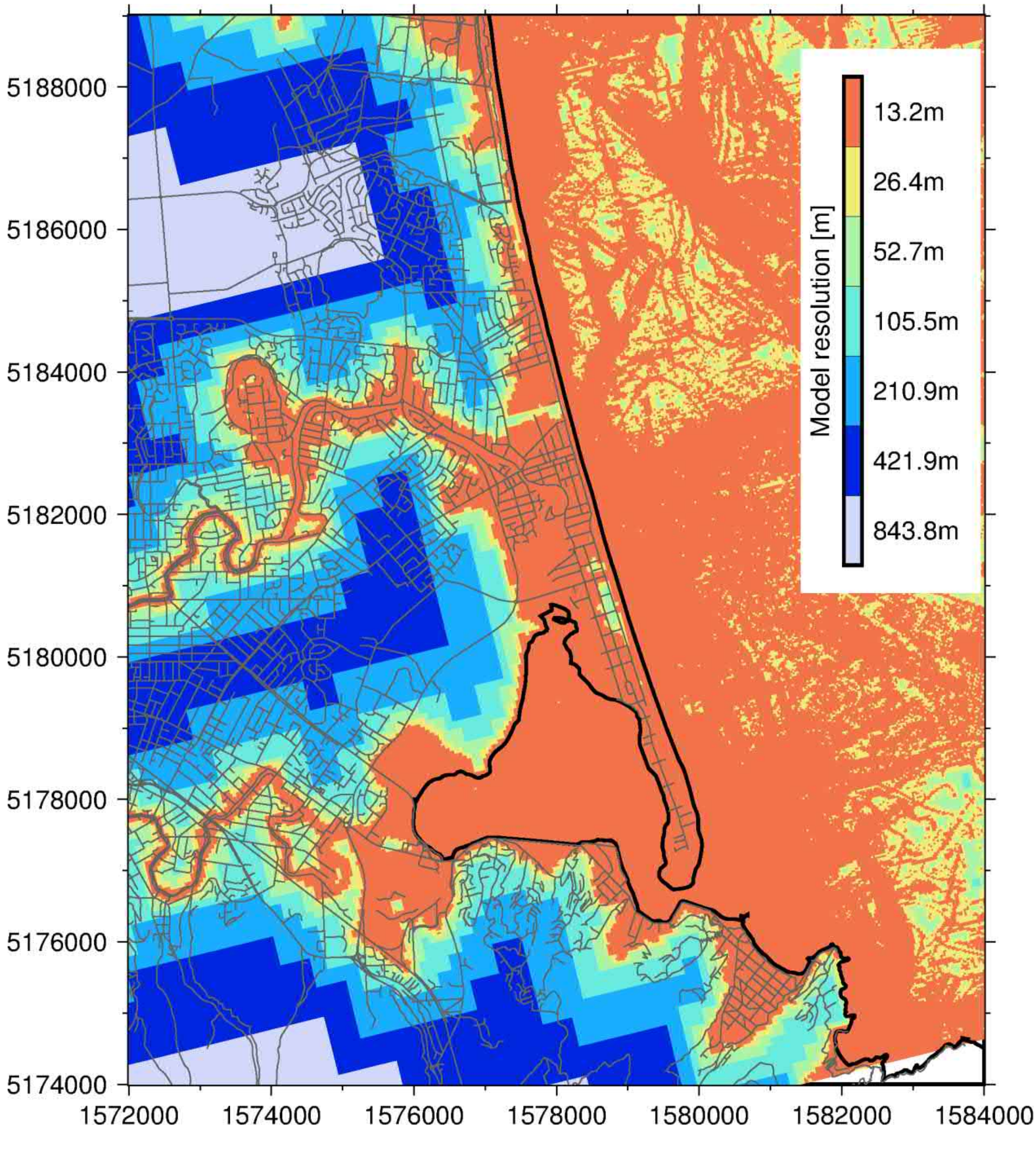

Figure 2-2: Snapshot of model resolution (shading) at the end of inundation for the 1:500-year return period at present mean sea level. The thick black line is the shoreline and the grey lines are roads. Note that higher resolutions occur in the inundated area and resolution gradually decreases on the dry land.

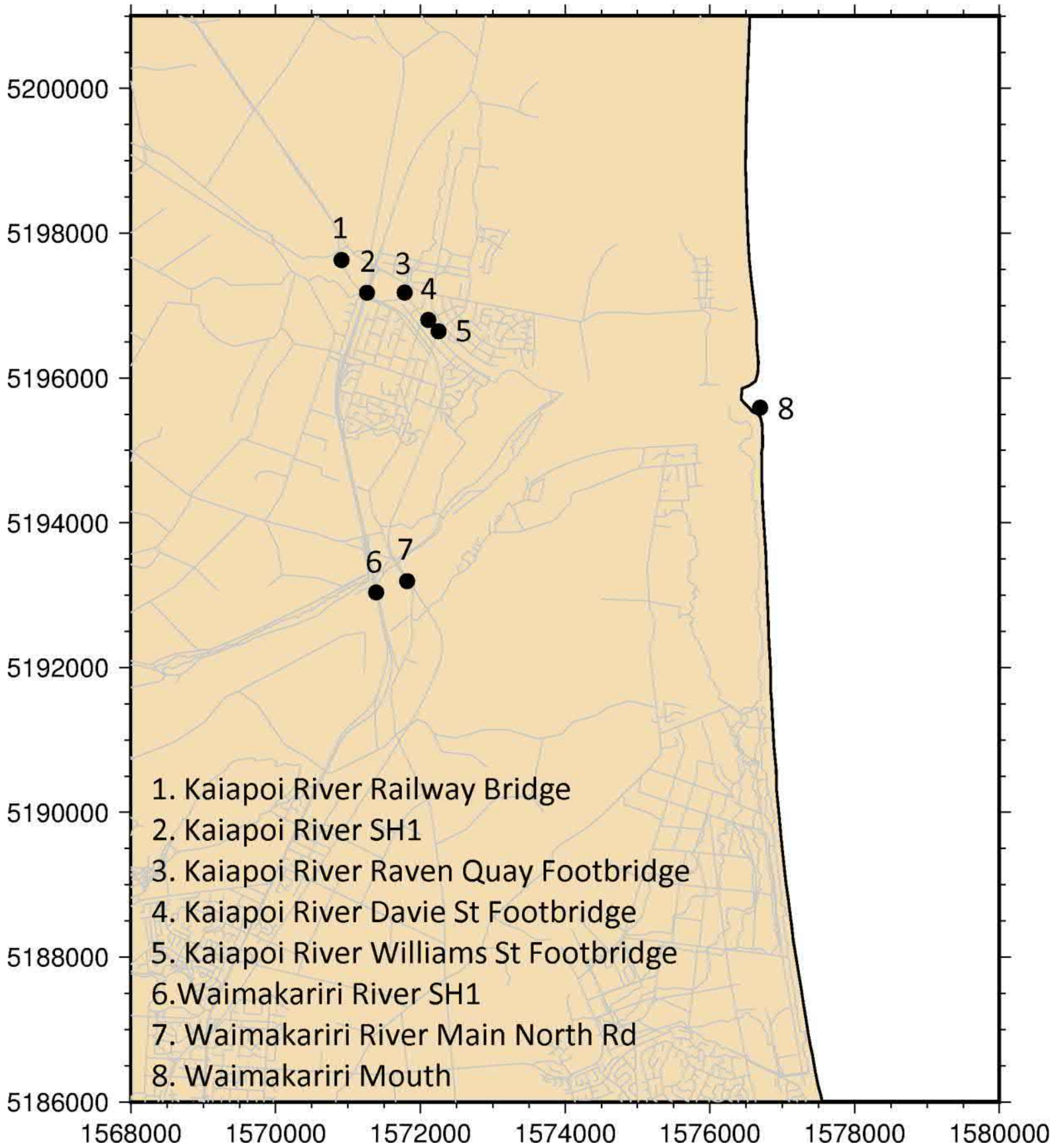

Figure 2-3: Bridge locations for the Northern Section.

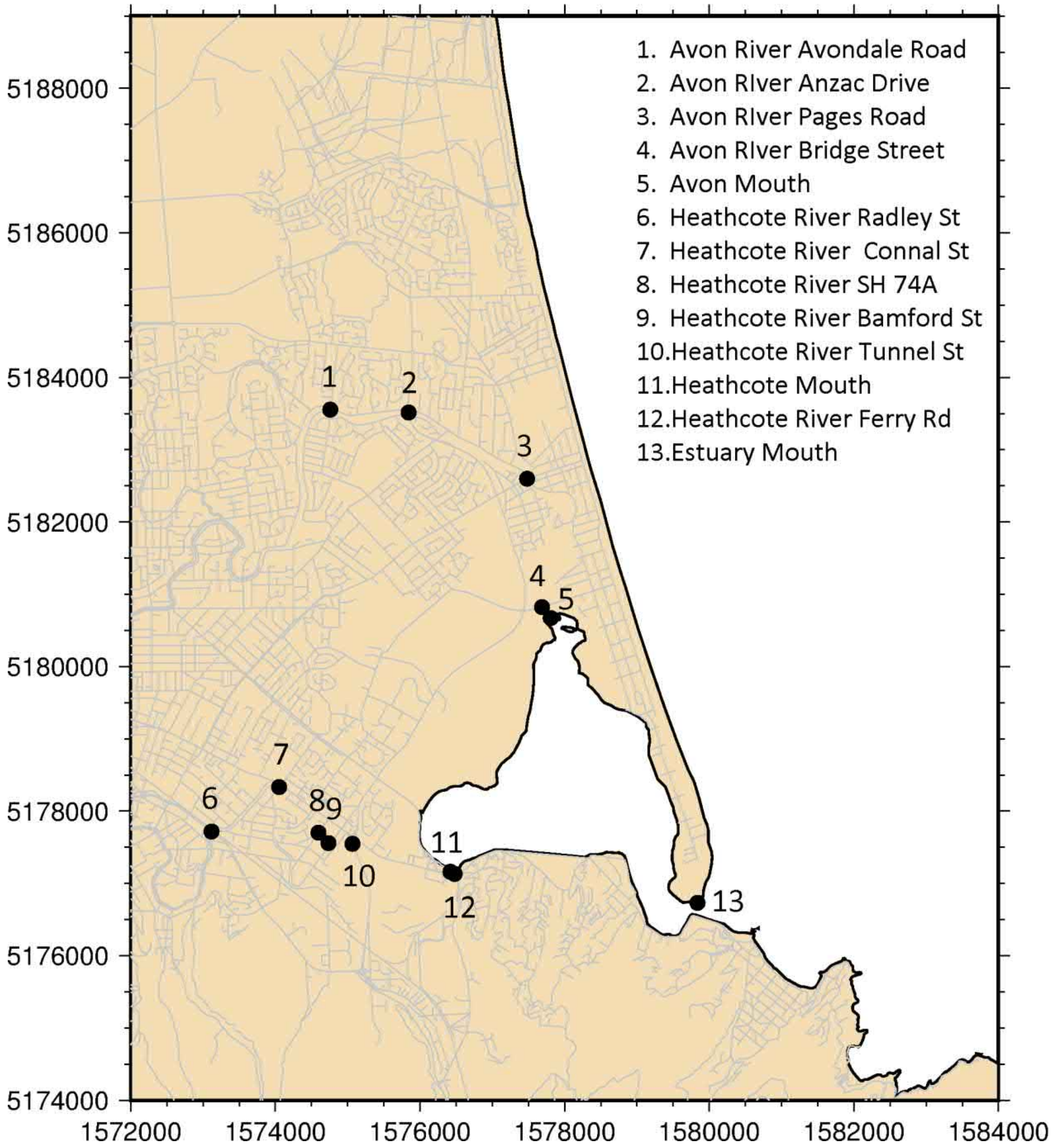

Figure 2-4: Bridge locations for the Southern Section.

2.4 Model outputs

The outputs listed below were produced using the numerical models:

A. Detailed spatial data depicting the maximum inundation depth (as water depth above ground for places that are normally dry and height above pre-tsunami level for rivers and estuaries) and extent, maximum flow speed, and maximum shear stress for the specified sea levels for each scenario. The modelling covered Christchurch City from Godley Head in the south, to the Waimakariri River Mouth in the north.

a. 1:500-year far-field tsunami under current sea level and sea-level rise for 2040 (0.19 m), 2065 (0.41 m) and 2120 (1.06 m).

b. 1:2,500-year far-field tsunami (i.e., maximum credible tsunami) under sea level rise for 2040 (0.19 m), 2065 (0.41 m) and 2120 (1.06 m).

B. Qualitative assessments of the likely geomorphic changes of the river mouths and scour and deposition within the regions of interest:

- The mouth of the Avon-Heathcote Estuary.
- The mouth of the Waimakariri River.
- Bridge locations in the lower reaches of the rivers.

These outputs describe the propagation and magnitude of the tsunami arriving at the Christchurch coastline and the inundation at the locations of interest. The maps are presented and discussed in this report are all in NZTM coordinate system. Detailed spatial data (in digital ArcGIS format) is provided to CCC in addition to this report.

2.5 Uncertainties

Inherent uncertainties associated with the tsunami modelling stem from the bathymetric resolution of the grid used, the fault rupture scenarios used, the numerical equations and the solver used for the modelling. These uncertainties are described in more detail below.

The quality of the topographic data and the bathymetric data in inshore waters strongly influences the simulation of inundation. For this modelling, we used available DEM data for the land topography and near-shore bathymetry in the vicinity of Christchurch, but in order to capture some of the more complex small-scale processes in harbours and embayed areas, higher resolution data is required. Known topographic uncertainties associated with the DEM used for this study include the bathymetry of the Waimakariri River. Also, in order to resolve the Waimakariri and Avon stop-banks and Sumner seawall, we refined cells in these regions to the highest resolution and then set their elevation to the specified stop-bank and seawall crest levels. Given that the finest resolution is 13.2 m, this means that the stop-banks and seawalls were modelled as having at least that width. In the case of the Sumner seawall, this is wider than the actual sea wall. This resolution also limits how well the dunes can be resolved. Although the model finest resolution is 13.2 m the GIS files that shows model output have been rotated back to a New Zealand Transverse Mercator coordinate system and resampled to a uniform resolution of 15 m for compliance with GIS format.

Other uncertainties in the modelling study include the gridded representation of a continuous coastline (grid-stepping), which can deform the shape of bays and estuaries, and the effects of building and land features on form drag. The latter could substantially modify the onshore propagation of tsunamis. Improving the drag representation remains a goal of current research. Eradication of the other errors is constrained by limitations of data quality and the practicalities of grid resolution. Models always represent an approximation of reality.

The model presented here did not include sediment transport and morphological changes associated with tsunami and hence in places where dunes are severely eroded by tsunami the model is likely to be underestimating the inundation. Lane et al. (2017) investigated the effect of dune breach on tsunami inundation near Christchurch.

Model uncertainty can be quantified by running multiple simulations with small variations in key parameters, an approach known as ensemble prediction or sensitivity analysis. Such an approach provides an envelope of predicted solutions, rather than single "worst-case" or "scenario-type" predictions, on which to base emergency response procedures. However, running many simulations increases the computational and research costs, and, in any event, model forecasts can never be certain because our knowledge of all the geophysical processes involved in tsunami generation, propagation and inundation remains incomplete.

Quantitative calibration of the tsunami inundation model against real measurements is difficult due to the uncertain nature of tsunami impact data from New Zealand and the consequent difficulty in identifying events from the past. Nevertheless, the Gerris and Basilisk models have been continuously validated against standard analytical test cases (e.g., Popinet 2003, Popinet 2011, Popinet 2012, Popinet 2015).

In addition to the uncertainty in the model there is always additional aleatory uncertainty. Changes to ground levels from future local earthquakes could change the results - especially if the epicentres were close to the coast. However, the changes could raise or lower the land depending on the details of where and how the fault ruptures so very little can be said a priori about this. If the earthquake were to cause liquefaction and this was then removed it would cause a lowering of the land with respect to sea level and could increase the flooding hazard. Likewise, effects on the sea level (e.g. relative sea level rise and the geomorphological changes it could cause; tidal cycle, storm surge and sea state at the time of a tsunami) could also change the results given here.

3 Model results

3.1 Water level at coast

For the 1:500-year return period event, the tsunami wave reached a maximum height of 4.4 m above LVD (wave height of 5.7 m from crest to trough) near the Waimakariri River Mouth (Figure 3-1) and 4.7 m at the Estuary mouth (Figure 3-2). For the 1:2,500-year return period event, the maximum level was 7.23 m above LVD (wave height of 8.6 m from crest to trough) at the Waimakariri River mouth (Figure 3-3) and 7.25 m above LVD at the Estuary mouth (Figure 3-4).

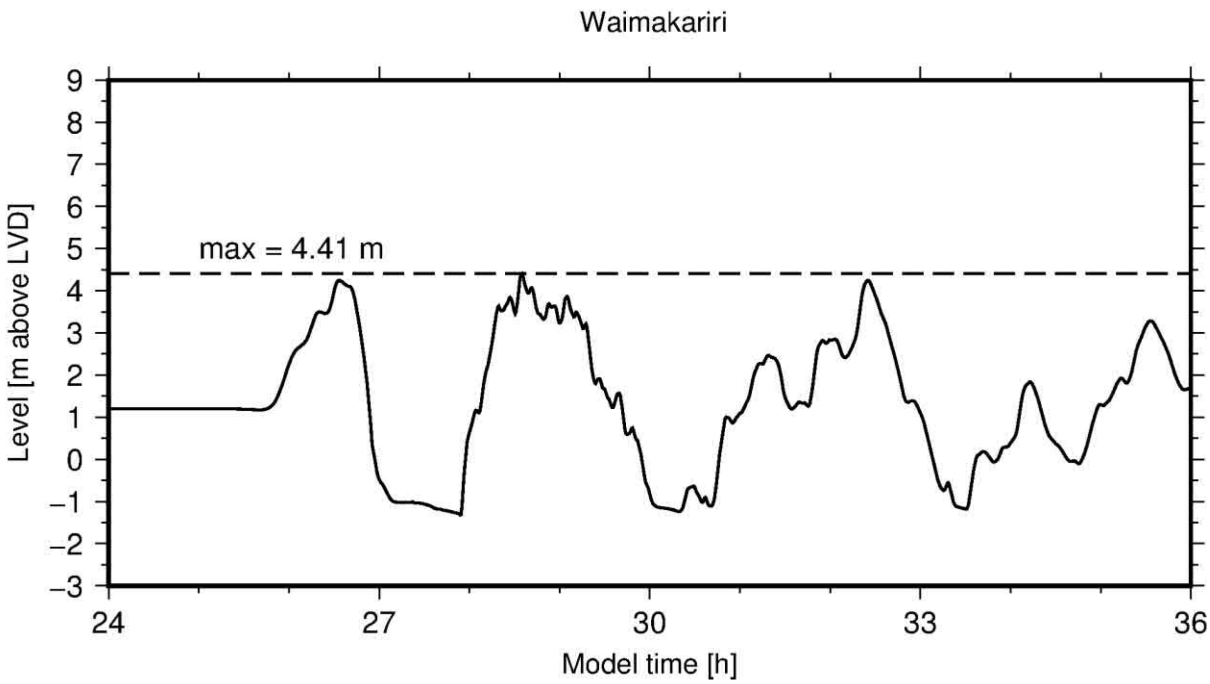

Figure 3-1: Water level at the Waimakariri river mouth for the 1:500-year return period event at present sea level.

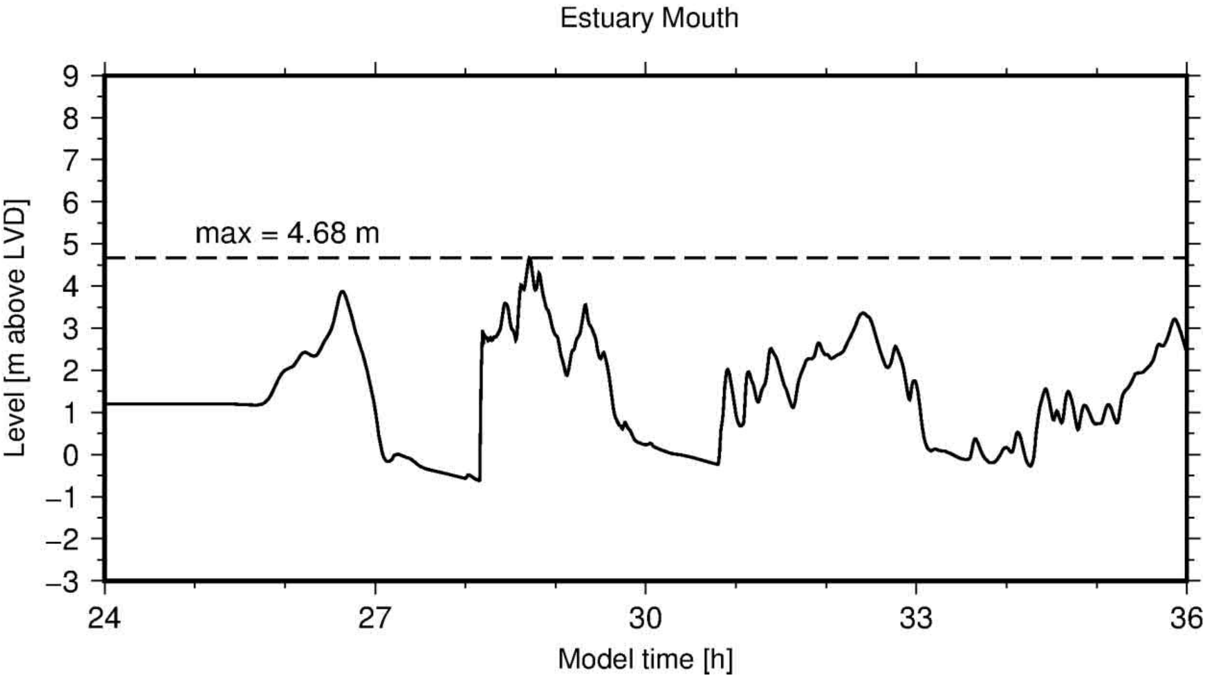

Figure 3-2: Water level at the Estuary mouth for the 1:500-year return period event at present sea level.

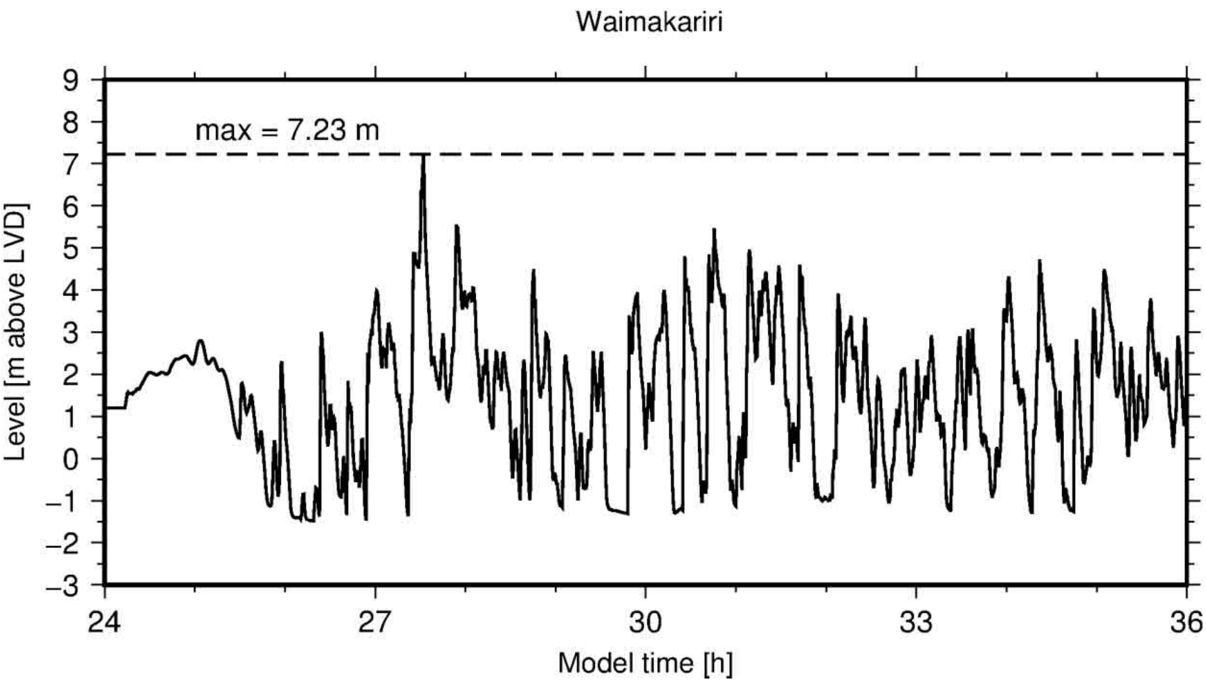

Figure 3-3: Water level at the Waimakariri river mouth for the 1:2,500-year return period event at 2040 Sea Level Scenario – 0.19 m Sea Level Rise.

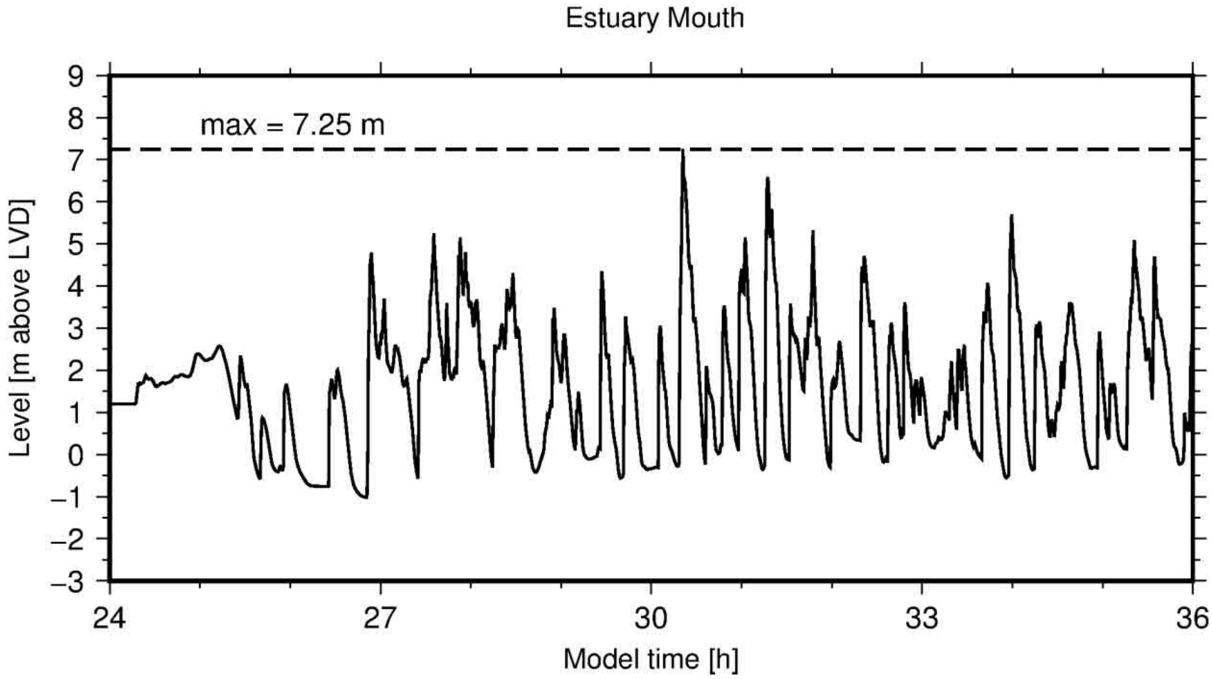

Figure 3-4: Water level at the Estuary mouth for the 1:2,500-year return period event at 2040 Sea Level Scenario – 0.19 m Sea Level Rise.

3.2 Water level at the main bridges.

Tsunami wave propagating along river channels can cause severe damage to infrastructure far upstream. The maximum elevation of tsunami waves at each of the main bridges in the lower reaches of the Waimakariri, Avon and Heathcote rivers is presented in Table 3-1 and Table 3-2. Elevation of the soffit (i.e., underside of the bridge decks) (LVD37) are also presented (where the value is known) and the modelled tsunami heights above LVD37 at each location.

Tsunami waves reached the highest levels at the Waimakariri River SH1 bridge (Figure 3-5 and Figure 3-6). For most scenarios the tsunami waves did not reach the soffit height (where elevation is known) except for the Heathcote River Bamford Street bridge (Figure 3-7 – Figure 3-10) where the soffit elevation is reached by the tsunami wave for all the scenarios. For the 1:500-year return period at the predicted sea level of 2120 (1.06m), the tsunami level reaches within less than 1 m of the soffit for the Avon River Pages Road bridge (Figure 3-11 – Figure 3-14), the Avon River Avondale Road bridge (Figure 3-15 and Figure 3-16), the Heathcote River Ferry Road Bridge (Figure 3-17 and Figure 3-18) and the Heathcote River Tunnel Road bridge (Figure 3-19 and Figure 3-20). This would make these bridges more vulnerable to debris transported by the tsunami waves.

The water level has not yet peaked at the end of the simulation at the Avon River Avondale Road bridge (Figure 3-15 and Figure 3-16). This is because the bridge is at a point that drains the inundation for a large area and water levels are likely to remain high long after the tsunami as the inundation drains back to the sea.

For some of the bridges (e.g., Waimakariri River SH1, Heathcote River Ferry Road) the maximum water level reached with the 1:500-year return period event exceeds the level reached by the 1:2,500-year return period event. While this may appear counter-intuitive, this is the result of the higher frequency waves from the 1:2,500-year scenario losing a large amount of energy while propagating along the river channels. The 1:500-year scenarios do not include such high frequency waves. This highlights the potential differences in impacts caused by different tsunami scenarios.

Table 3-1: Bridges on Waimakariri, Avon and Heathcote rivers with heights above LVD37 and modelled maximum tsunami height at those locations for the 1:500-year return period scenario.

Bridge	Bridge soffit level above LVD37 (m)	1:500-year return period Tsunami height above LVD37 (m) Current Sea Level	2040 Sea Level 0.19 m Rise	2065 Sea Level 0.41 m Rise	2120 Sea Level 1.06 m Rise
Waimakariri River Main North Rd	7.8	3.96	4.17	4.39	4.90
Waimakariri River SH1		4.02	4.20	4.43	4.95
Avon River Bridge Street	6.2	2.66	2.83	3.12	3.72
Avon River Pages Road	4.2	2.57	2.77	3.02	3.71
Avon River Anzac Drive	4.2	2.09	2.21	2.39	2.84
Avon River Avondale Road	3.8	1.99	2.08	2.23	2.82
Heathcote River Ferry Road	4.6	2.57	2.77	2.96	3.57
Heathcote River Tunnel Road	4.3	2.51	2.65	2.84	3.55
Heathcote River Bamford Street	2.1	2.51	2.66	2.83	3.55
Heathcote River SH 74A		2.50	2.65	2.81	3.50
Heathcote River Connal Street		2.38	2.53	2.69	3.21
Heathcote River Radley Street		2.38	2.54	2.70	3.20

Table 3-2: Bridges on Waimakariri, Avon and Heathcote rivers with heights above LVD37 and modelled maximum tsunami height at those locations for the 1:2,500-year return period scenario.

Bridge	Bridge soffit level above LVD37 (m)	1:2,500-year return period Tsunami height above LVD37 (m)		
		2040 Sea Level 0.19 m Rise	2065 Sea Level 0.41 m Rise	2120 Sea Level 1.06 m Rise
Waimakariri River Main North Rd	7.8	3.85	4.04	4.65
Waimakariri River SH1		3.86	4.07	4.70
Avon River Bridge Street	6.2	3.12	3.34	3.90
Avon River Pages Road	4.2	2.97	3.22	3.96
Avon River Anzac Drive	4.2	2.28	2.40	2.93
Avon River Avondale Road	3.8	2.19	2.31	2.9
Heathcote River Ferry Road	4.6	2.82	2.98	3.49
Heathcote River Tunnel Road	4.3	2.66	2.81	3.41
Heathcote River Bamford Street	2.1	2.66	2.81	3.40
Heathcote River SH 74A		2.65	2.80	3.37
Heathcote River Connal Street		2.60	2.75	3.15
Heathcote River Radley Street		2.60	2.76	3.16

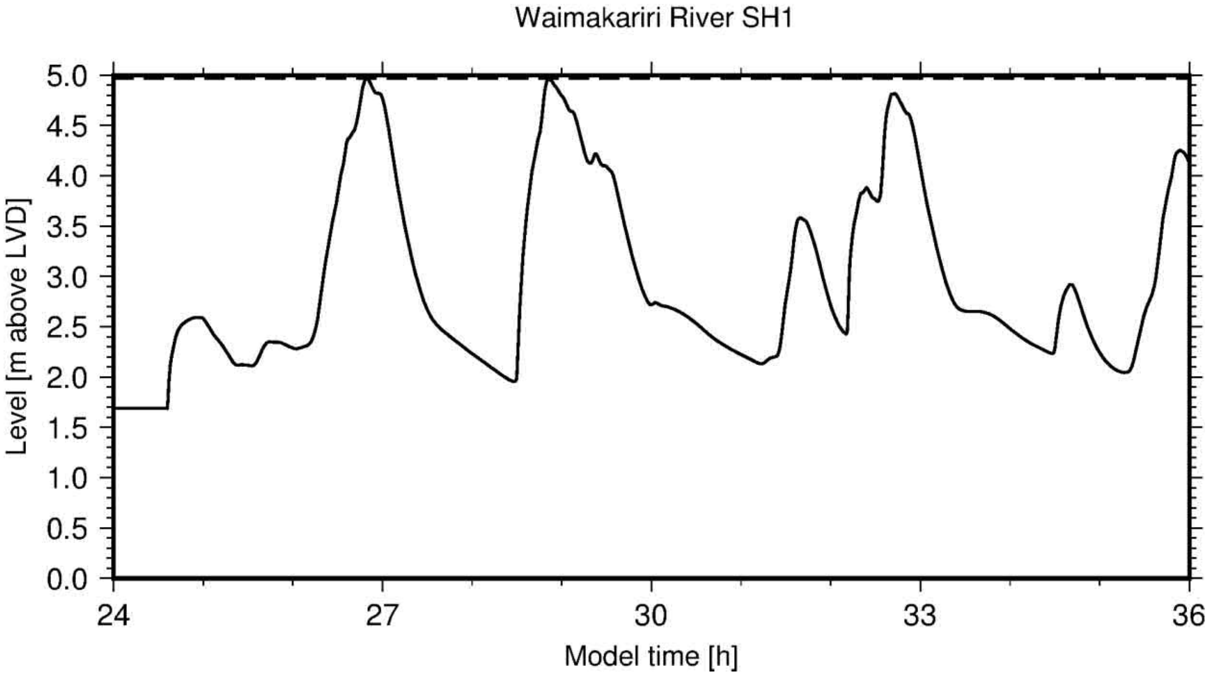

Figure 3-5: Tsunami height timeseries for 1:500-year return period – 2120 Sea Level Scenario – 1.06 m Sea Level Rise at the Waimakariri River SH1 bridge.

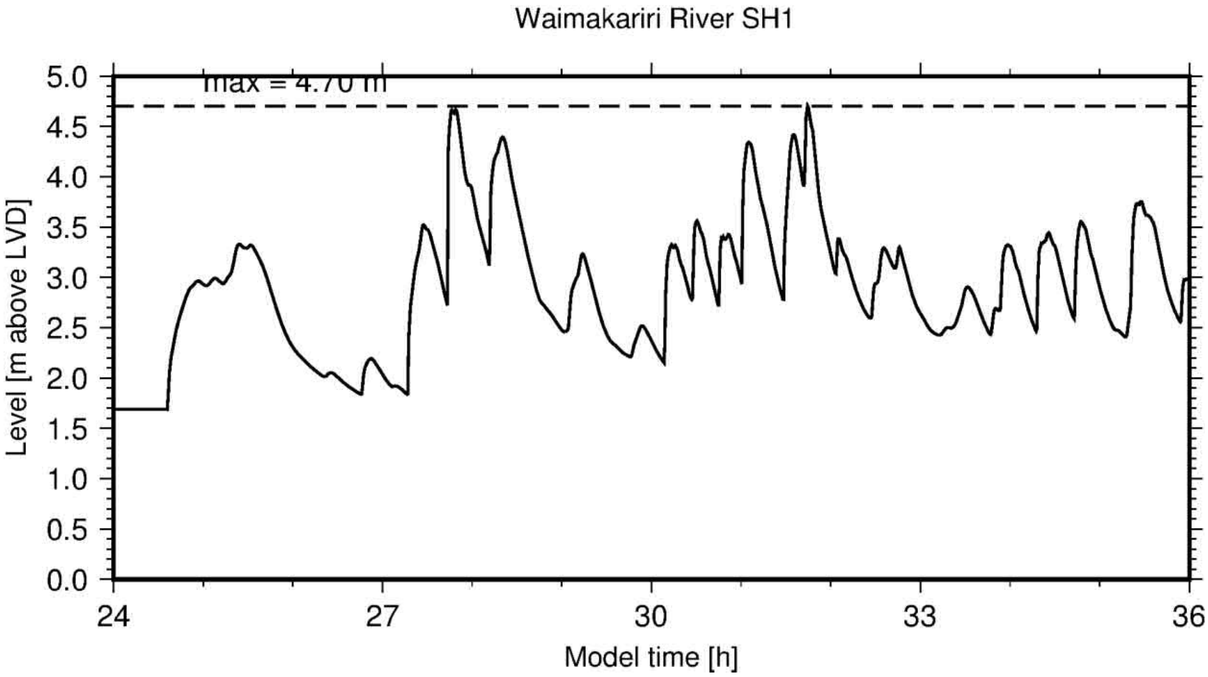

Figure 3-6: Tsunami height timeseries for 1:2,500-year return period – 2120 Sea Level Scenario – 1.06 m Sea Level Rise at the Waimakariri River SH1 bridge.

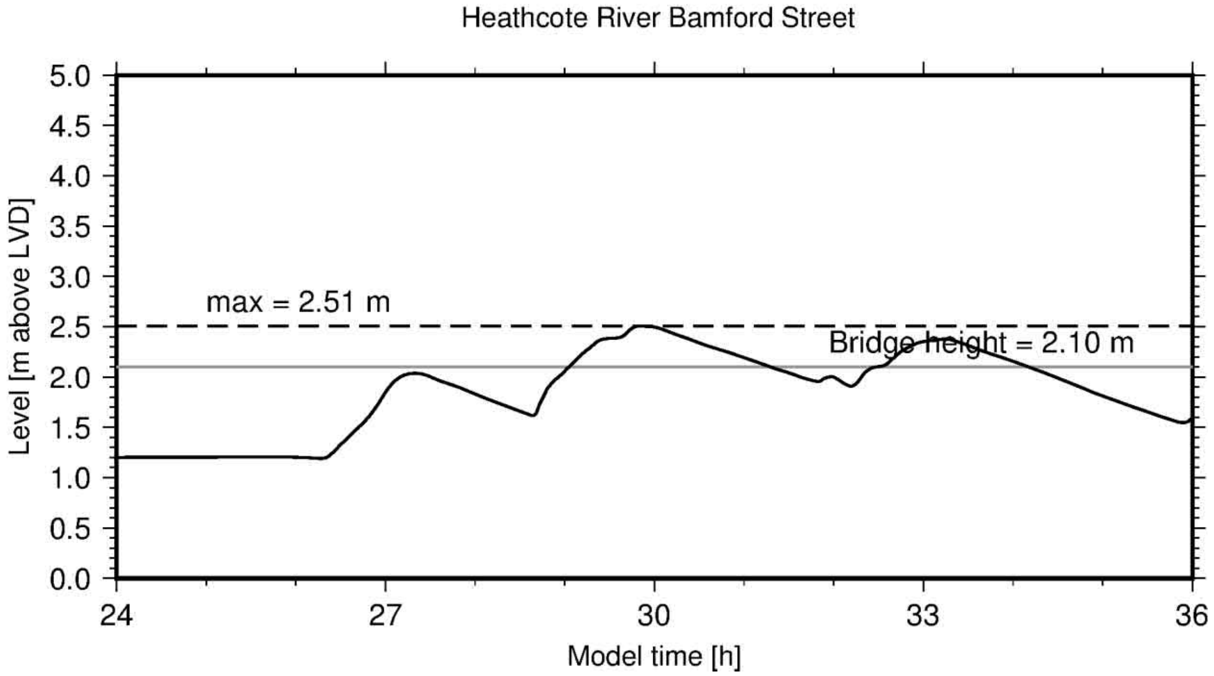

Figure 3-7: Tsunami height timeseries for 1:500-year return period - Current Sea Level at Heathcote River Bamford Street.

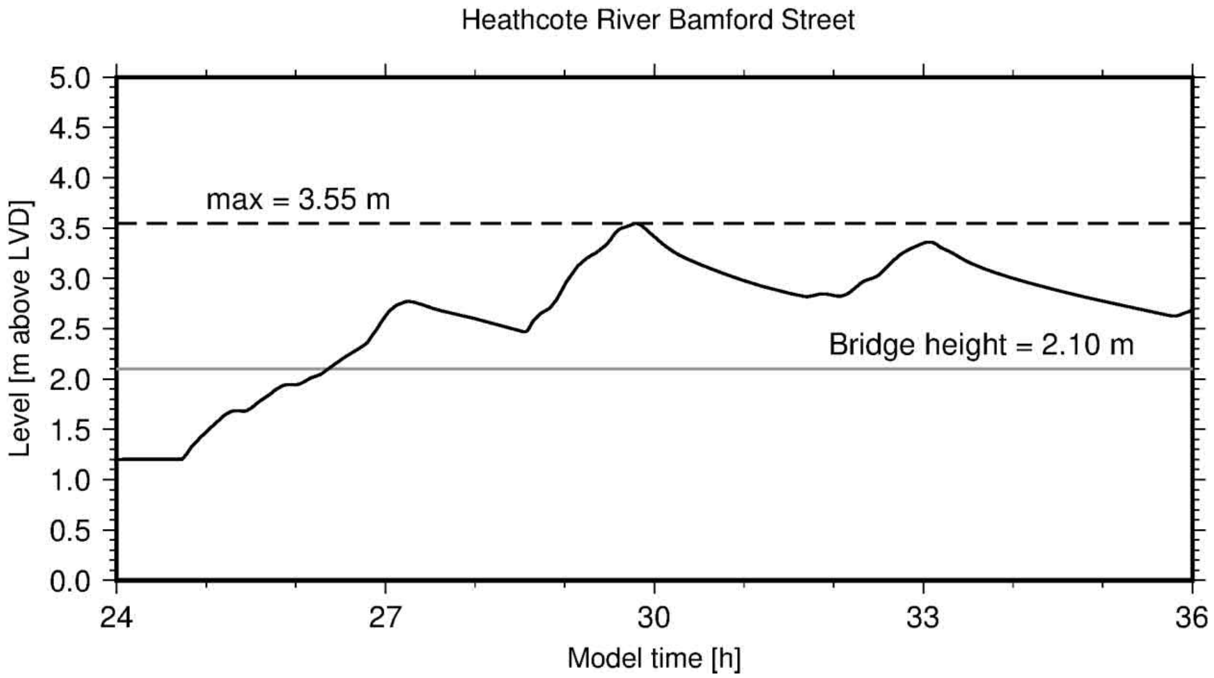

Figure 3-8: Tsunami height timeseries for 1:500-year return period – 2120 Sea Level Scenario – 1.06 m Sea Level Rise at Heathcote River Bamford Street.

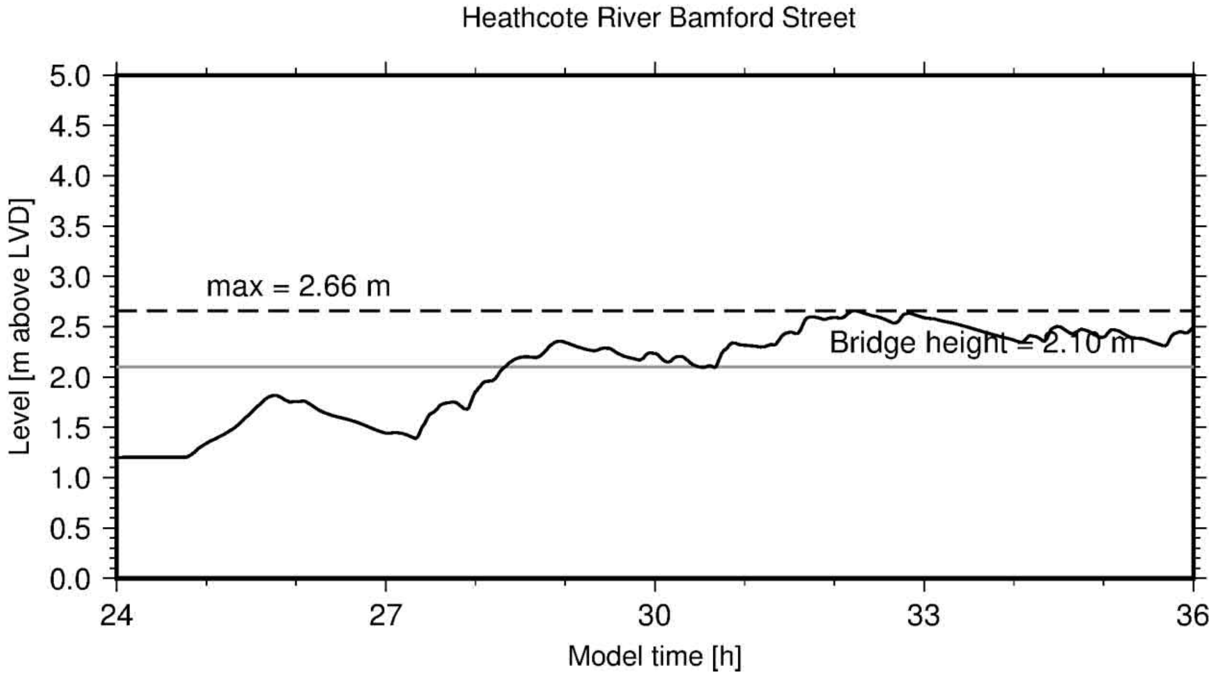

Figure 3-9: Tsunami height timeseries for 1:2,500-year return period - 2040 Sea Level Scenario – 0.19 m Sea Level Rise at Heathcote River Bamford Street.

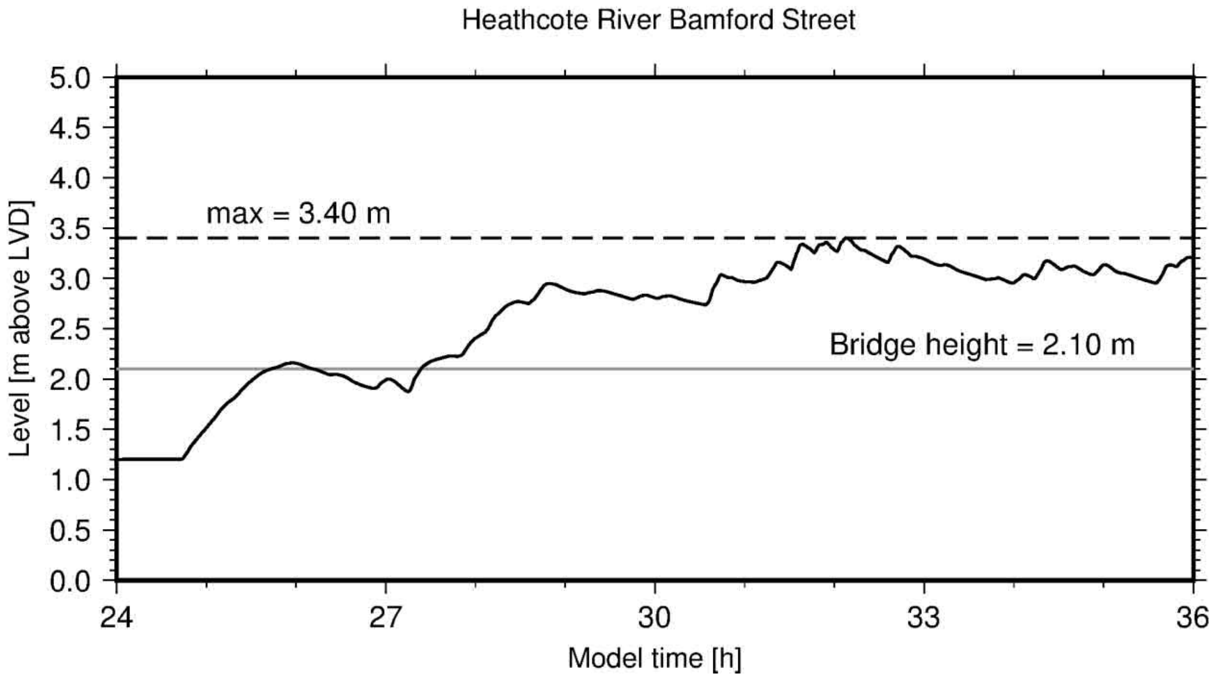

Figure 3-10: Tsunami height timeseries for 1:2,500-year return period – 2120 Sea Level Scenario – 1.06 m Sea Level Rise at Heathcote River Bamford Street.

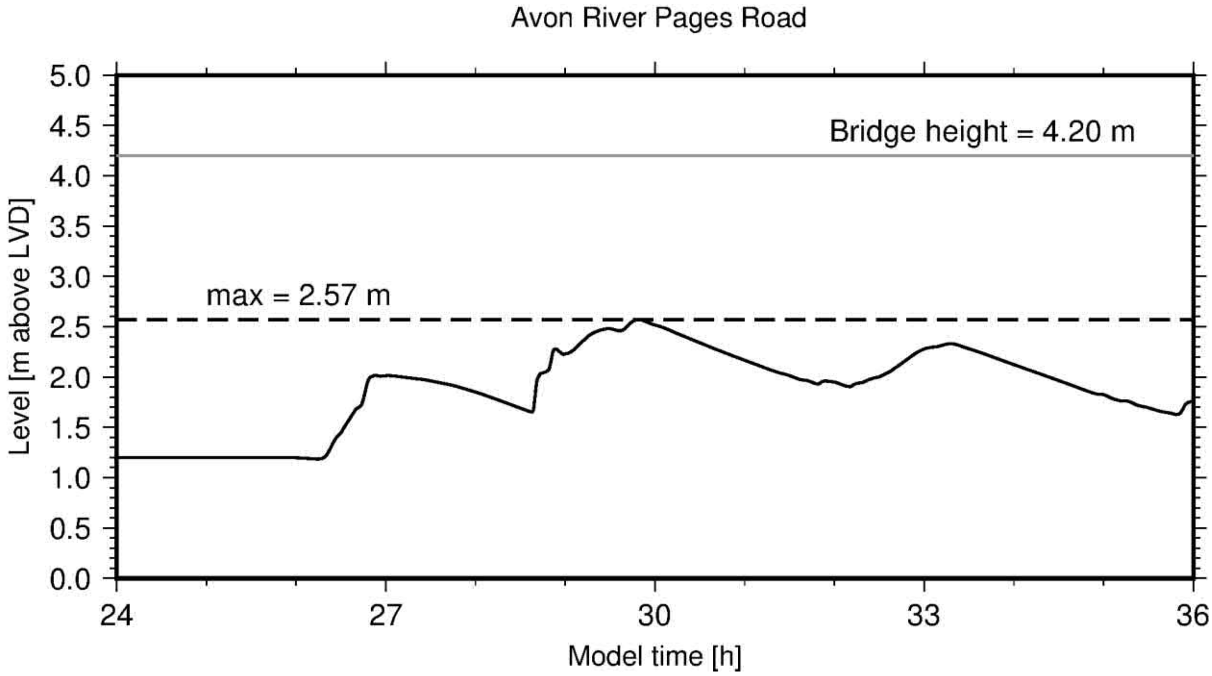

Figure 3-11: Tsunami height timeseries for 1:500-year return period - Current Sea Level at Avon River Pages Road.

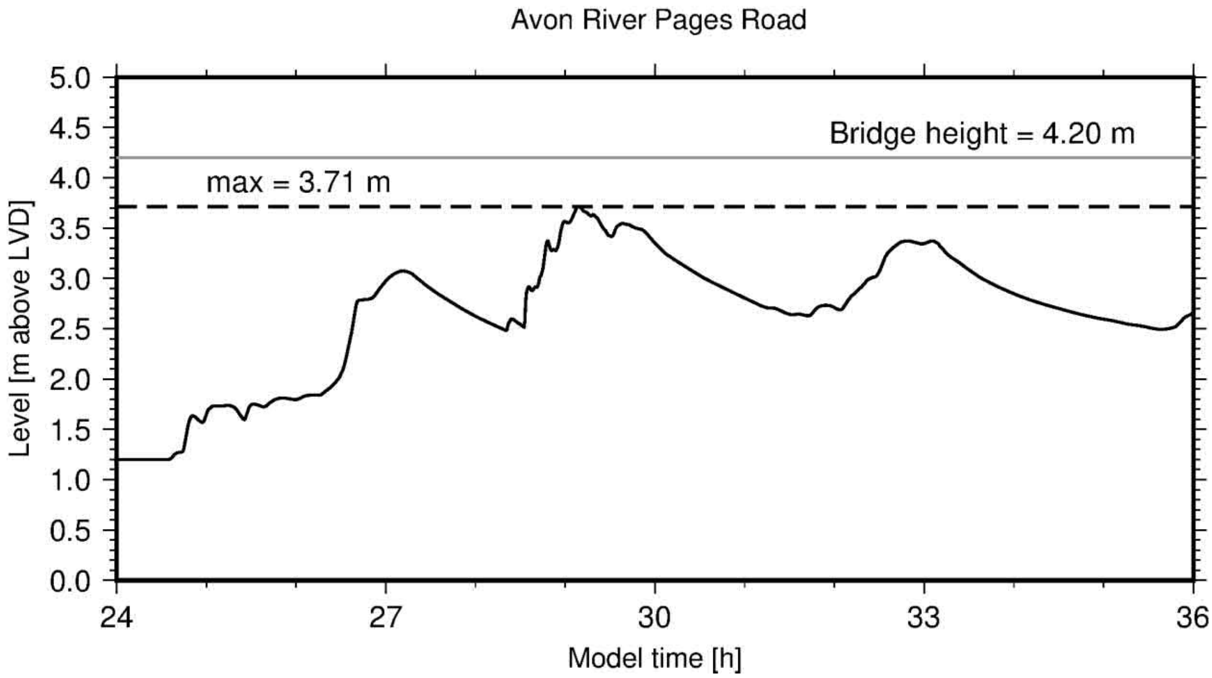

Figure 3-12: Tsunami height timeseries for 1:500-year return period – 2120 Sea Level Scenario – 1.06 m Sea Level Rise at Avon River Pages Road.

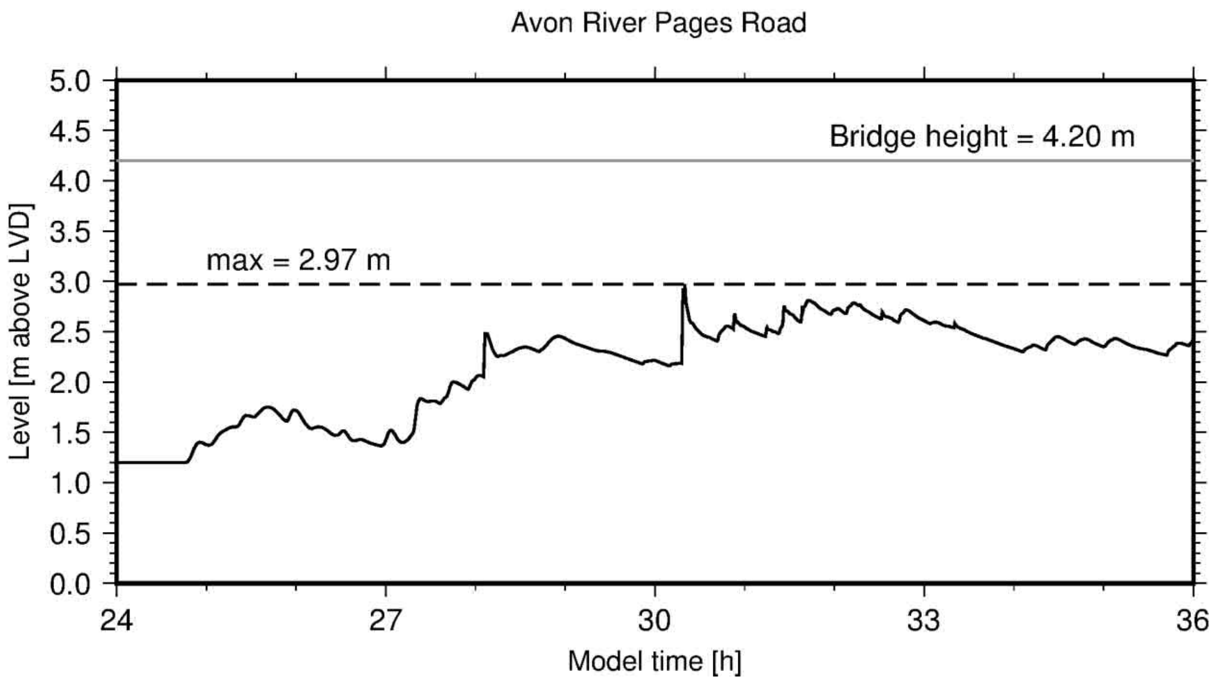

Figure 3-13: Tsunami height timeseries for 1:2,500-year return period - 2040 Sea Level Scenario – 0.19 m Sea Level Rise at Avon River Pages Road.

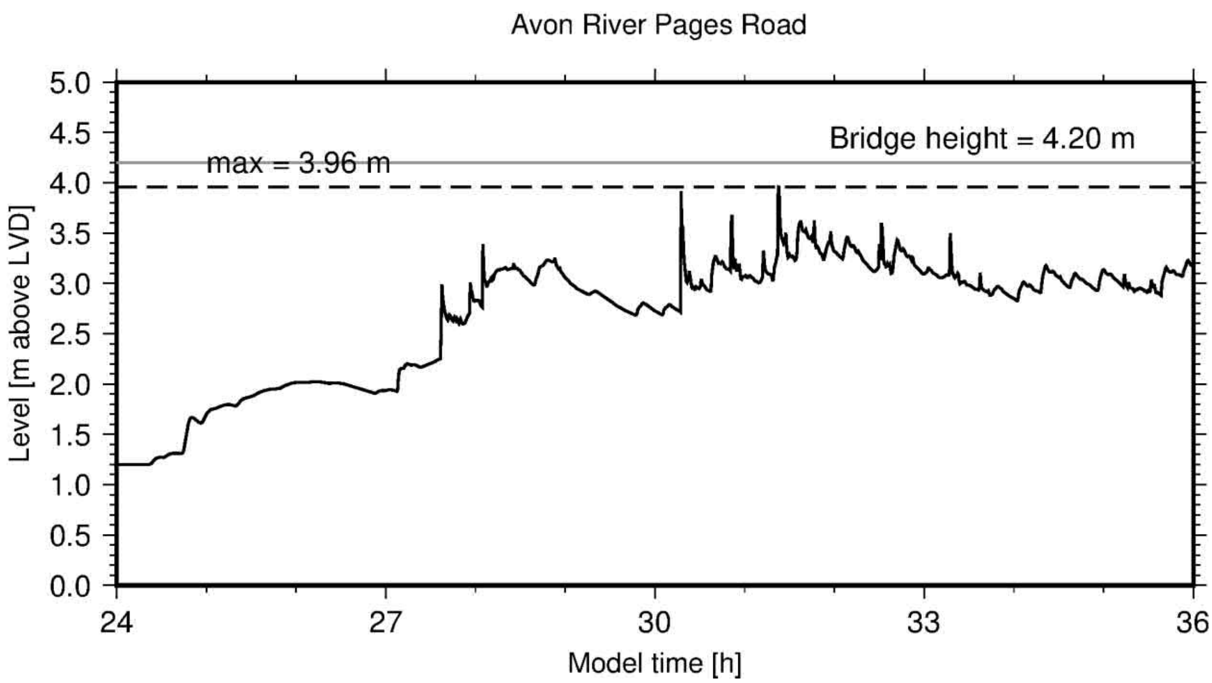

Figure 3-14: Tsunami height timeseries for 1:2,500-year return period – 2120 Sea Level Scenario – 1.06 m Sea Level Rise at Avon River Pages Road.

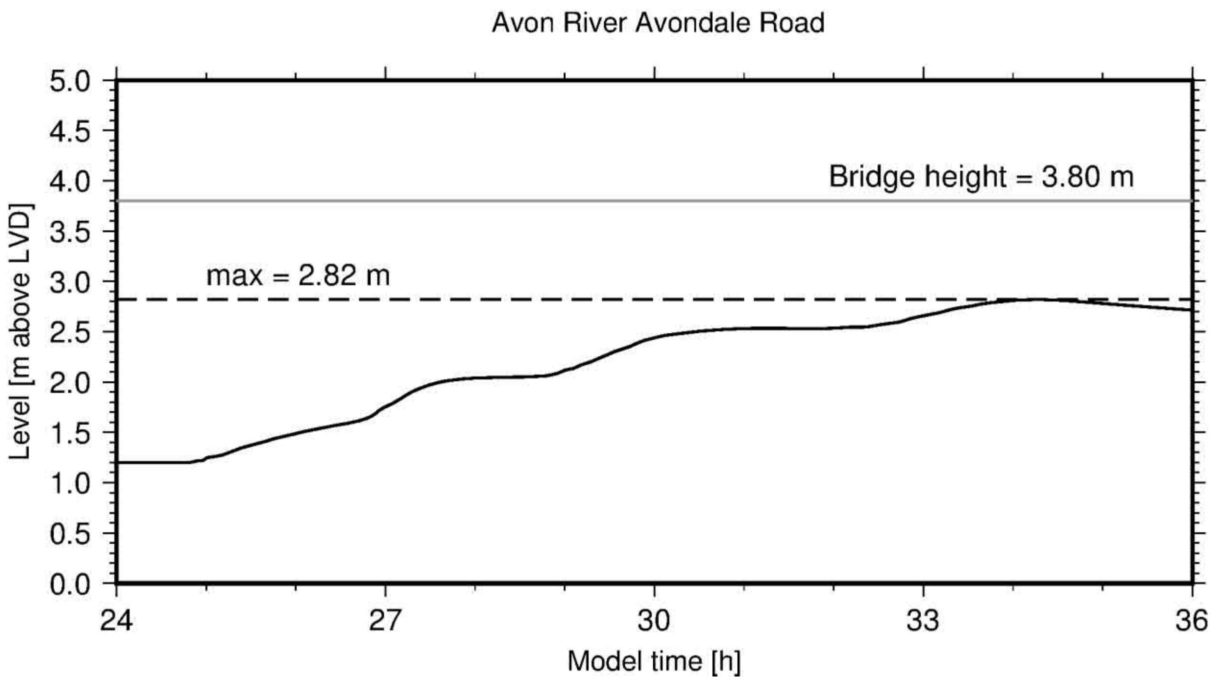

Figure 3-15: Tsunami height timeseries for 1:500-year return period – 2120 Sea Level Scenario – 1.06 m Sea Level Rise at Avon River Avondale Road bridge.

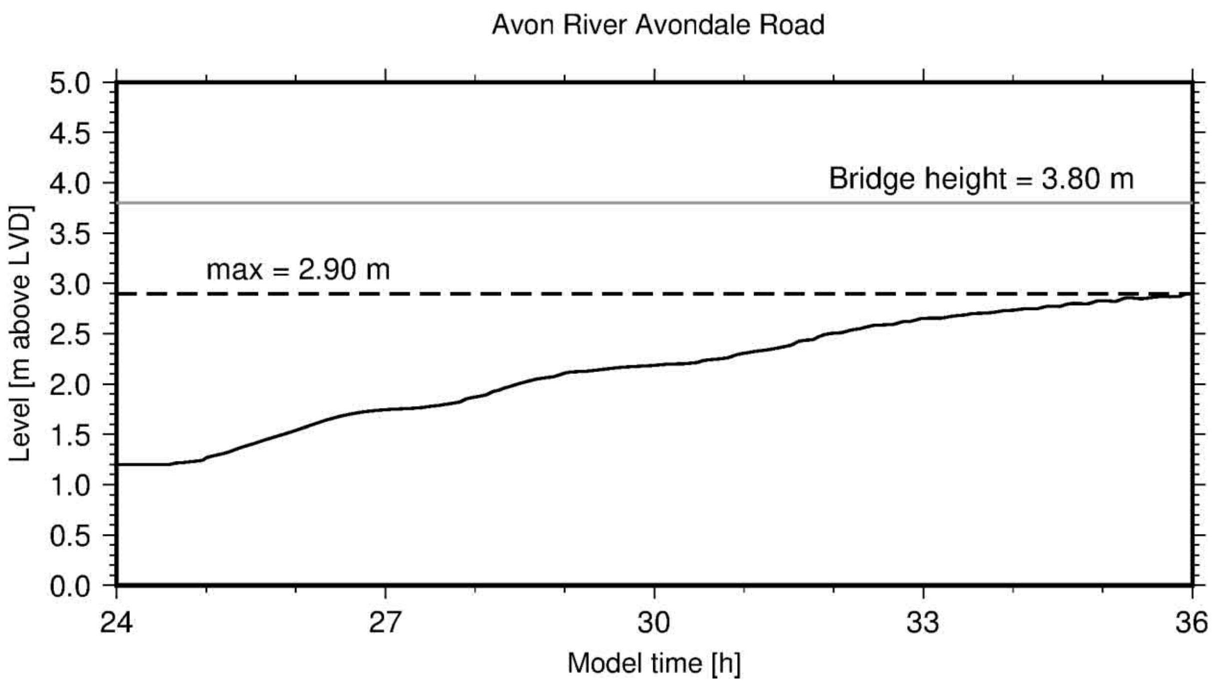

Figure 3-16: Tsunami height timeseries for 1:2,500-year return period – 2120 Sea Level Scenario – 1.06 m Sea Level Rise at Avon River Avondale Road bridge.

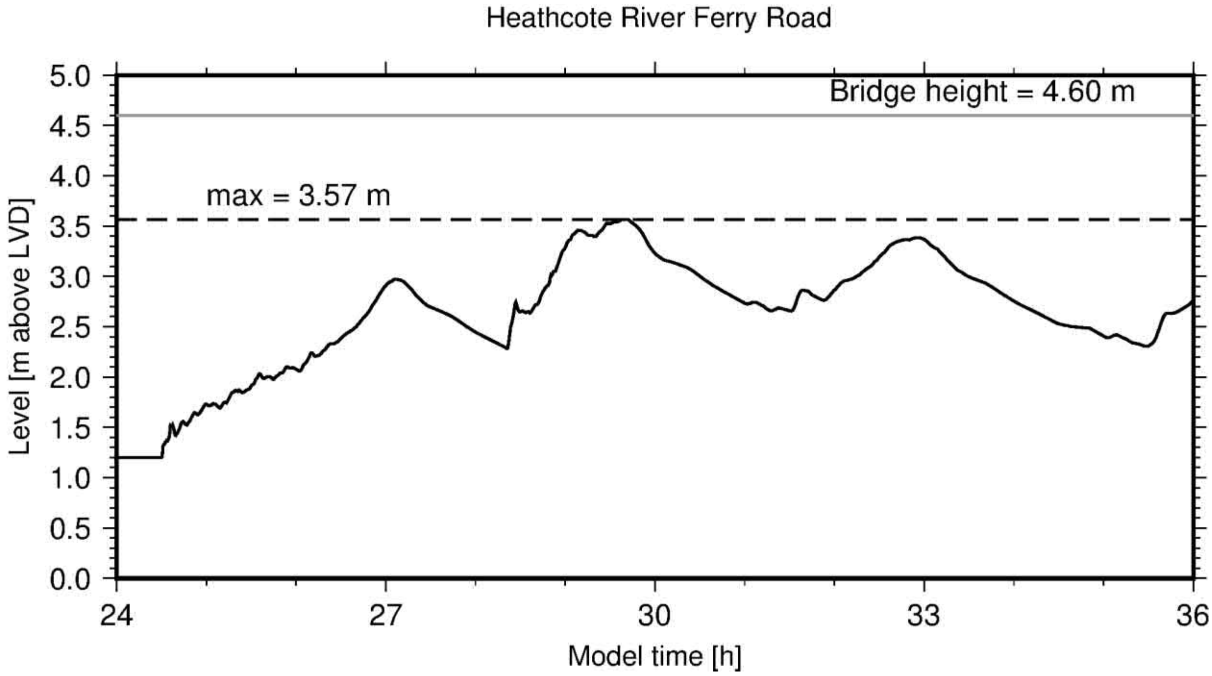

Figure 3-17: Tsunami height timeseries for 1:500-year return period – 2120 Sea Level Scenario – 1.06 m Sea Level Rise at the Heathcote River Ferry Road bridge.

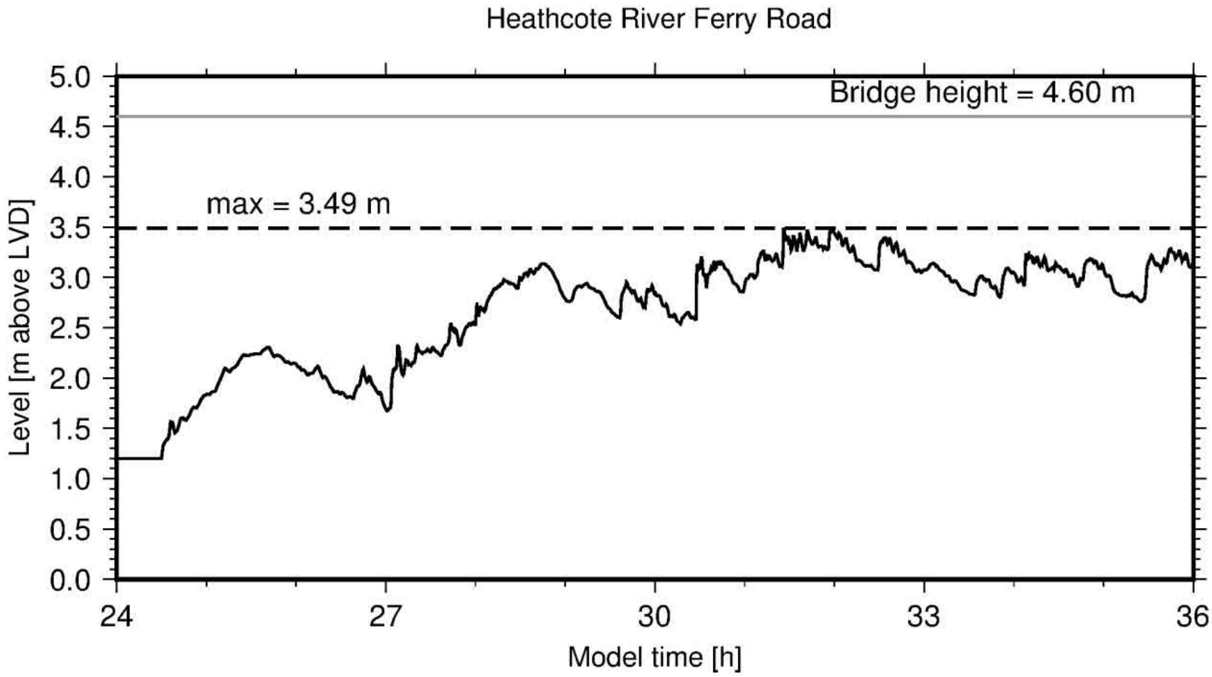

Figure 3-18: Tsunami height timeseries for 1:2,500-year return period – 2120 Sea Level Scenario – 1.06 m Sea Level Rise at the Heathcote River Ferry Road bridge.

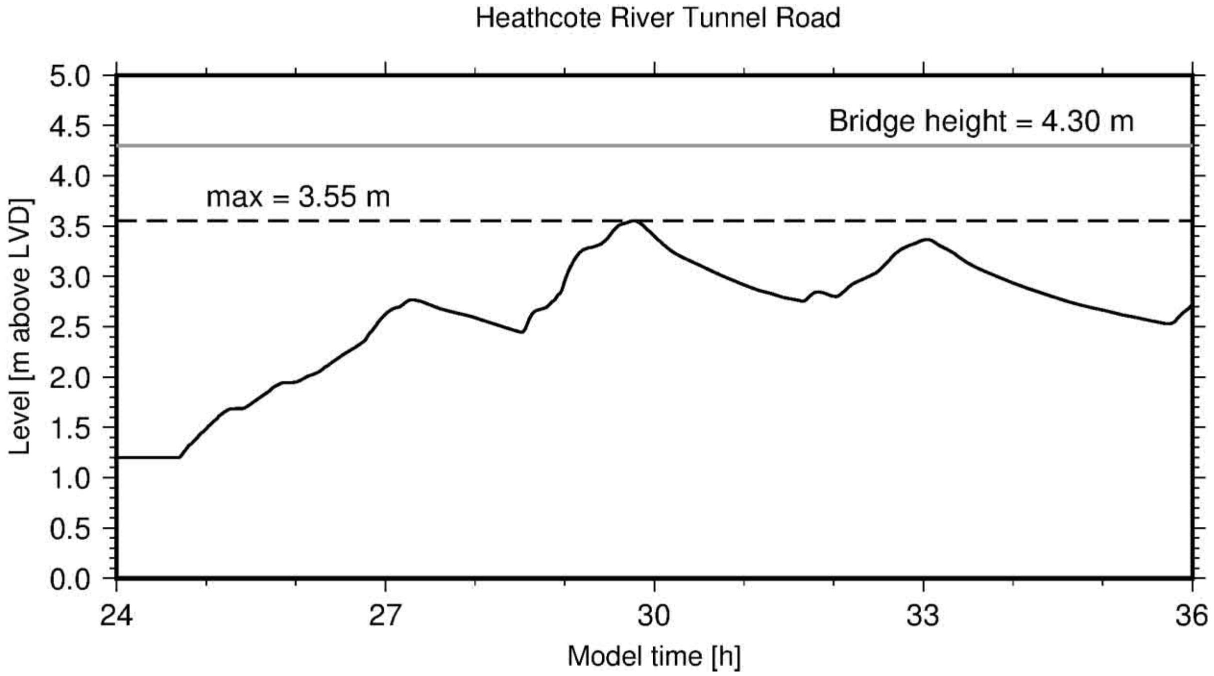

Figure 3-19: Tsunami height timeseries for 1:500-year return period – 2120 Sea Level Scenario – 1.06 m Sea Level Rise at the Heathcote River Tunnel Road bridge.

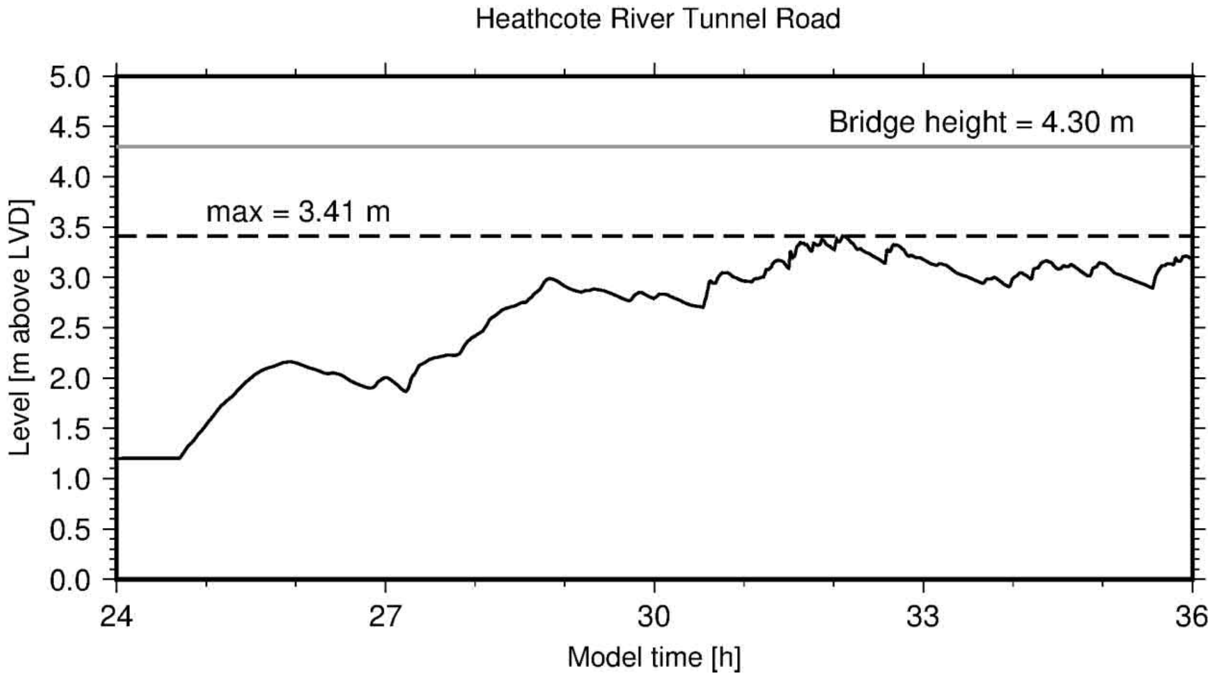

Figure 3-20: Tsunami height timeseries for 1:2,500-year return period – 2120 Sea Level Scenario – 1.06 m Sea Level Rise at the Heathcote River Tunnel Road bridge.

3.3 Maximum inundation, speed and shear stress.

3.3.1 1:500-year return period tsunami - Current Sea Level

The inundation extent for the 1:500-year return period tsunami at current mean sea-level covers an area of 39 km^2 and reaches a maximum depth of 5.4 m near the Waimakariri River entrance. The main inundation locations on the northern side of the area of interest are the flood plain of the Brooklands Lagoon and the Styx River floodplain (Figure 3-21). In this area the high flow speed (>2 m/s) is constrained to the Waimakariri River Channel, the Kaiapoi River channel, Brooklands Lagoon and the Waimakariri River Mouth (Figure 3-22). On the southern side of the area of interest, inundation for the 1:500-year tsunami occurs in the floodplain of the Avon River, near the mouth of the Heathcote River, on the low-lying area along the Avon-Heathcote Estuary (e.g., South Shore) and near low lying "breaches" in the dunes near the New Brighton pier, and the Waimairi Beach surf club (North New Brighton) (Figure 3-23). Extremely high flow velocities are predicted in the Estuary mouth (8 m/s) and the Waimakariri River Mouth (7 m/s). High velocities are predicted near the dune breaches (New Brighton Pier, North New Brighton surf club, South Sumner) (3-4 m/s) and near the main bridges where the flow is constricted (Avon River Bridge Street bridge, 3.2 m/s, and Heathcote River Ferry Road bridge, 2.7 m/s) (Figure 3-24).

The high velocities predicted in the model would entrain large quantities of sediment and radically modify the topography and bathymetry from what was used in the model. This could affect later inundation but is not captured in the modelling.

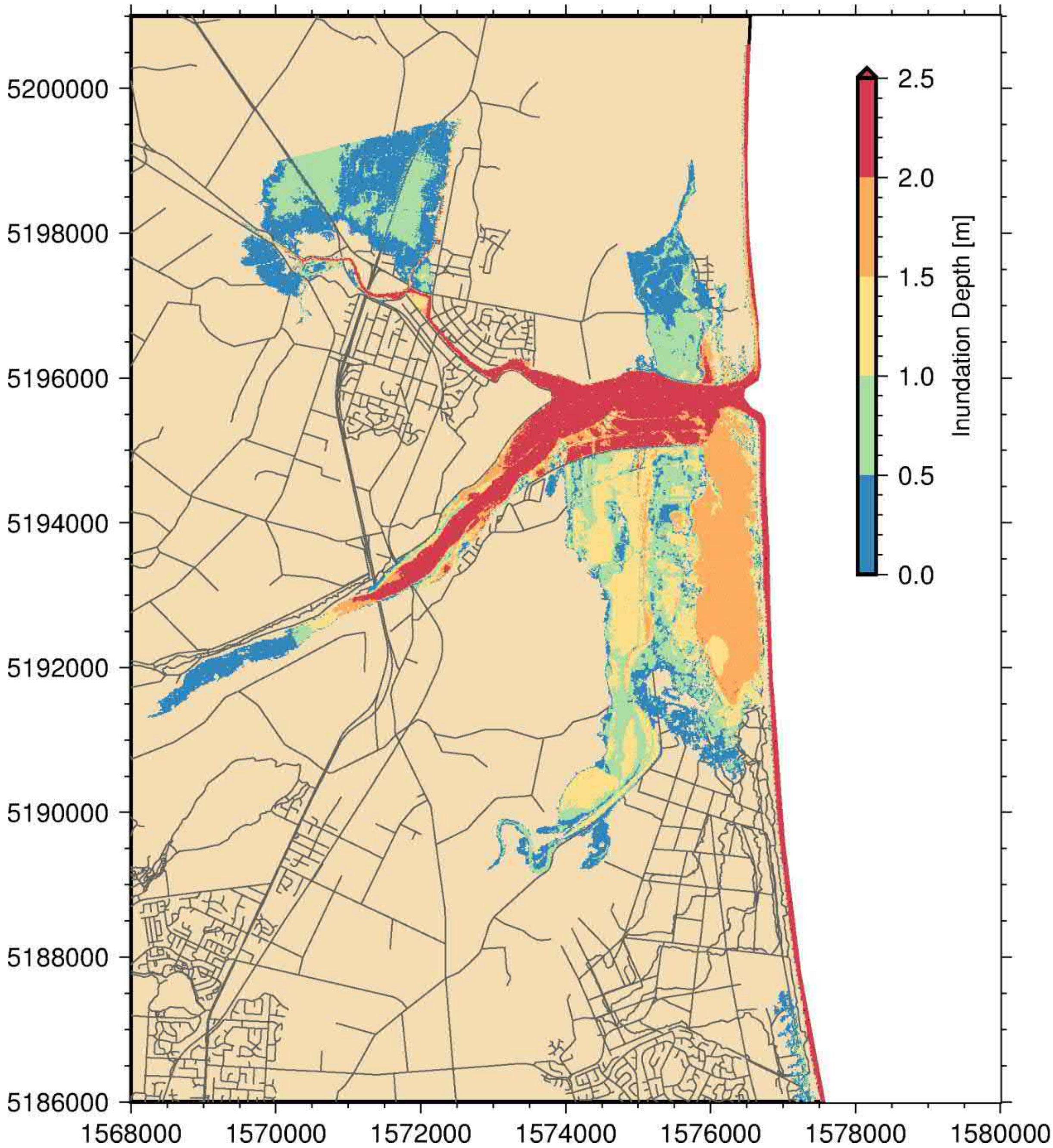

Figure 3-21: Maximum inundation depth (i.e., height above ground) for 1:500-year return period event Current Sea Level - Northern Section. Note that for the river channels the value given is the height above the pre-tsunami water level.

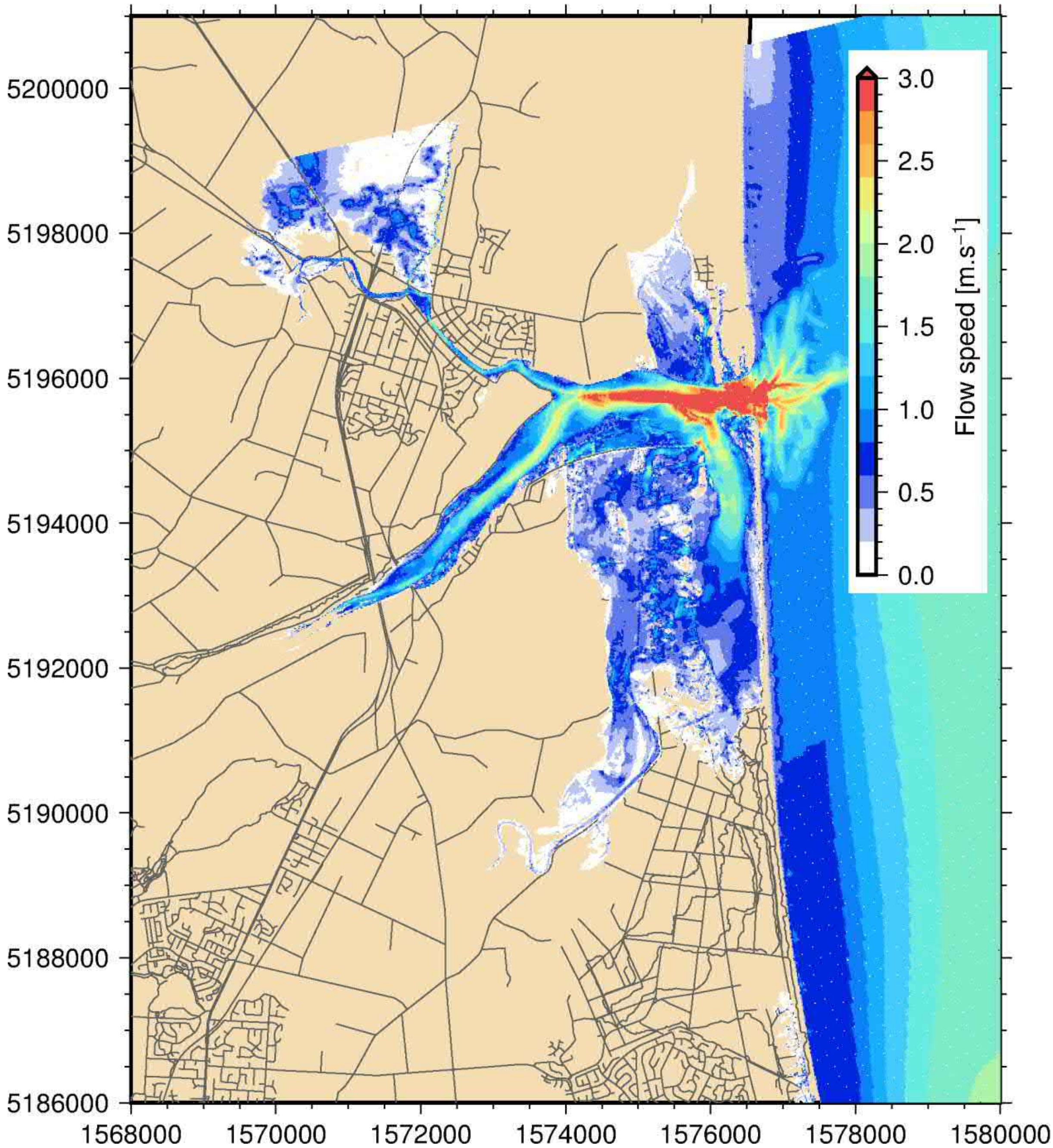

Figure 3-22: Maximum flow velocity for 1:500-year return period event Current Sea Level - Northern Section.

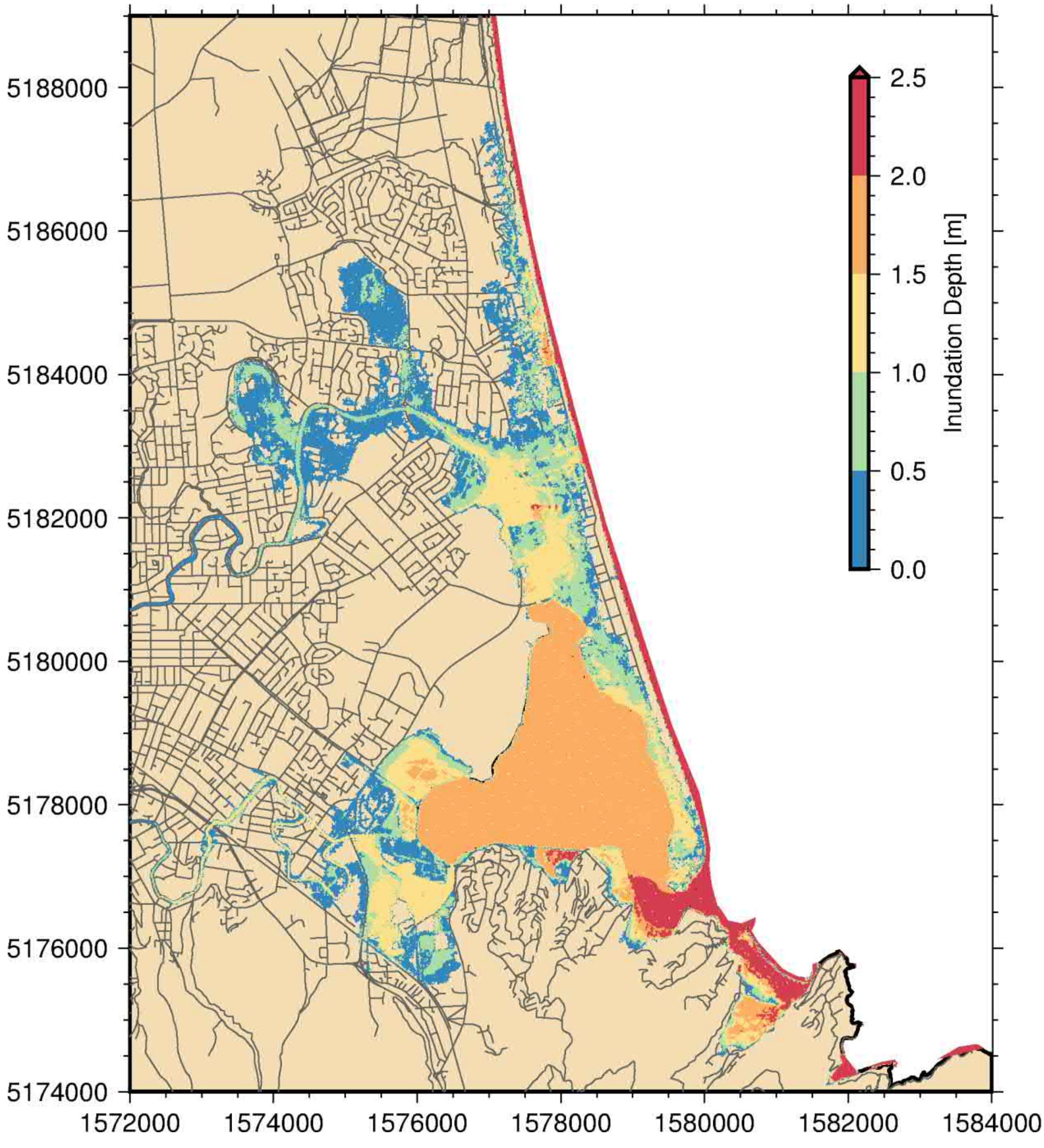

Figure 3-23: Maximum inundation depth (i.e., height above ground) for 1:500-year return period event Current Sea Level - Southern Section. Note that for the river channels the value given is the height above the pre-tsunami water level.

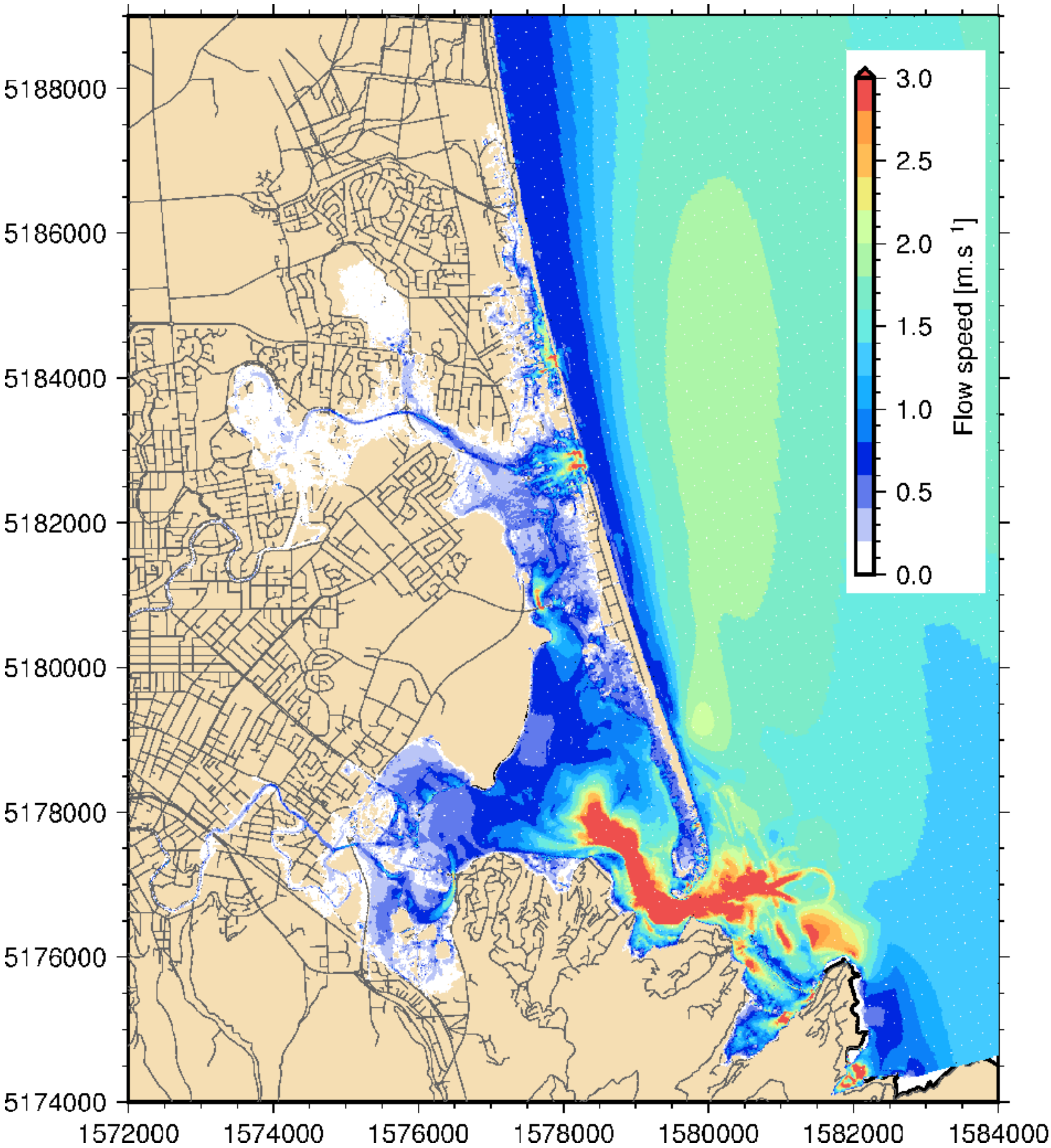

Figure 3-24: Maximum flow velocity for 1:500-year return period event Current Sea Level - Southern Section.

3.3.2 1:500-year return period - 2040 Sea Level Scenario – 0.19 m Sea Level Rise

For the 1:500-year return period tsunami at 0.19 m above present mean sea-level (2040 scenario), the inundation covers an area of 45 km^2 and reaches a maximum depth of 5.6 m. The inundation naturally extends further than the scenario with present day sea level (Figure 3-25 and Figure 3-27). Flow velocity patterns are similar to the present day sea-level and similar flow speeds are observed at the main bridges (Figure 3-26 and Figure 3-28).

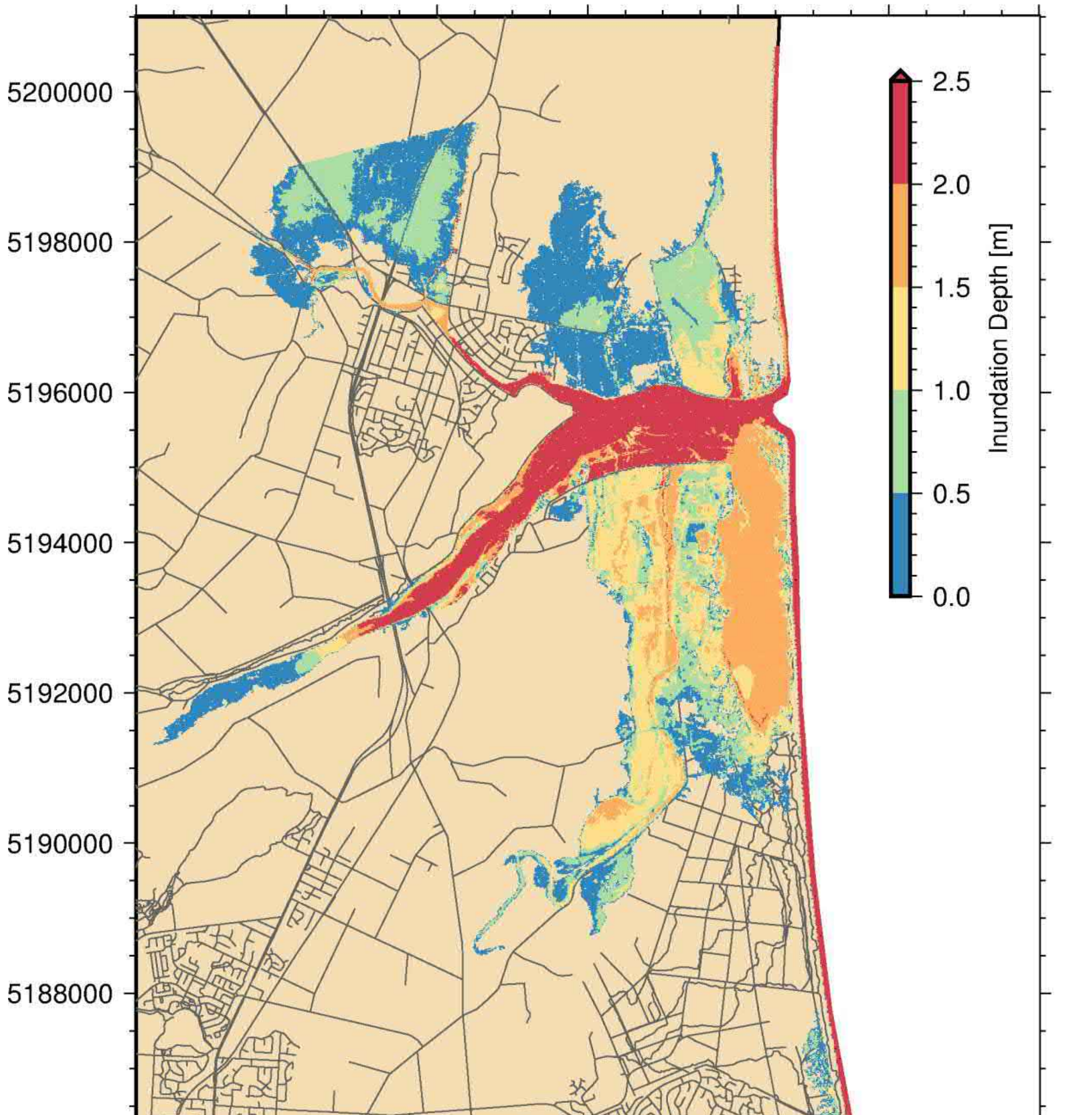

Figure 3-25: Maximum inundation depth (i.e., height above ground) for 1:500-year return period event 2040 Sea Level Scenario – 0.19 m Sea Level Rise - Northern Section. Note that for the river channels the value given is the height above the pre-tsunami water level.

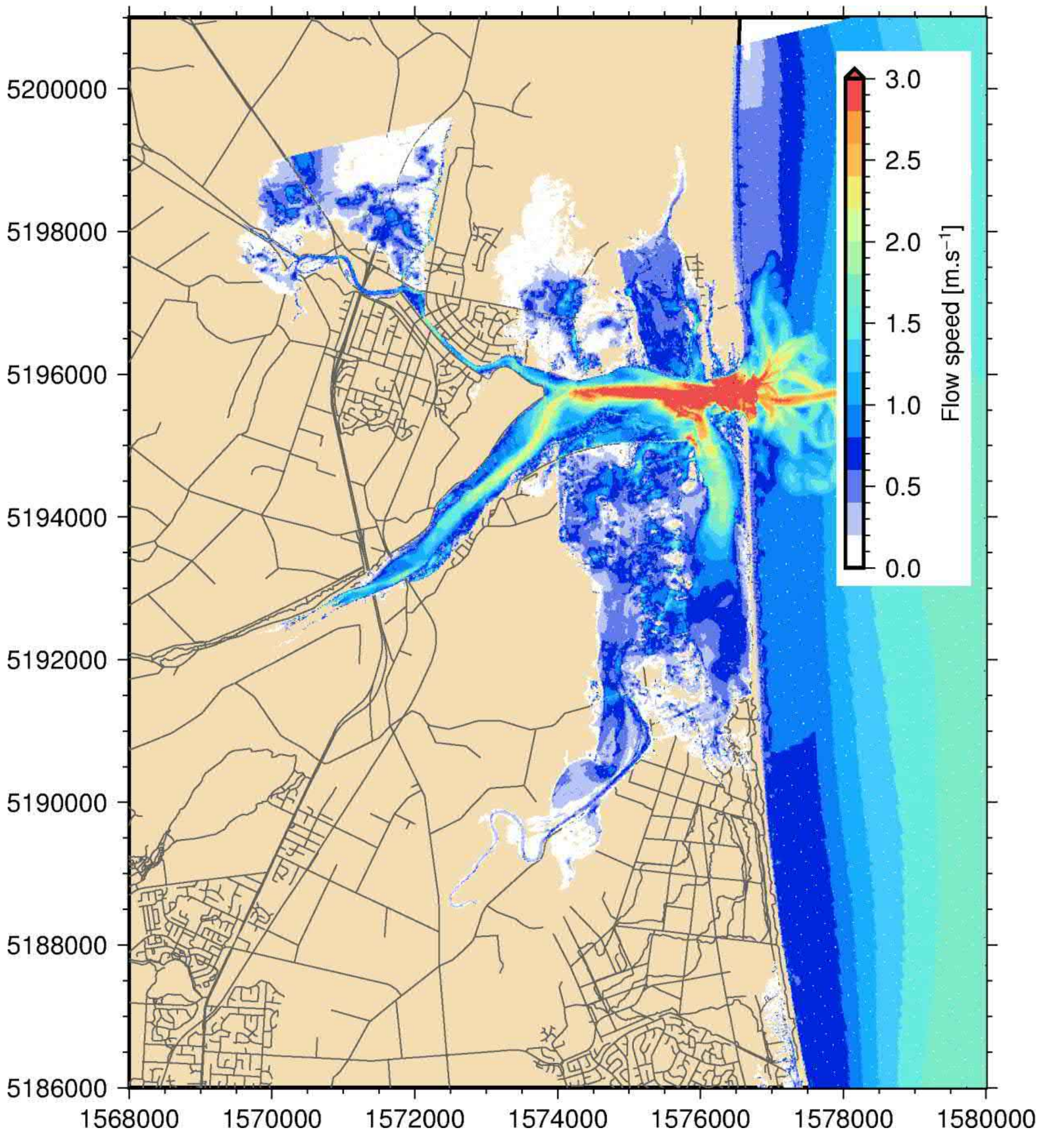

Figure 3-26: Maximum flow velocity for 1:500-year return period event 2040 Sea Level Scenario – 0.19 m Sea Level Rise - Northern Section.

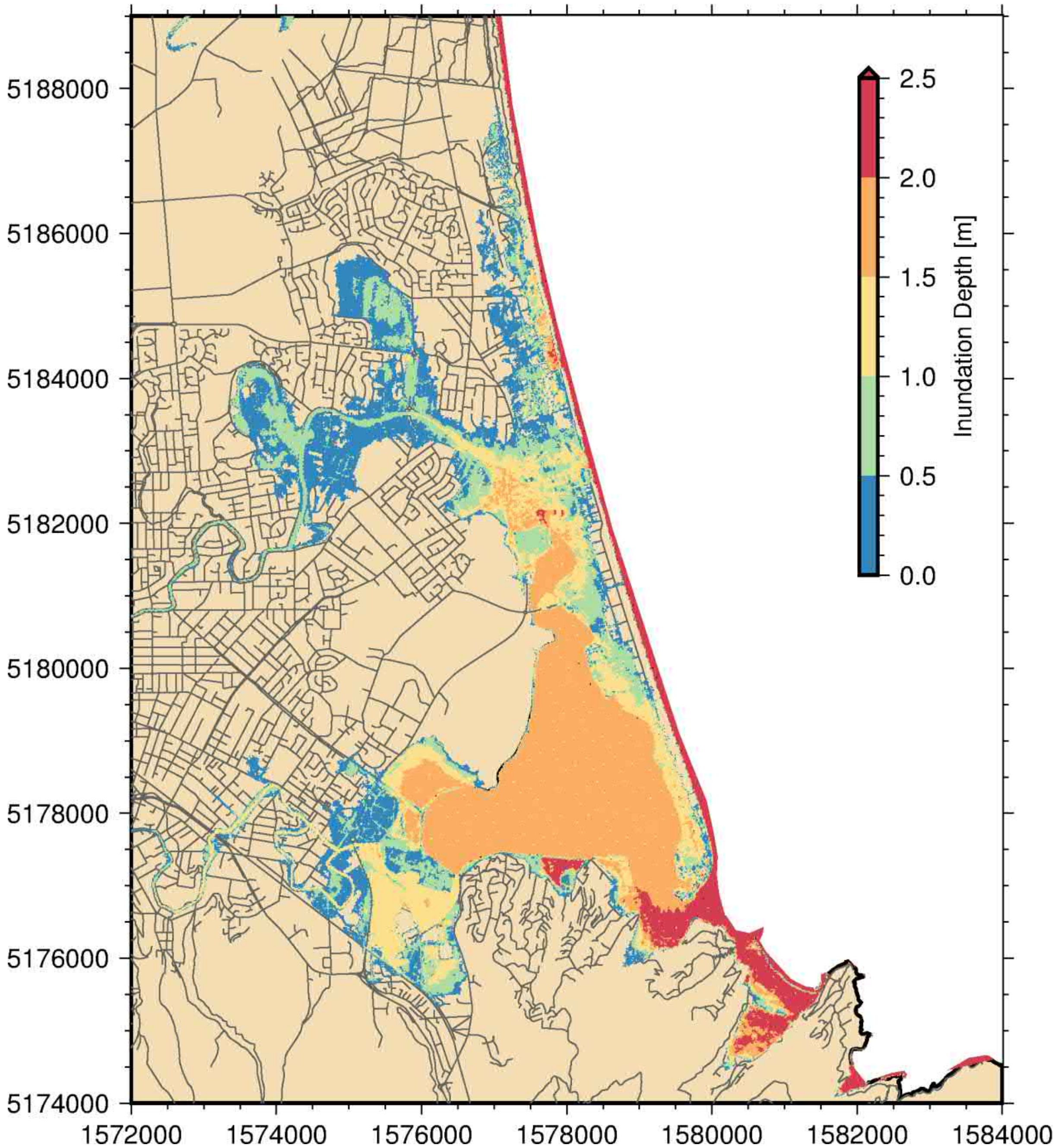

Figure 3-27: Maximum inundation depth (i.e., height above ground) for 1:500-year return period event 2040 Sea Level Scenario – 0.19 m Sea Level Rise - Southern Section. Note that for the river channels the value given is the height above the pre-tsunami water level.

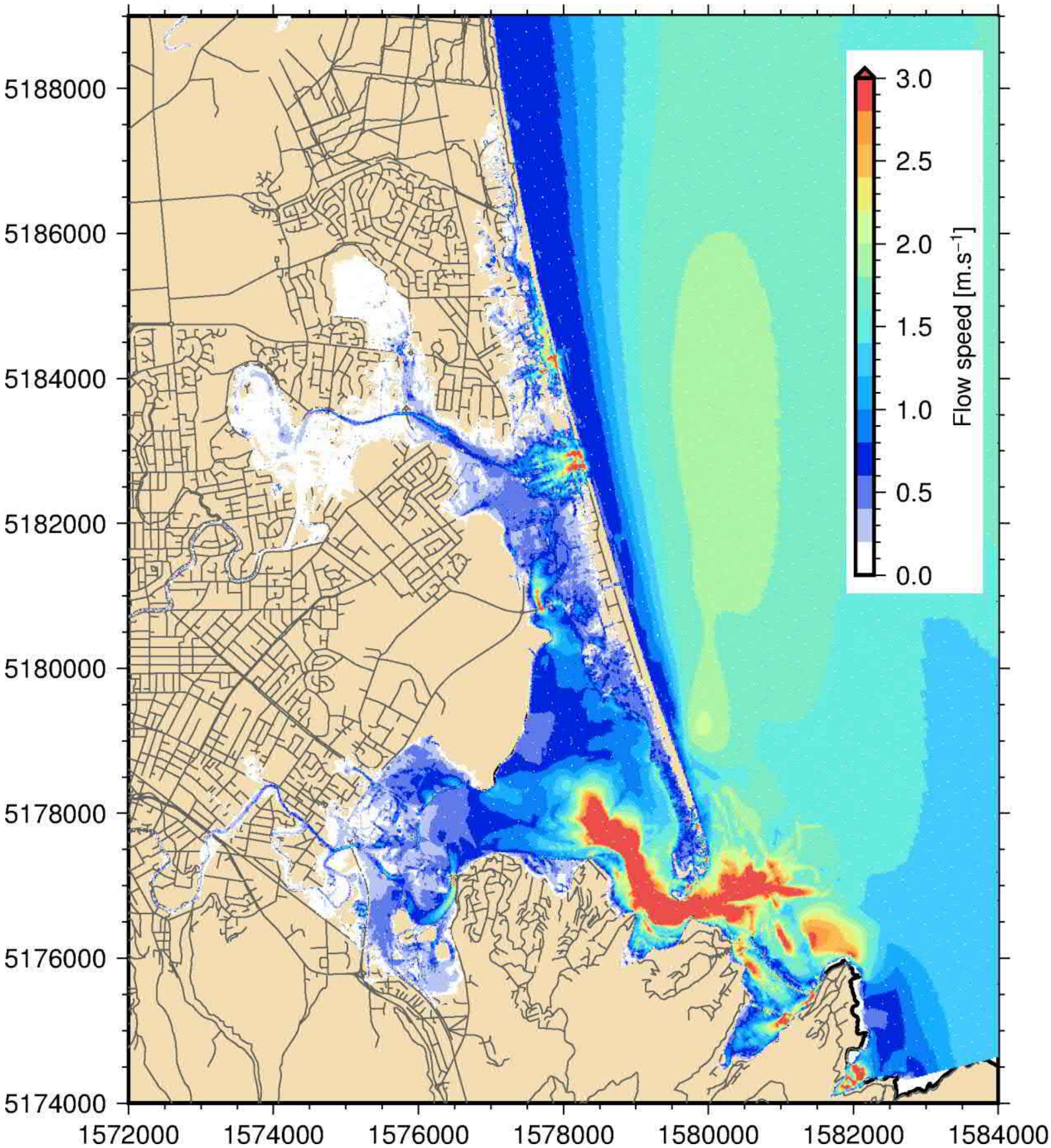

Figure 3-28: Maximum flow velocity for 1:500-year return period event 2040 Sea Level Scenario – 0.19 m Sea Level Rise - Southern Section.

3.3.3 1:500-year return period - 2065 Sea Level Scenario – 0.41 m Sea Level Rise

Inundation extent for the 1:500-year return period tsunami at 0.41 m sea-level rise (Figure 3-29 and Figure 3-31) covers an area of 47 km^2 and reaches a maximum depth of 5.1 m. Overall the flow patterns are similar (Figure 3-30 and Figure 3-32), however, more water can overtop the dunes near the New Brighton Pier than in the scenarios presented above and in the dune "breach" the flow speed exceed 4 m/s.

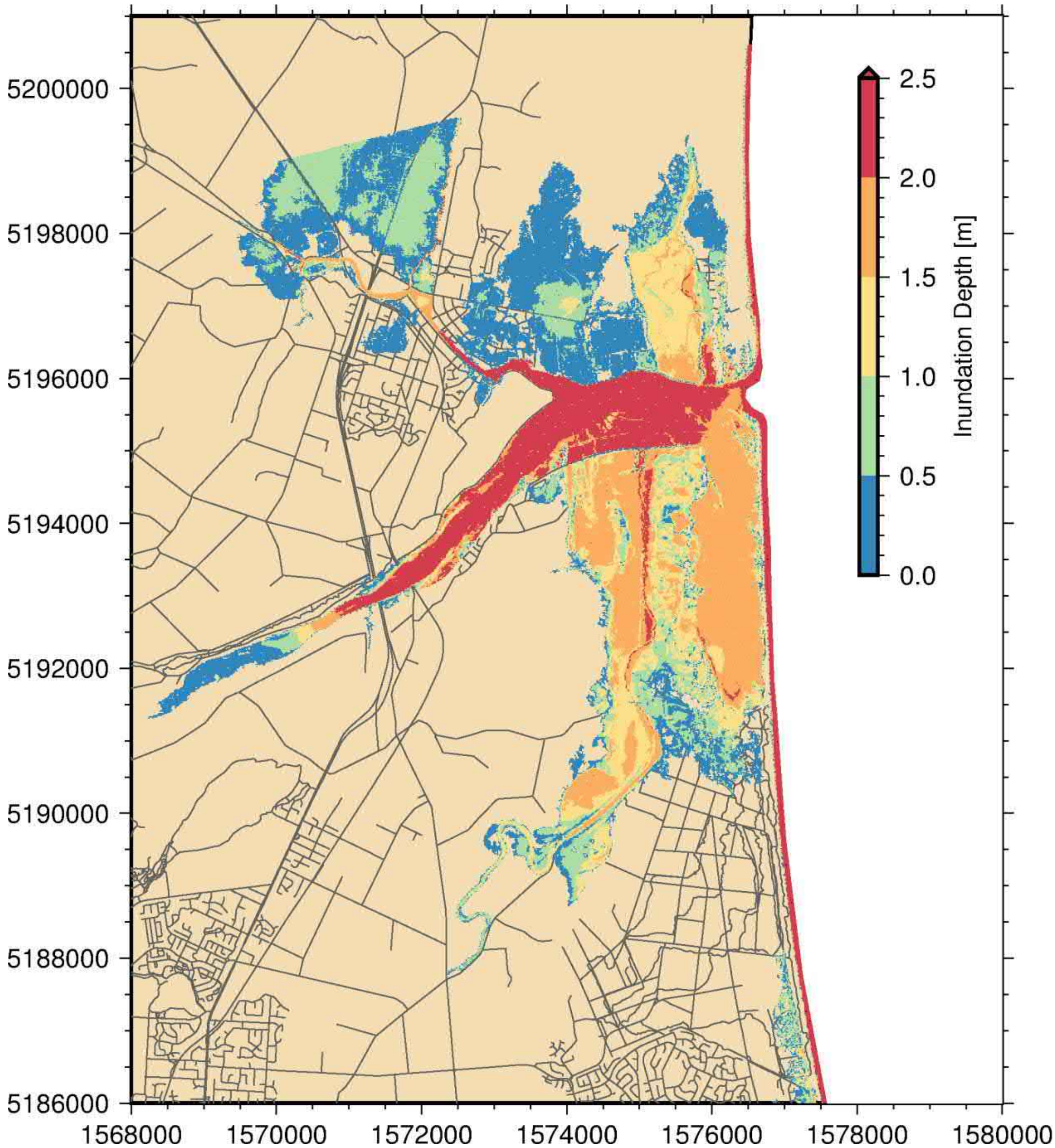

Figure 3-29: Maximum inundation depth (i.e., height above ground) for 1:500-year return period 2065 Sea Level Scenario – 0.41 m Sea Level Rise - Northern Section. Note that for the river channels the value given is the height above the pre-tsunami water level.

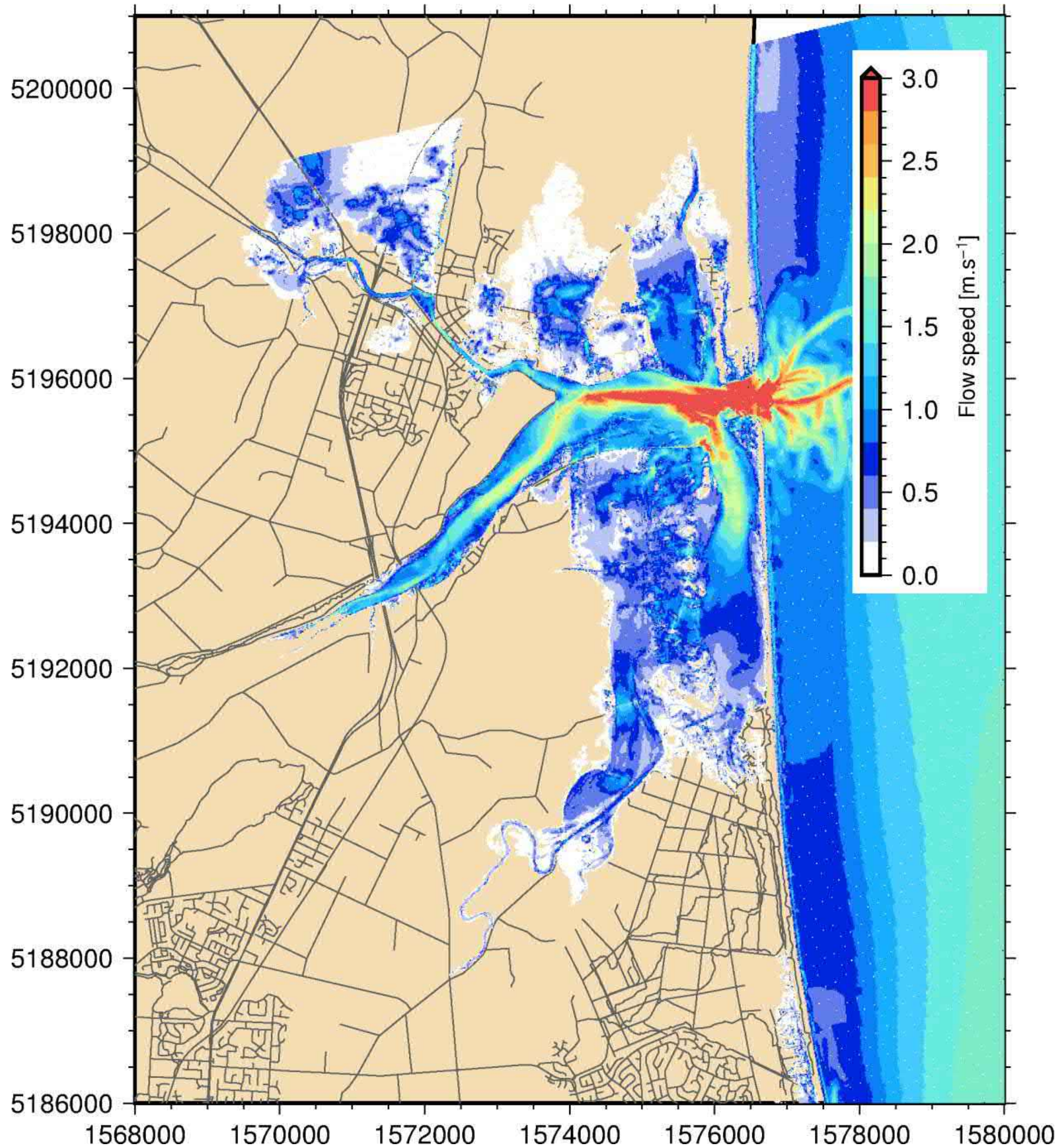

Figure 3-30: Maximum flow velocity for 1:500-year return period event 2065 Sea Level Scenario – 0.41 m Sea Level Rise - Northern Section.

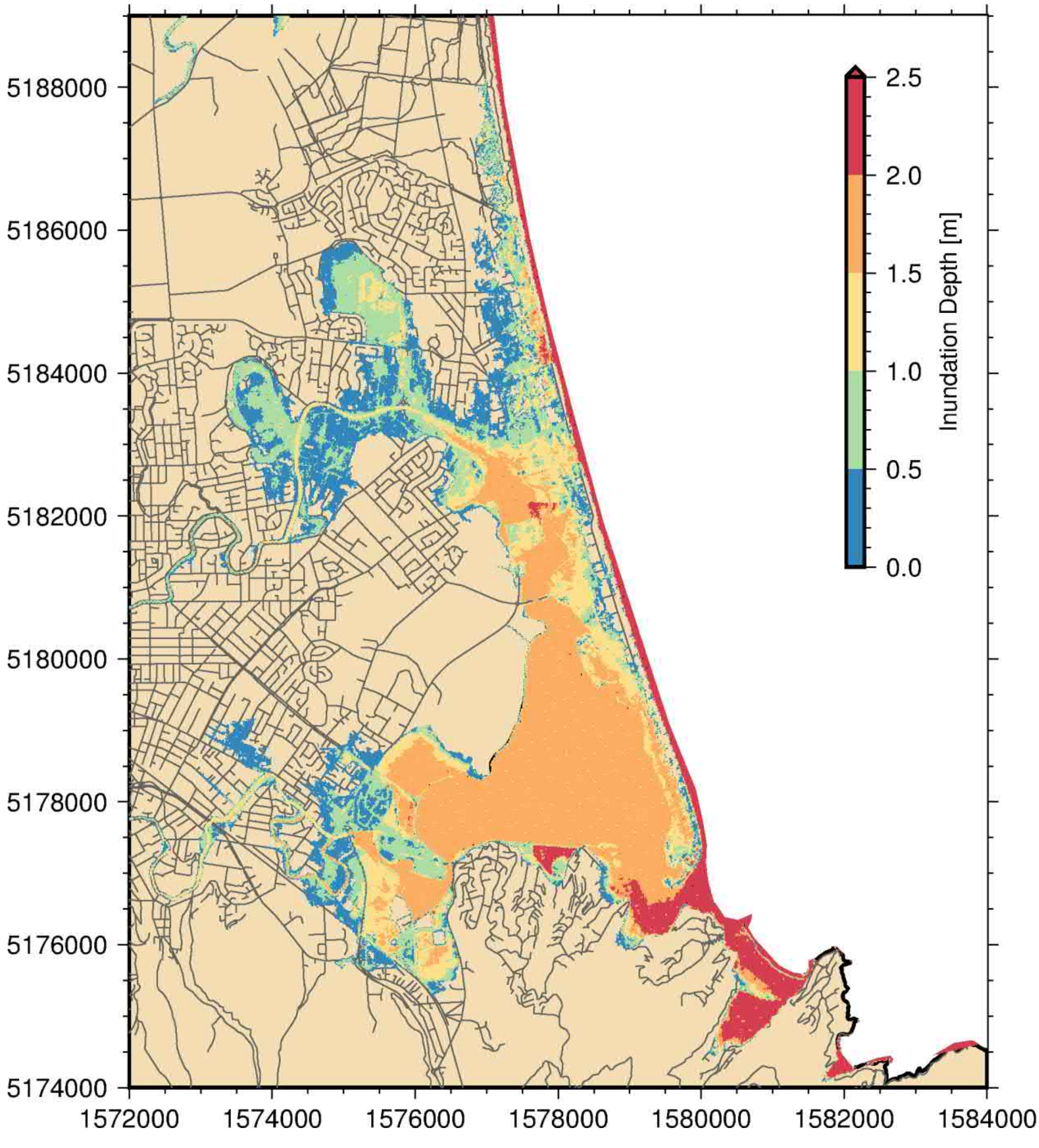

Figure 3-31: Maximum inundation depth (i.e., height above ground) for 1:500-year return period 2065 Sea Level Scenario – 0.41 m Sea Level Rise - Southern Section. Note that for the river channels the value given is the height above the pre-tsunami water level.

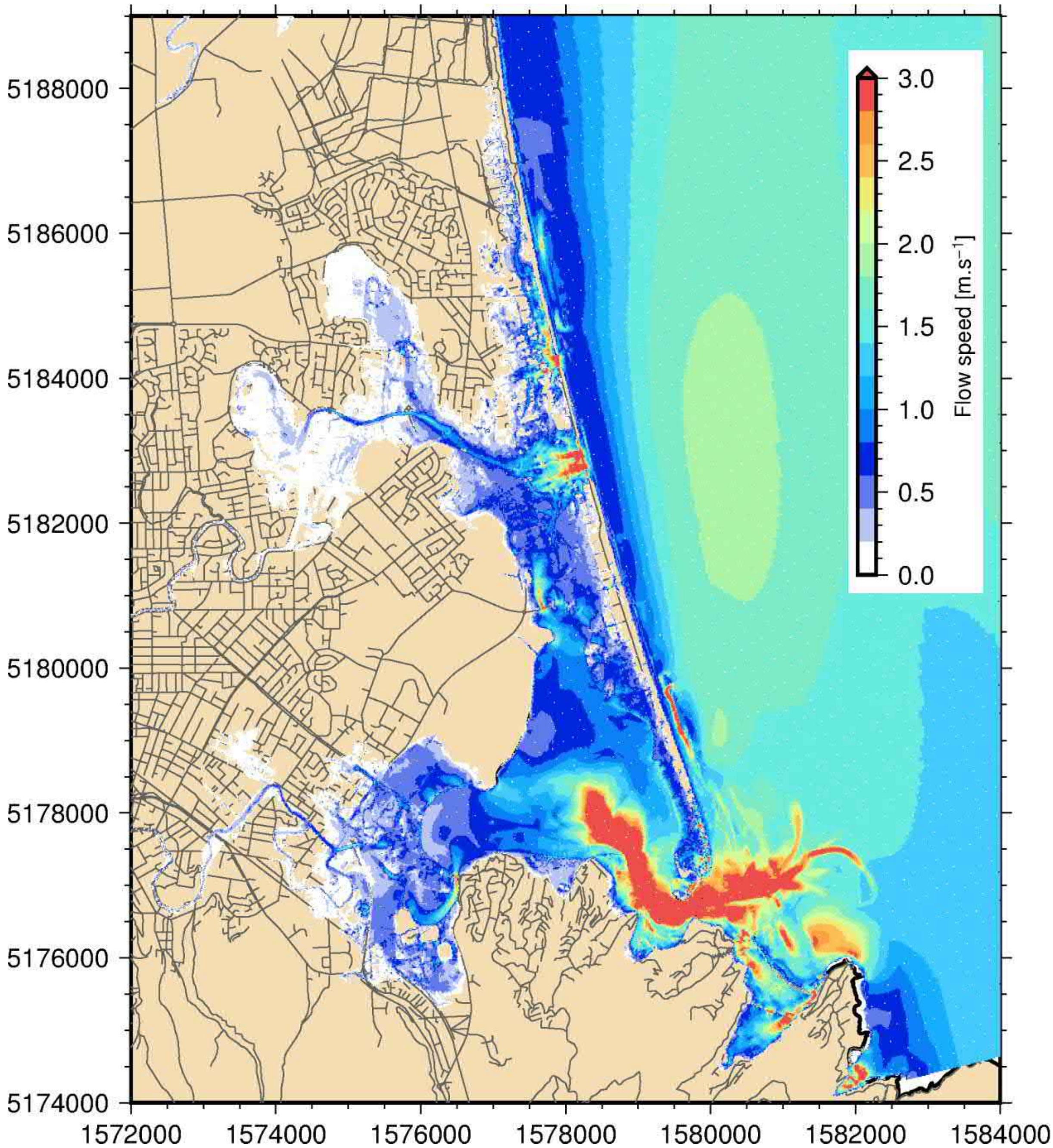

Figure 3-32: Maximum flow velocity for 1:500-year return period event 2065 Sea Level Scenario – 0.41 m Sea Level Rise - Southern Section.

3.3.4 1:500-year return period - 2120 Sea Level Scenario – 1.06 m Sea Level Rise

Inundation extent for the 1:500-year return period tsunami at 1.06 m sea-level rise covers an area of 70 km^2 and reaches a maximum depth of 5.8 m (Figure 3-33 and Figure 3-35). The dunes on the coastal strip are overtopped at numerous locations causing nearly continuous inundation of the dune backshore. Flow velocity does not increase at the main bridges but increases in the flooded area (e.g., South New Brighton, over the Sumner sea-wall) (Figure 3-34 and Figure 3-36). This overtopping would likely erode the dunes and could cause increased inundation, but this is not captured in this model.

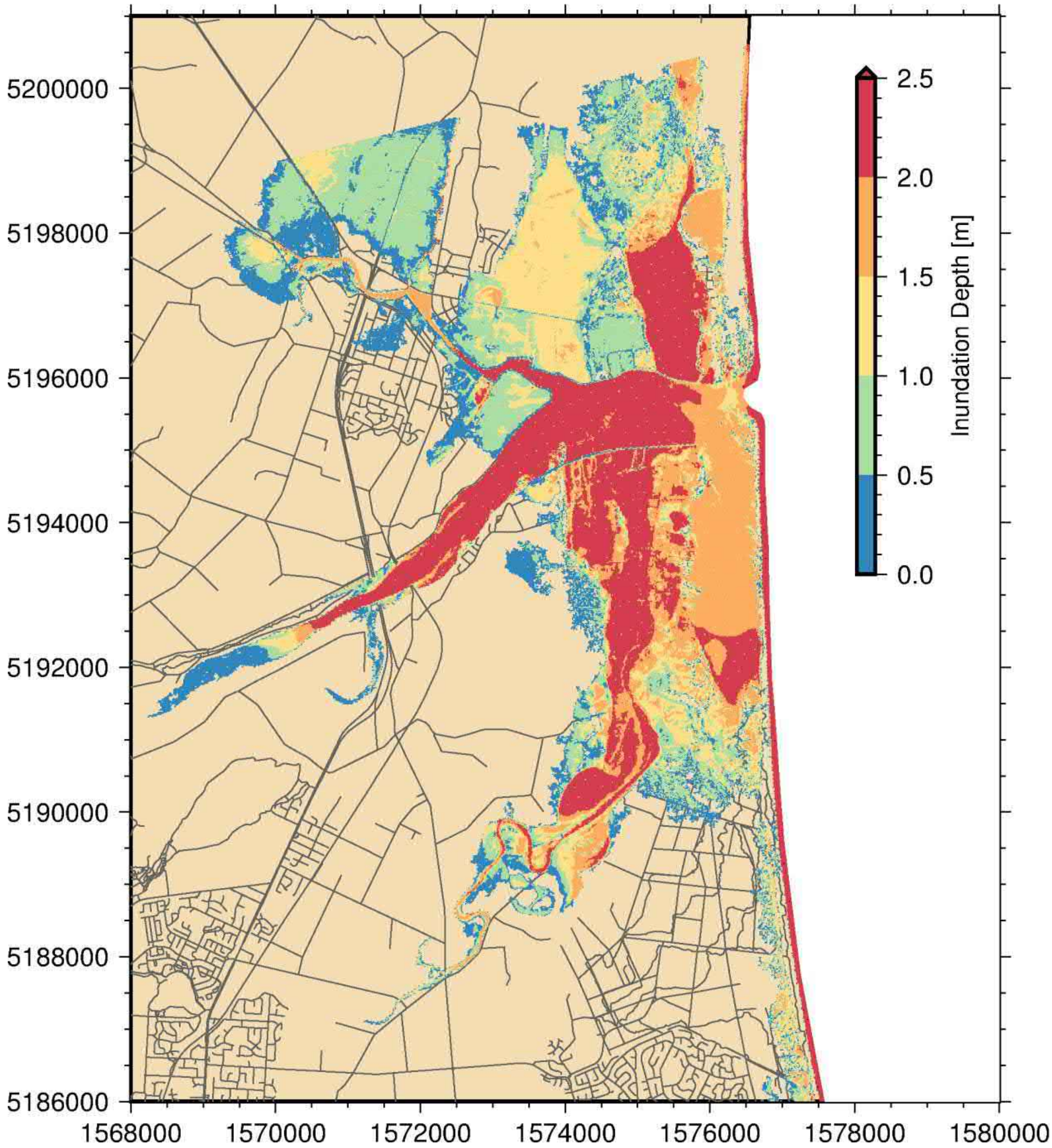

Figure 3-33: Maximum inundation depth (i.e., height above ground) for 1:500-year return period event 2120 Sea Level Scenario – 1.06 m Sea Level Rise - Northern Section. Note that for the river channels the value given is the height above the pre-tsunami water level.

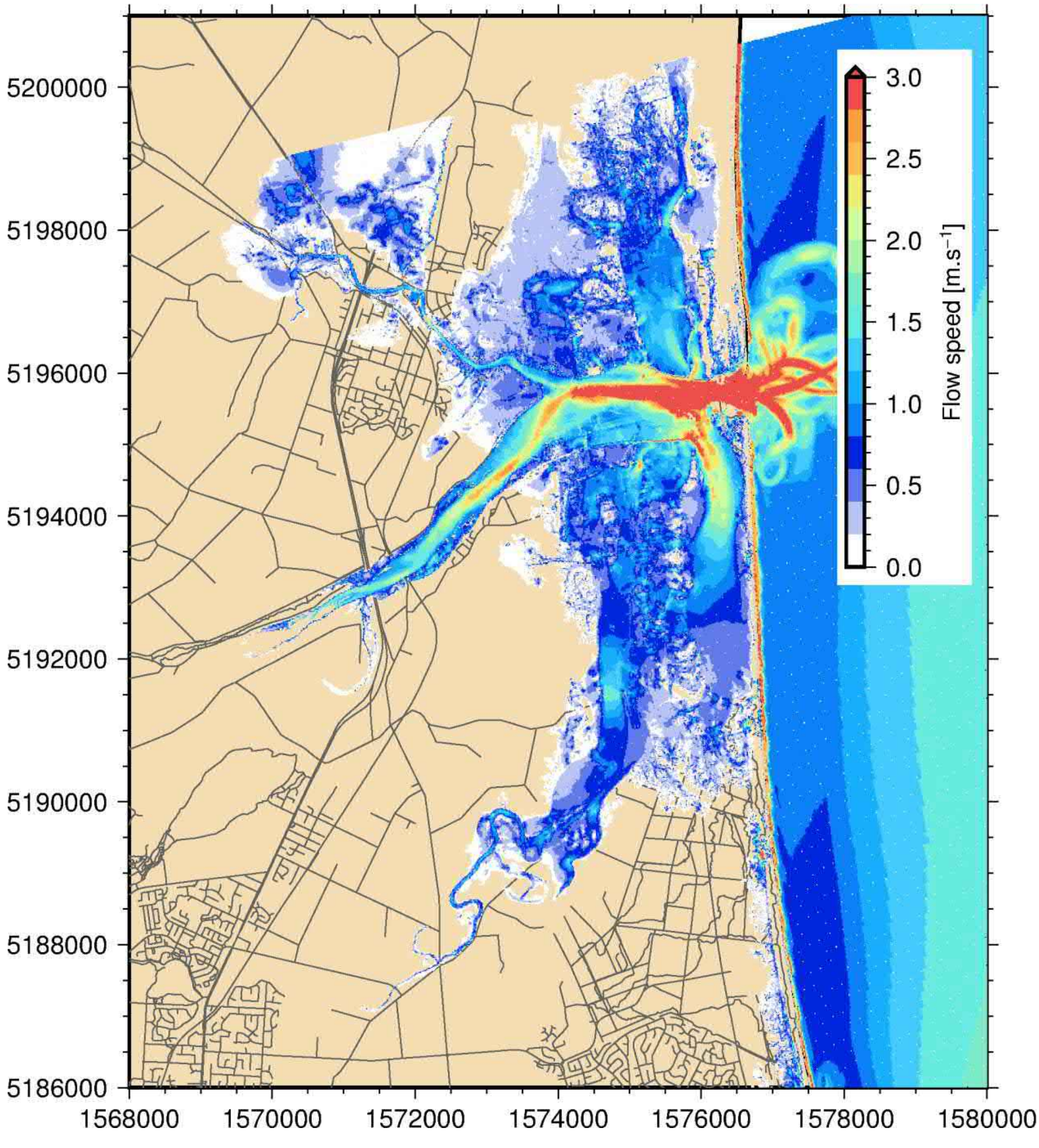

Figure 3-34: Maximum flow velocity for 1:500-year return period event 2120 Sea Level Scenario – 1.06 m Sea Level Rise - Northern Section.

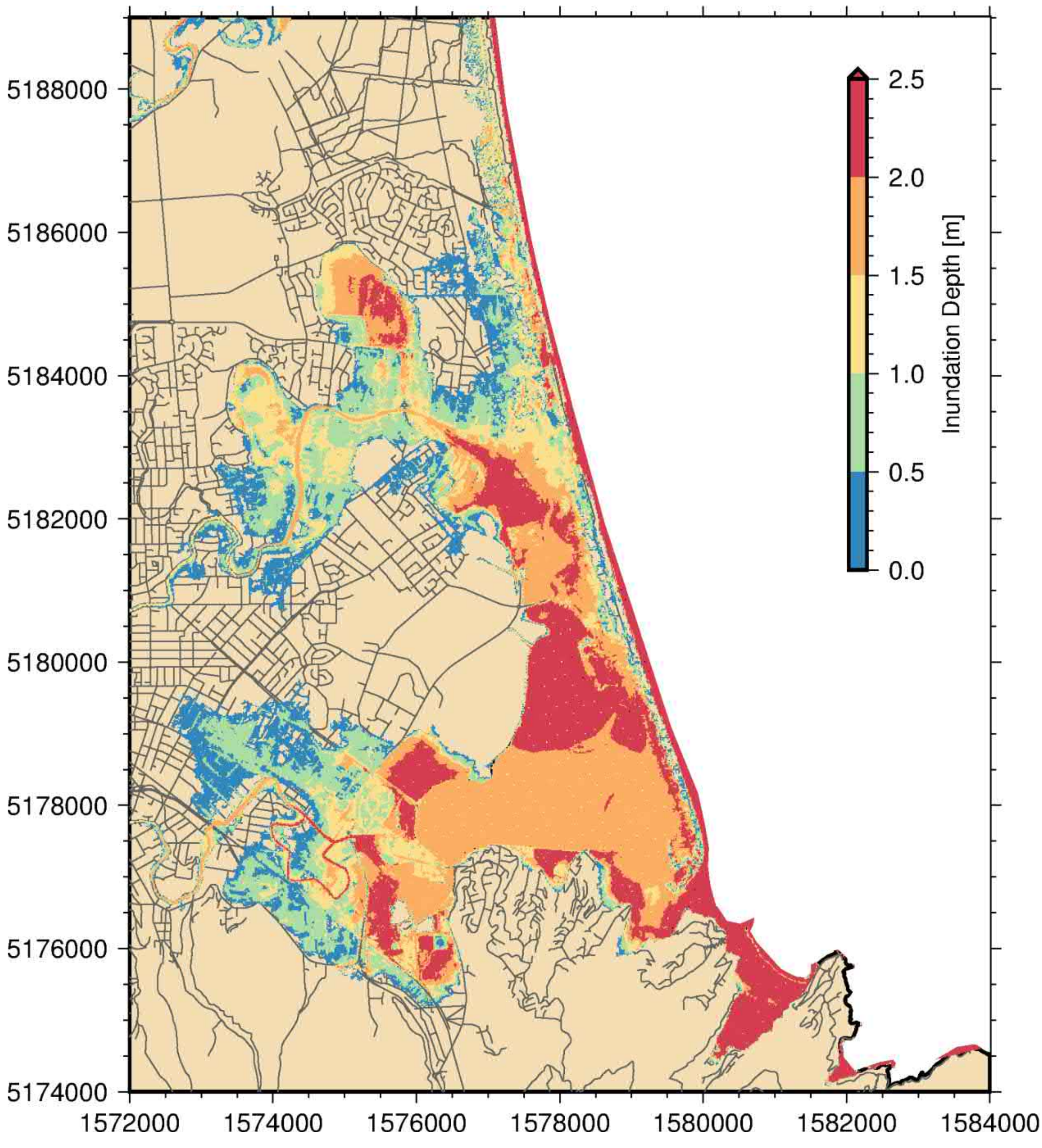

Figure 3-35: Maximum inundation depth (i.e., height above ground) for 1:500-year return period event 2120 Sea Level Scenario – 1.06 m Sea Level Rise - Southern Section. Note that for the river channels the value given is the height above the pre-tsunami water level.

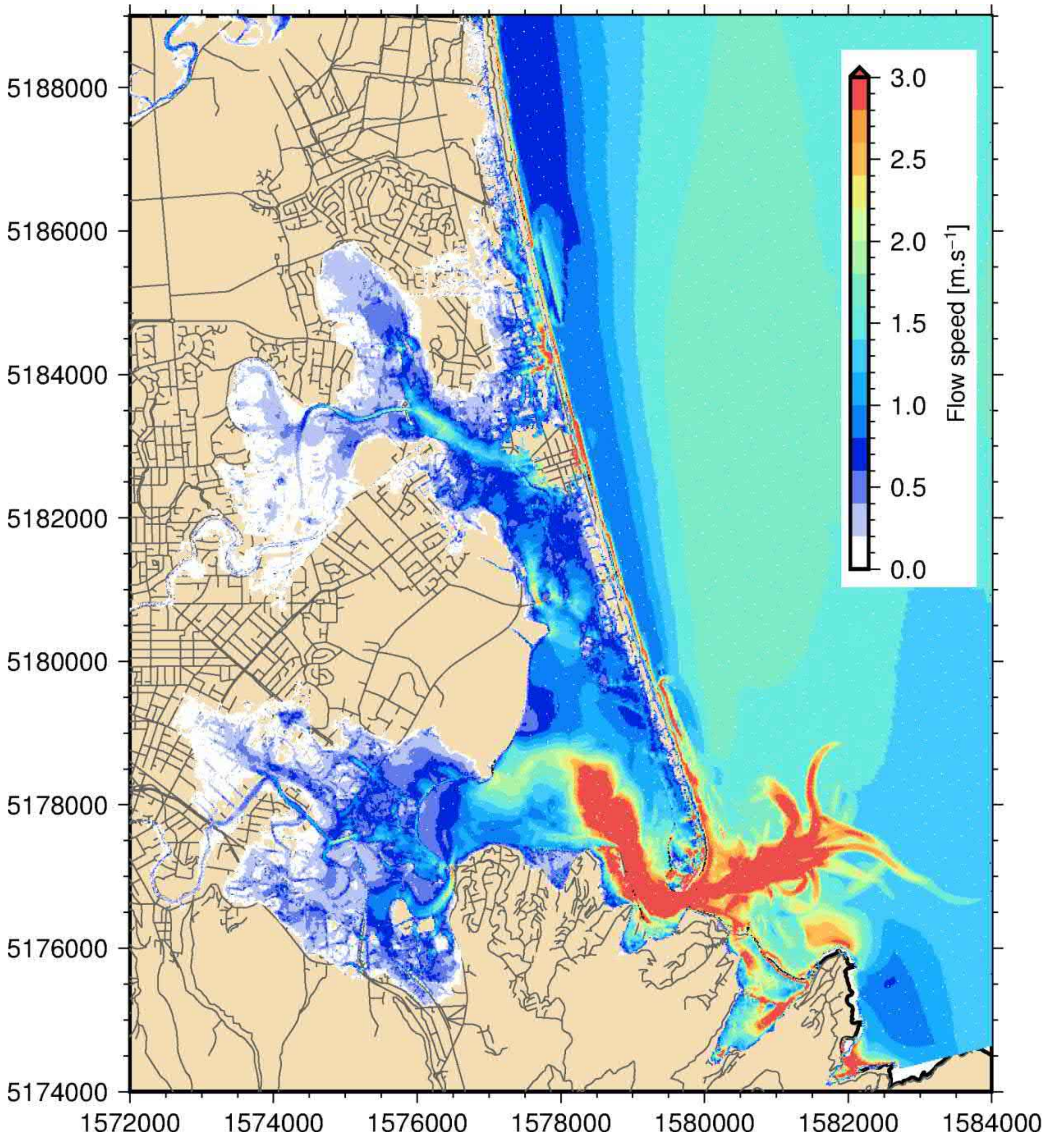

Figure 3-36: Maximum flow velocity for 1:500-year return period event 2120 Sea Level Scenario – 1.06 m Sea Level Rise - Southern Section.

3.3.5 1:2500-year return period tsunami - Current Sea Level

The inundation extent for the 1:2500-year return period tsunami at current mean sea-level covers an area of 50 km^2 and reaches a maximum depth of 9.5 m near the Waimakariri River mouth. The result of this simulation has previously been reported by Lane et al. (2017) and is not repeated here, however the results are given in Figure 3-37 to Figure 3-40 to allow comparison with simulations at higher sea levels.

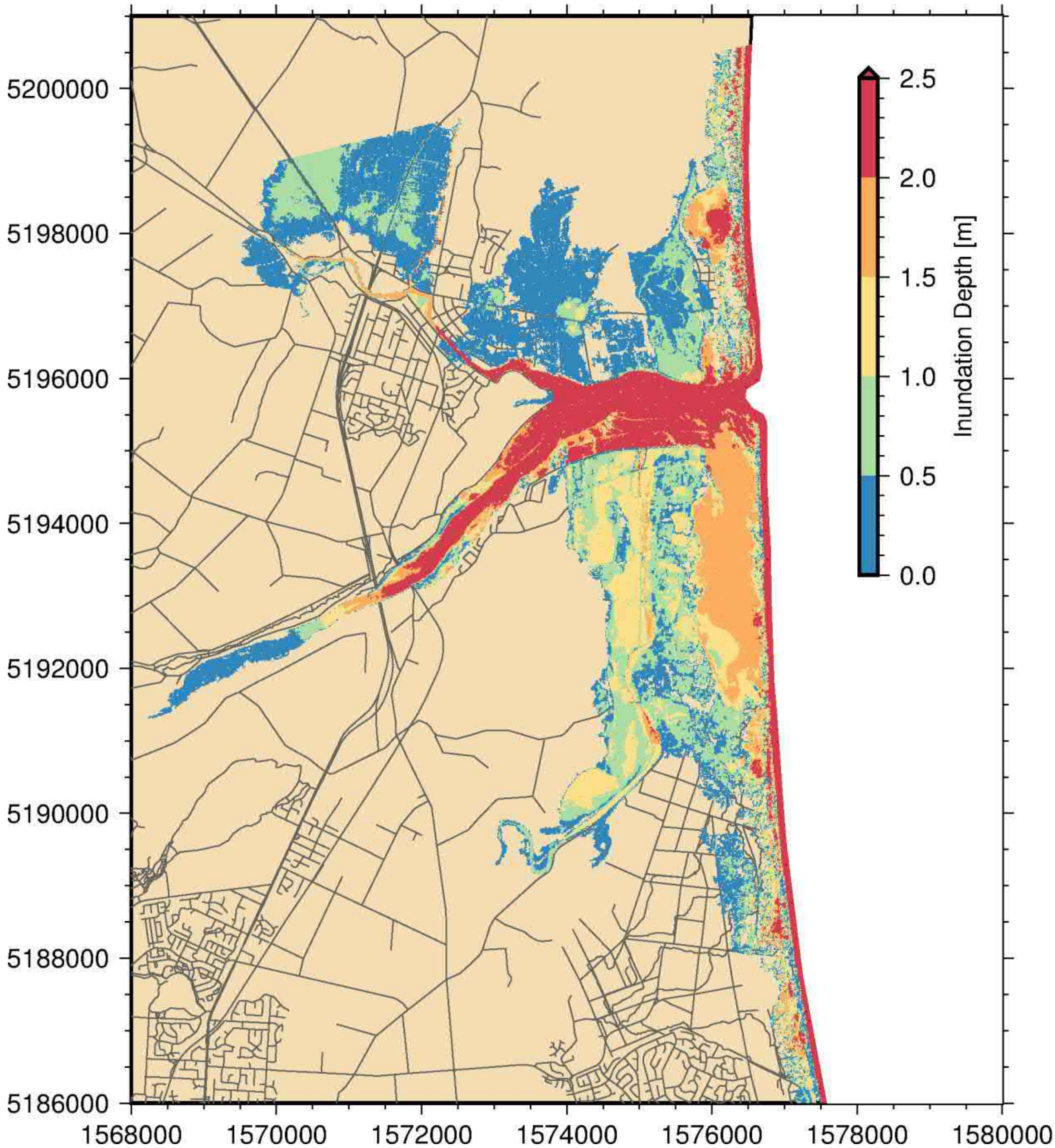

Figure 3-37: Maximum inundation depth (i.e., height above ground) for 1:2500-year return period event Current Sea Level - Northern Section. Note that for the river channels the value given is the height above the pre-tsunami water level.

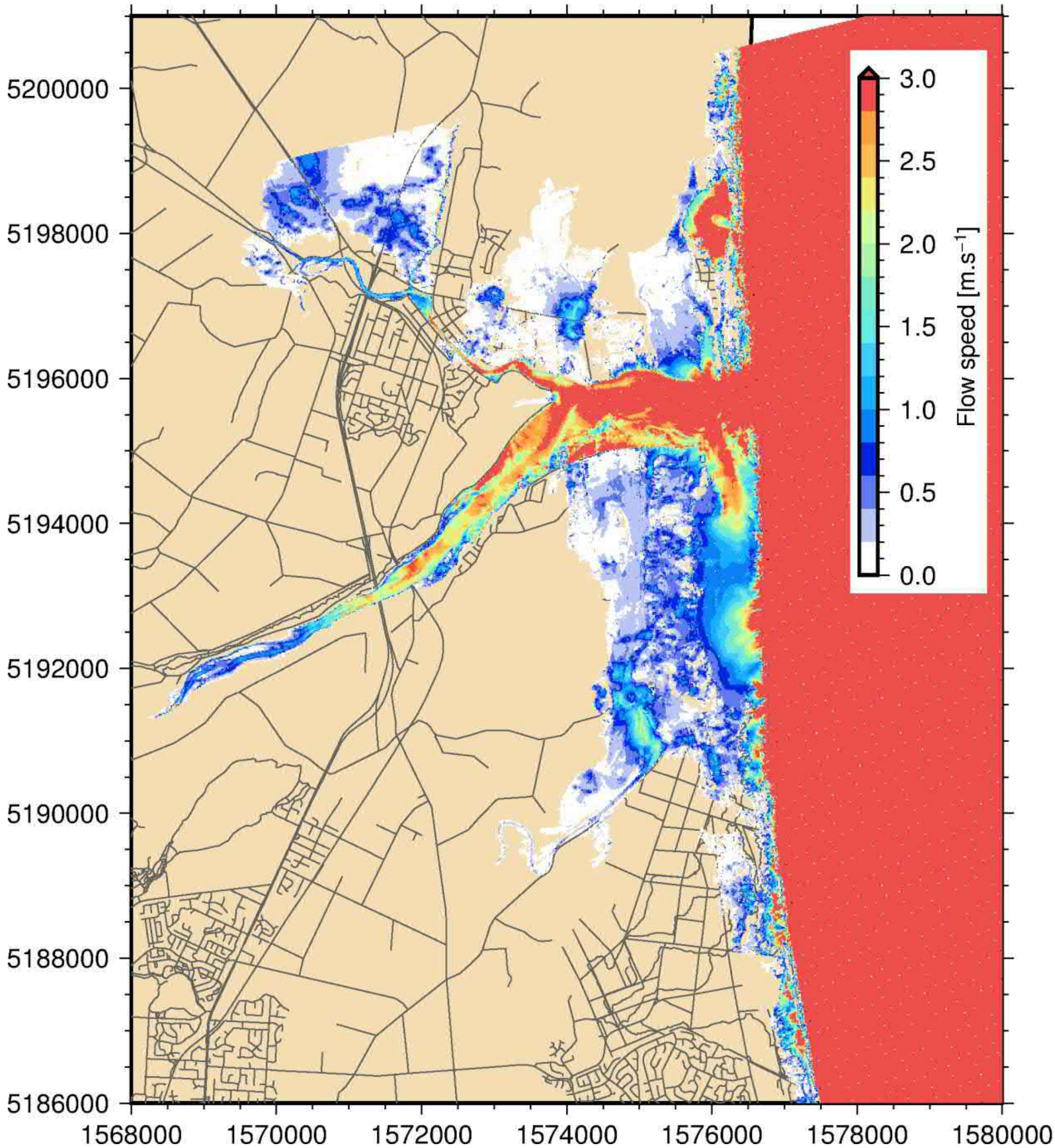

Figure 3-38: Maximum flow velocity for 1:2500-year return period event Current Sea Level - Northern Section.

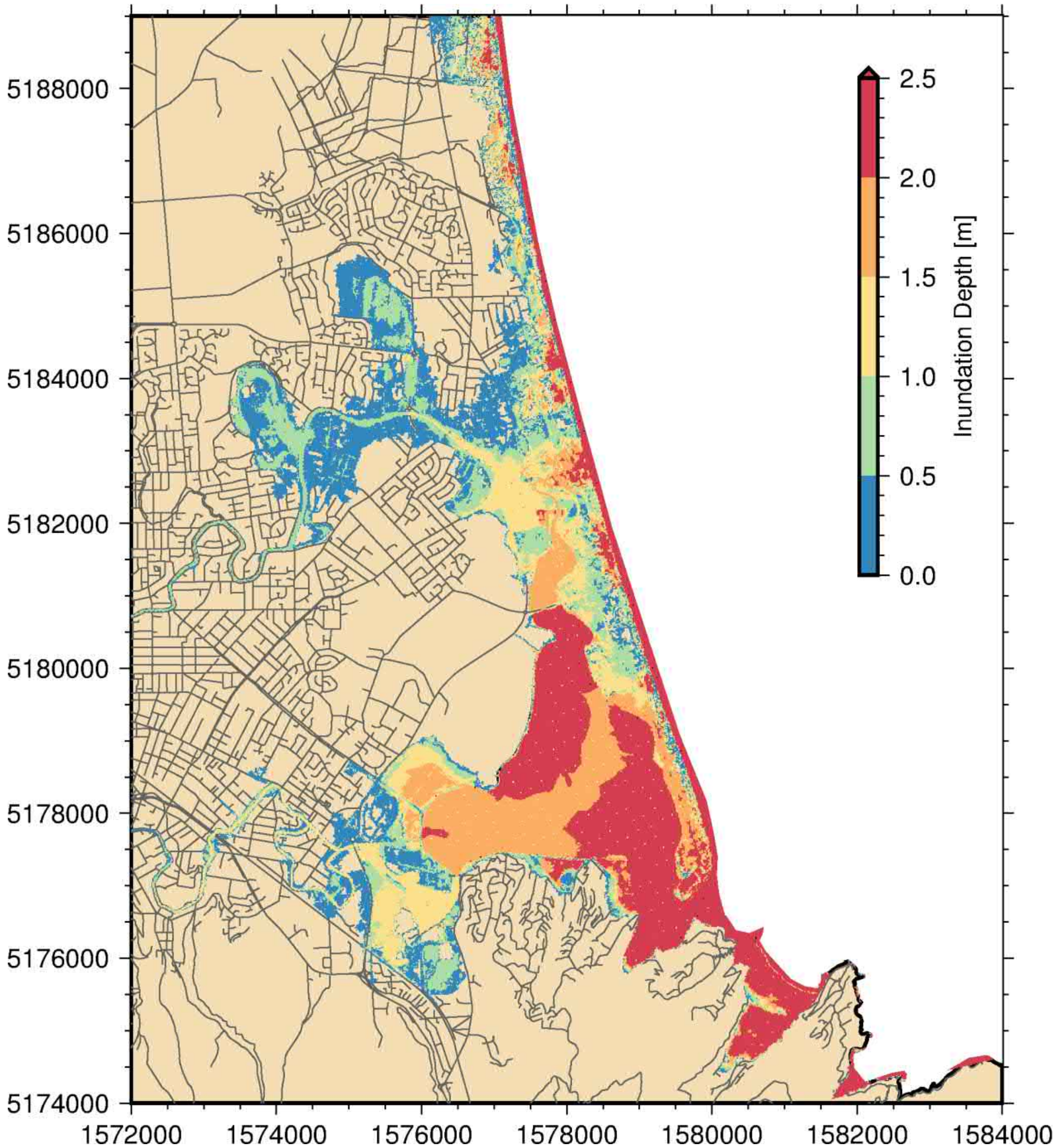

Figure 3-39: Maximum inundation depth (i.e., height above ground) for 1:2500-year return period event Current Sea Level - Southern Section. Note that for the river channels the value given is the height above the pre-tsunami water level.

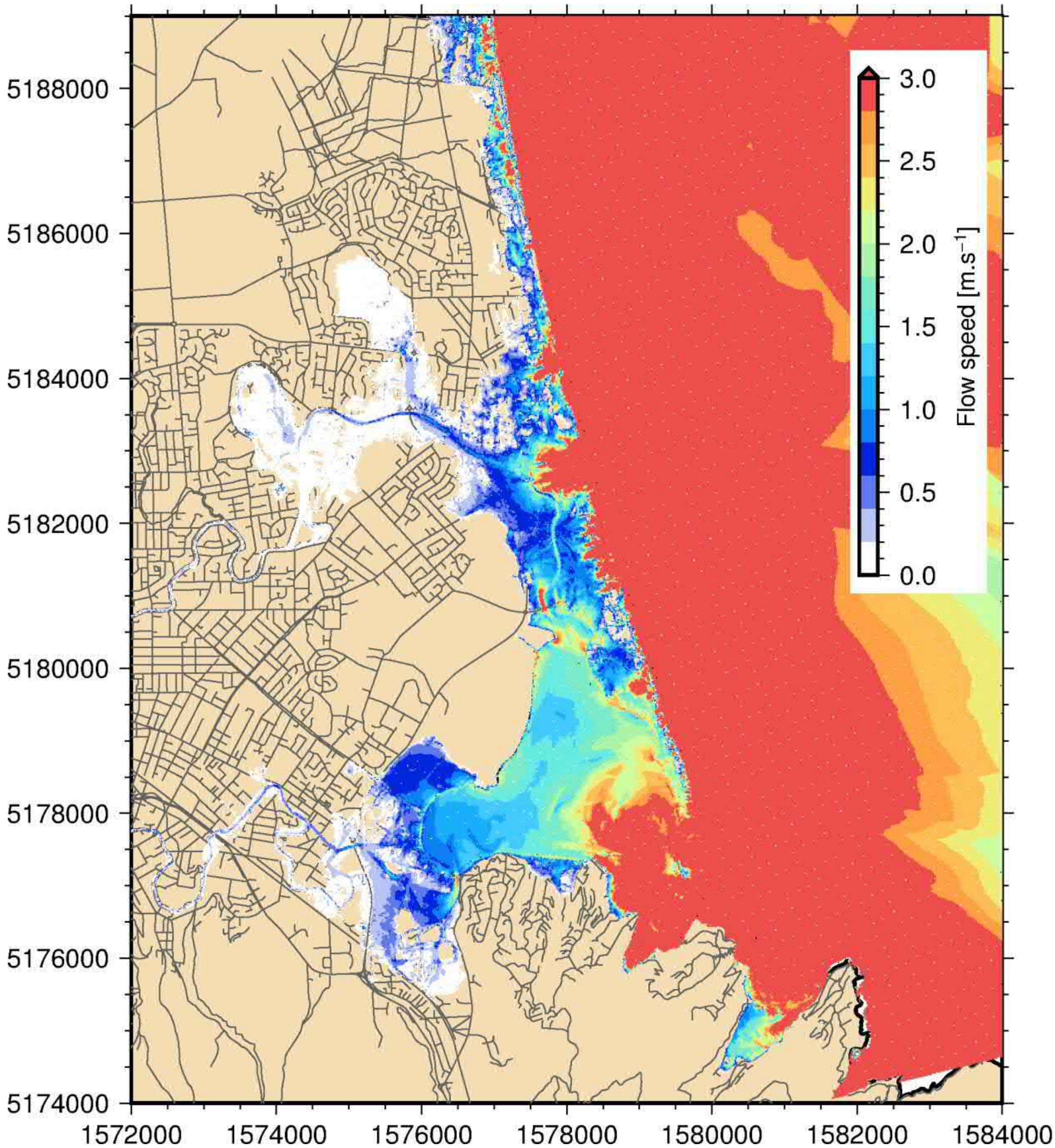

Figure 3-40: Maximum flow velocity for 1:2500-year return period event Current Sea Level - Southern Section.

3.3.6 1:2500-year return period - 2040 Sea Level Scenario – 0.19 m Sea Level Rise

Inundation extent for the 1:2500-year return period tsunami at 0.19 m sea-level rise covers an area of 55 km^2 and reaches a maximum depth of 8.4 m near the Waimakariri River mouth. It is unclear why this maximum value is lower than on the previous scenario but is likely due to the fact that the front of the first tsunami wave travels slightly faster than in scenarios with a lower water level which affect the shoaling of the tsunami waves. The inundation extent is comparable to the 1:500-year return period at 0.19 m sea-level but with higher inundation depth especially in the coastal strip. In this scenario the dunes along coastal strip are consistently overtopped by the tsunami waves leading to major inundation on the low-lying area of the backshore (Figure 3-41 and Figure 3-43). This overtopping would likely erode the dunes and could cause increased inundation, but this is not captured in this model. The simulated flow velocity over the dunes is also much faster than in the 1:500-year return period scenario exceeding 10 m/s at the Avon-Heathcote Estuary mouth and over the dunes in New Brighton (Figure 3-42 and Figure 3-44).

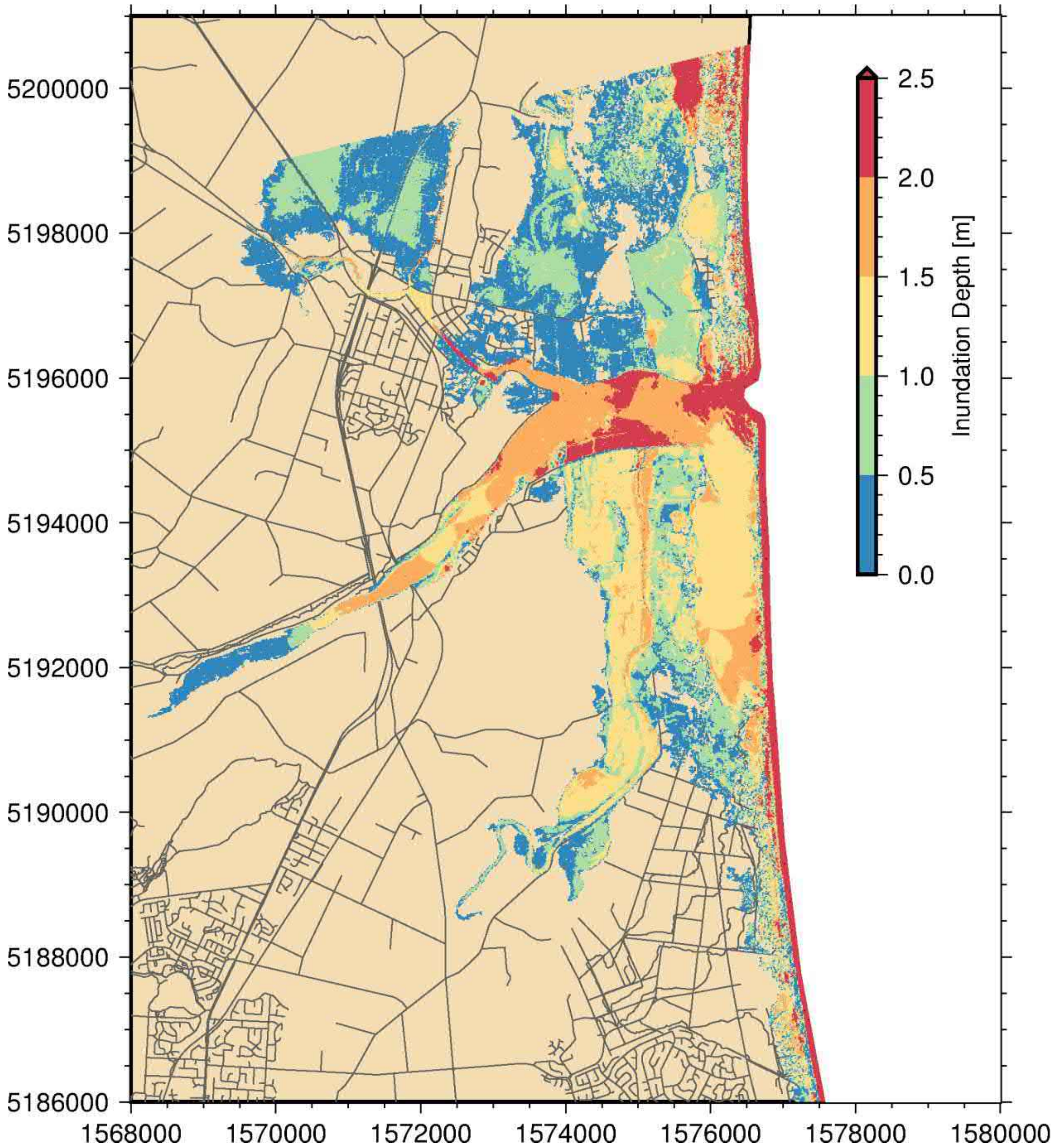

Figure 3-41: Maximum inundation depth (i.e., height above ground) for 1:2500-year return period - 2040 Sea Level Scenario – 0.19 m Sea Level Rise - Northern Section. Note that for the river channels the value given is the height above the pre-tsunami water level.

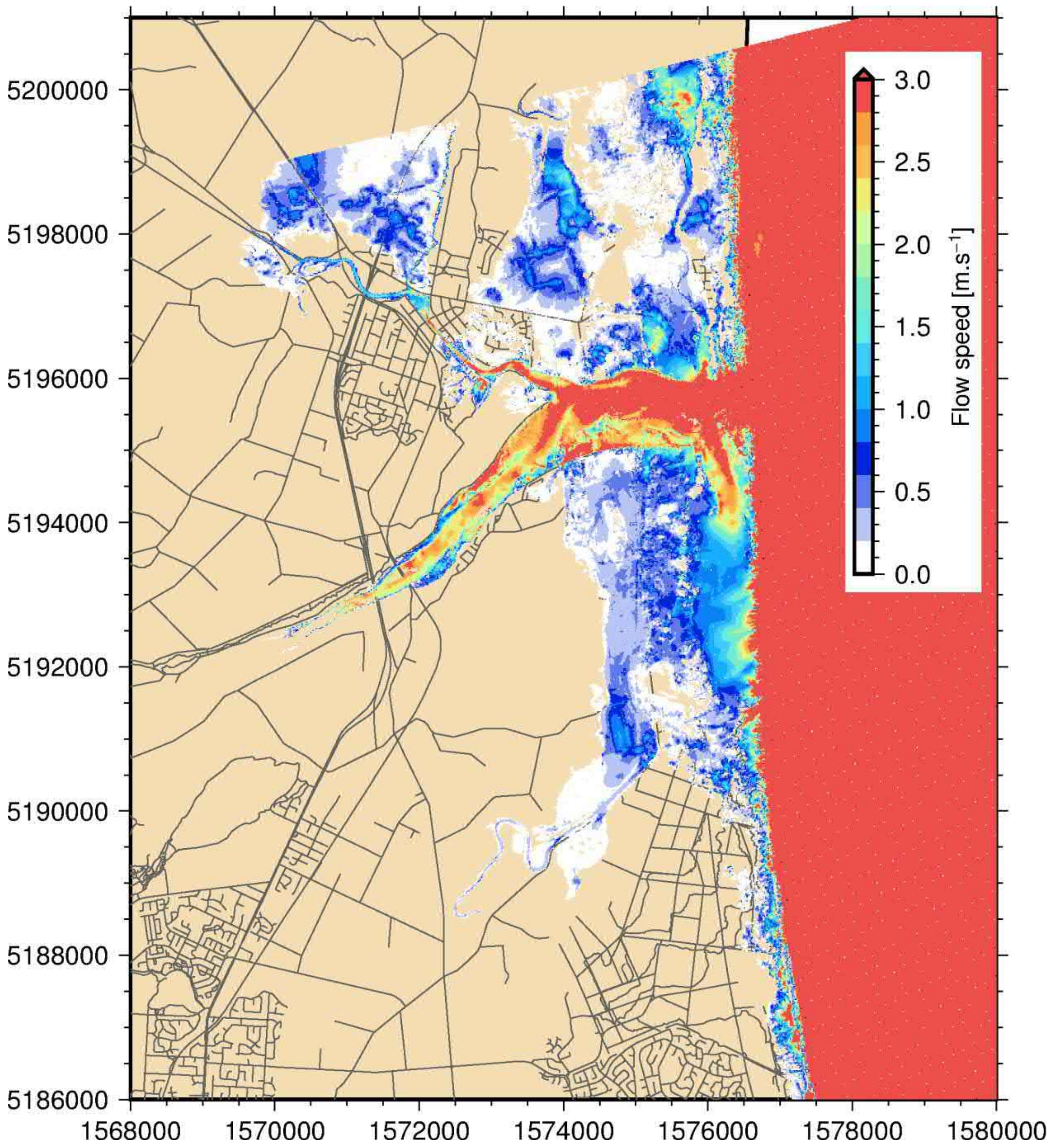

Figure 3-42: Maximum flow velocity for 1:2500-year return period - 2040 Sea Level Scenario – 0.19 m Sea Level Rise - Northern Section.

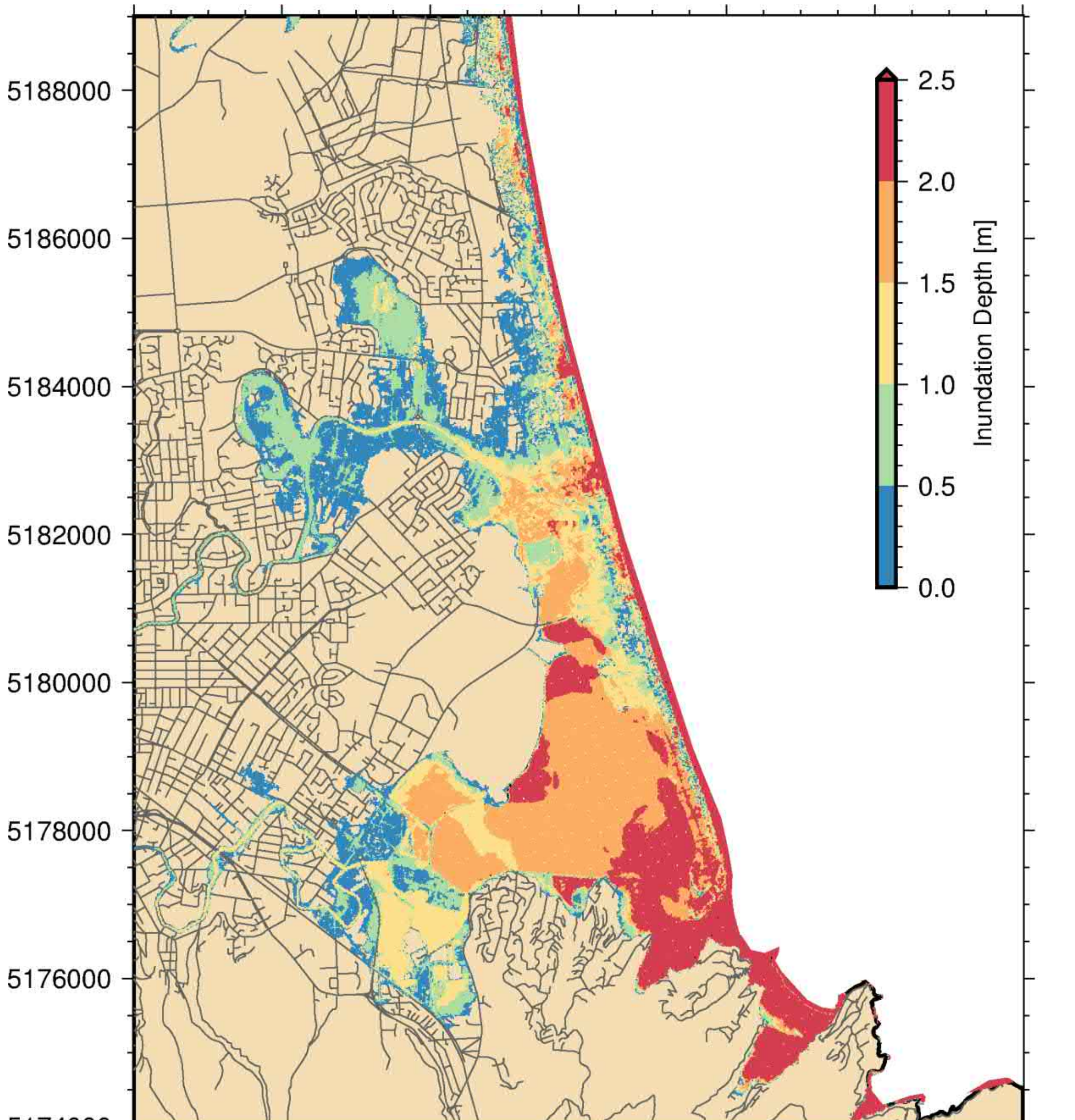

Figure 3-43: Maximum inundation depth (i.e., height above ground) for 1:2500-year return period - 2040 Sea Level Scenario – 0.19 m Sea Level Rise - Southern Section. Note that for the river channels the value given is the height above the pre-tsunami water level.

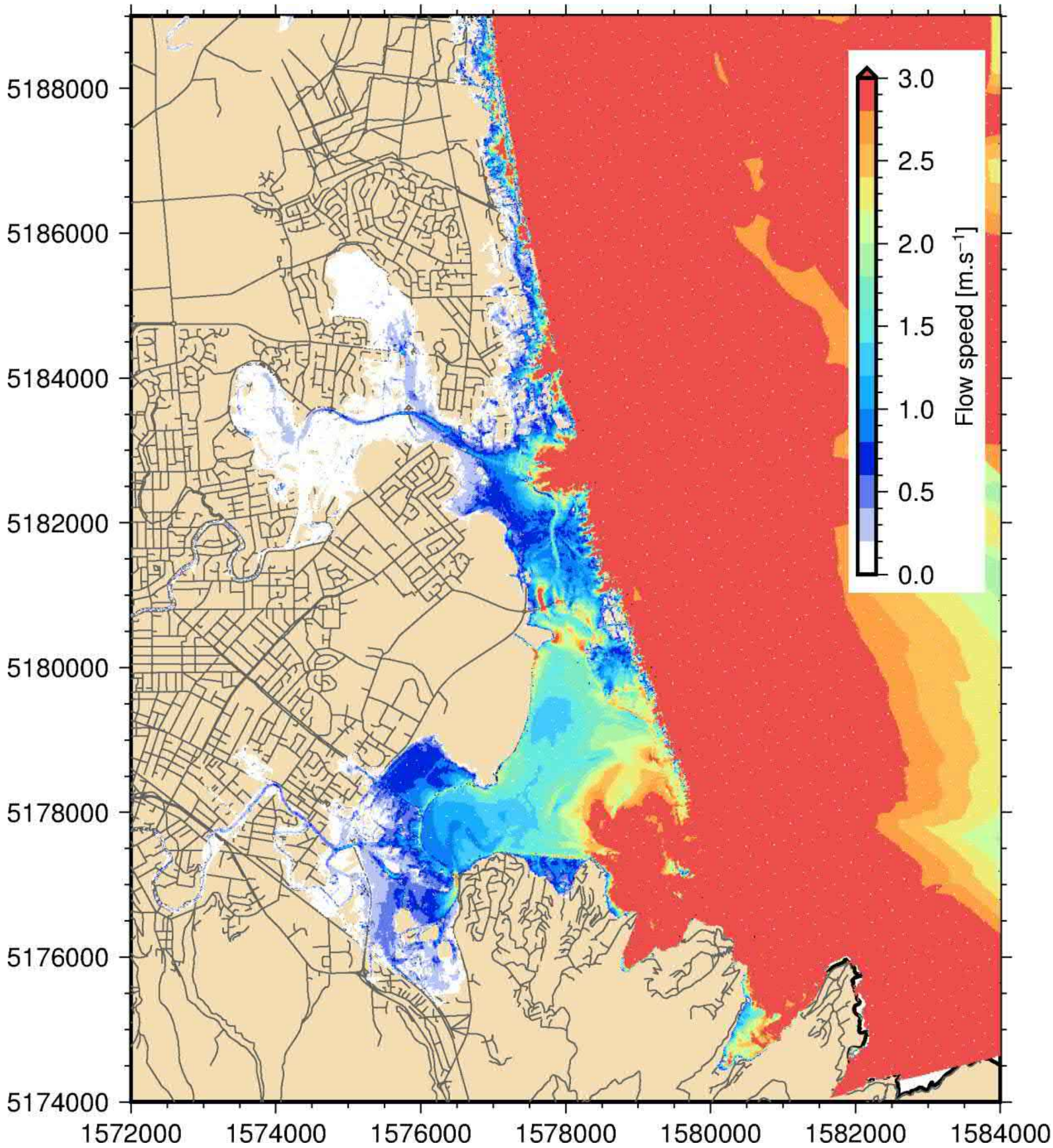

Figure 3-44: Maximum flow velocity for 1:2500-year return period - 2040 Sea Level Scenario – 0.19 m Sea Level Rise - Southern Section.

3.3.7 1:2500-year return period - 2065 Sea Level Scenario – 0.41 m Sea Level Rise

Inundation extent for the 1:2500-year return period tsunami at 0.41 m sea-level rise covers an area of 48 km^2 and reaches a maximum depth of 8.5 m near the Waimakariri River entrance. The tsunami waves in this scenario is slightly diverted southward compared with the scenario at 0.19 m sea-level rise causing less inundation on the north of the Waimakariri River. In the rest of the model area the inundation is slightly larger (Figure 3-45 and Figure 3-47). As with the previous sea level scenario, the dunes along coastal strip are consistently overtopped by the tsunami waves lead to major inundation on the low-lying area of the coastal strip with velocity exceeding 10 m/s where the dunes are overtopped (Figure 3-46 and Figure 3-48). This overtopping would likely erode the dunes and could cause increased inundation, but this is not captured in this model.

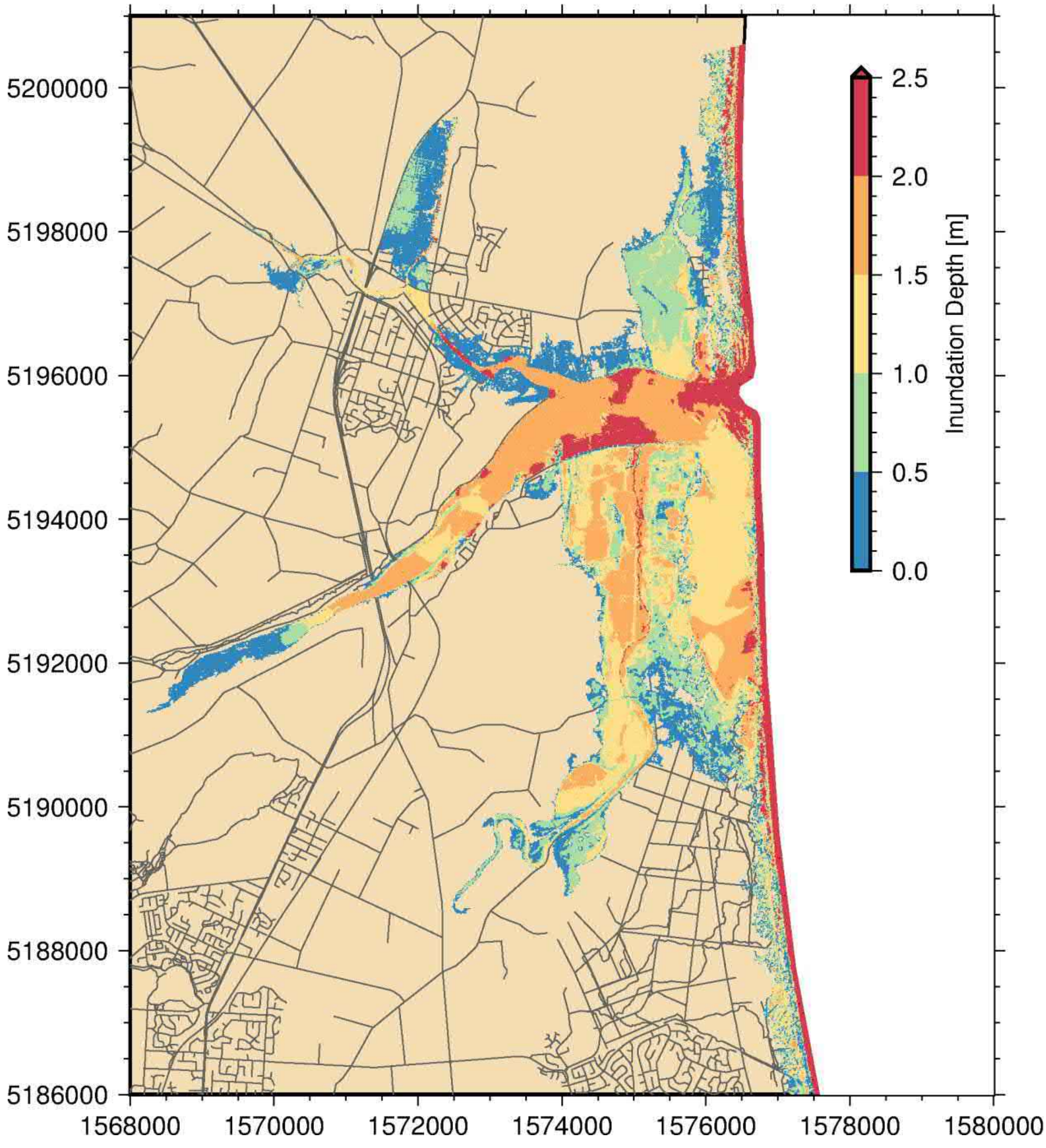

Figure 3-45: Maximum inundation depth (i.e., height above ground) for 1:2500-year return period - 2065 Sea Level Scenario – 0.41 m Sea Level Rise - Northern Section. Note that for the river channels the value given is the height above the pre-tsunami water level.

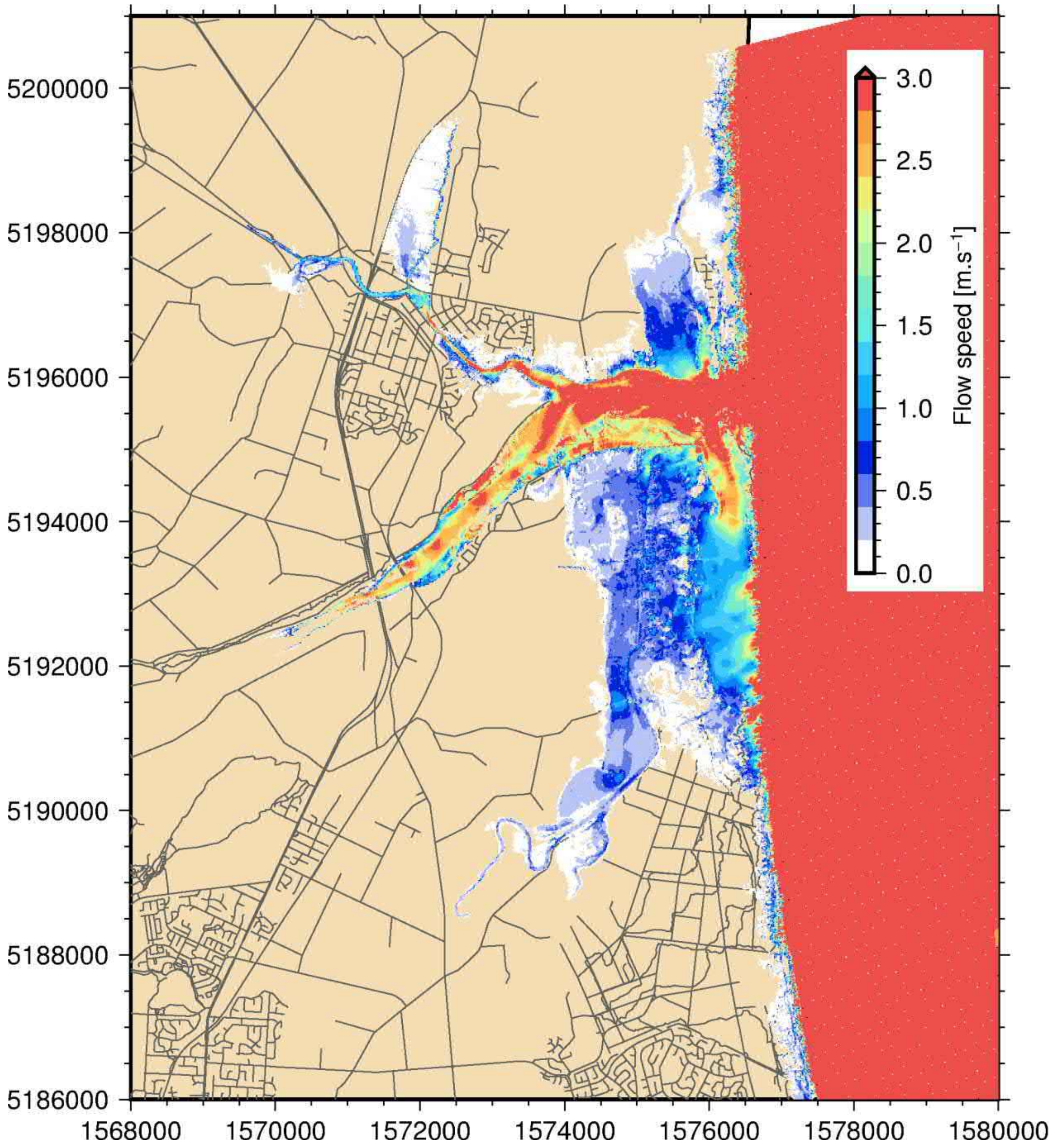

Figure 3-46: Maximum flow velocity for 1:2500-year return period - 2065 Sea Level Scenario – 0.41 m Sea Level Rise - Northern Section.

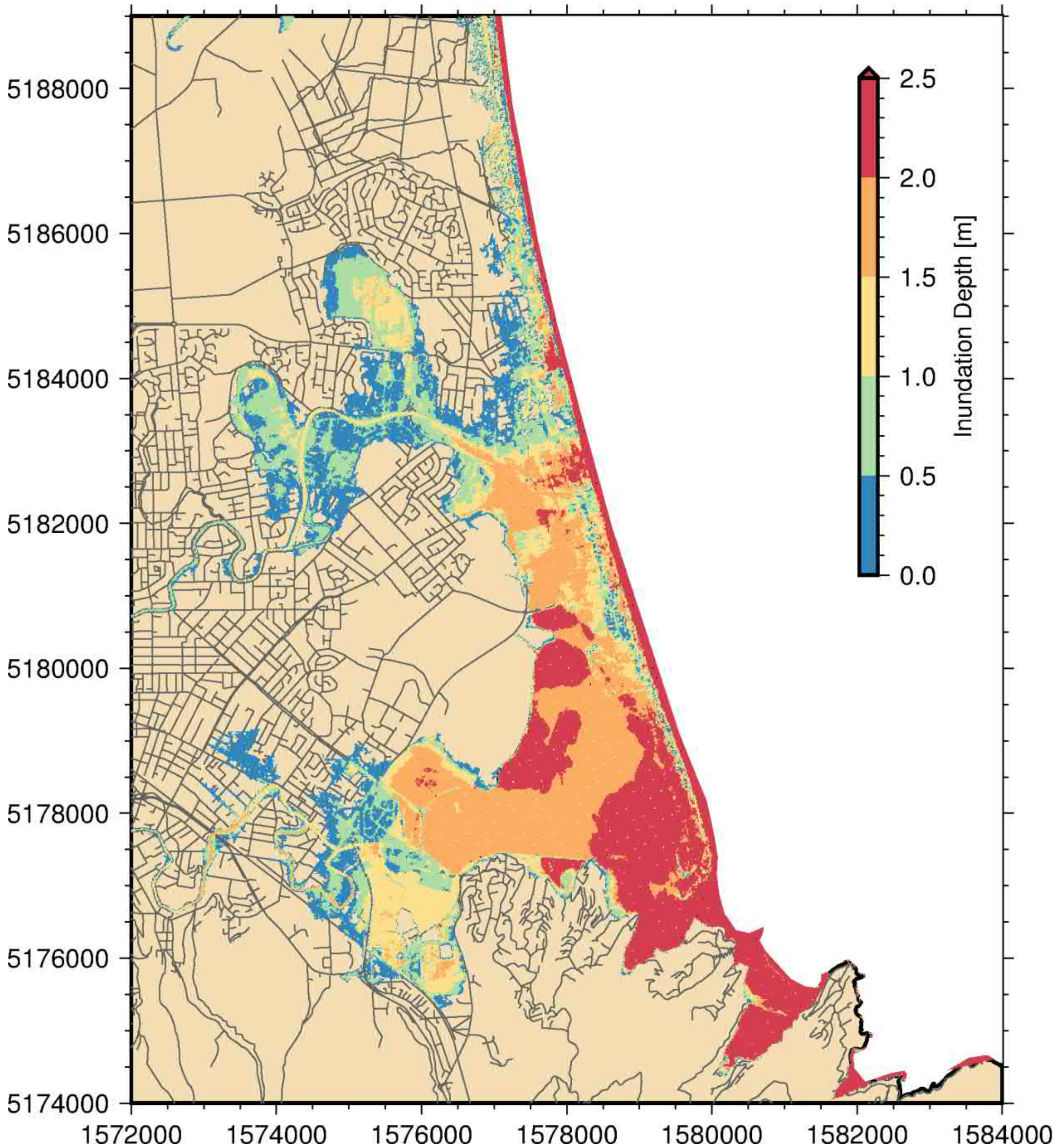

Figure 3-47: Maximum inundation depth (i.e., height above ground) for 1:2500-year return period - 2065 Sea Level Scenario – 0.41 m Sea Level Rise - Southern Section. Note that for the river channels the value given is the height above the pre-tsunami water level.

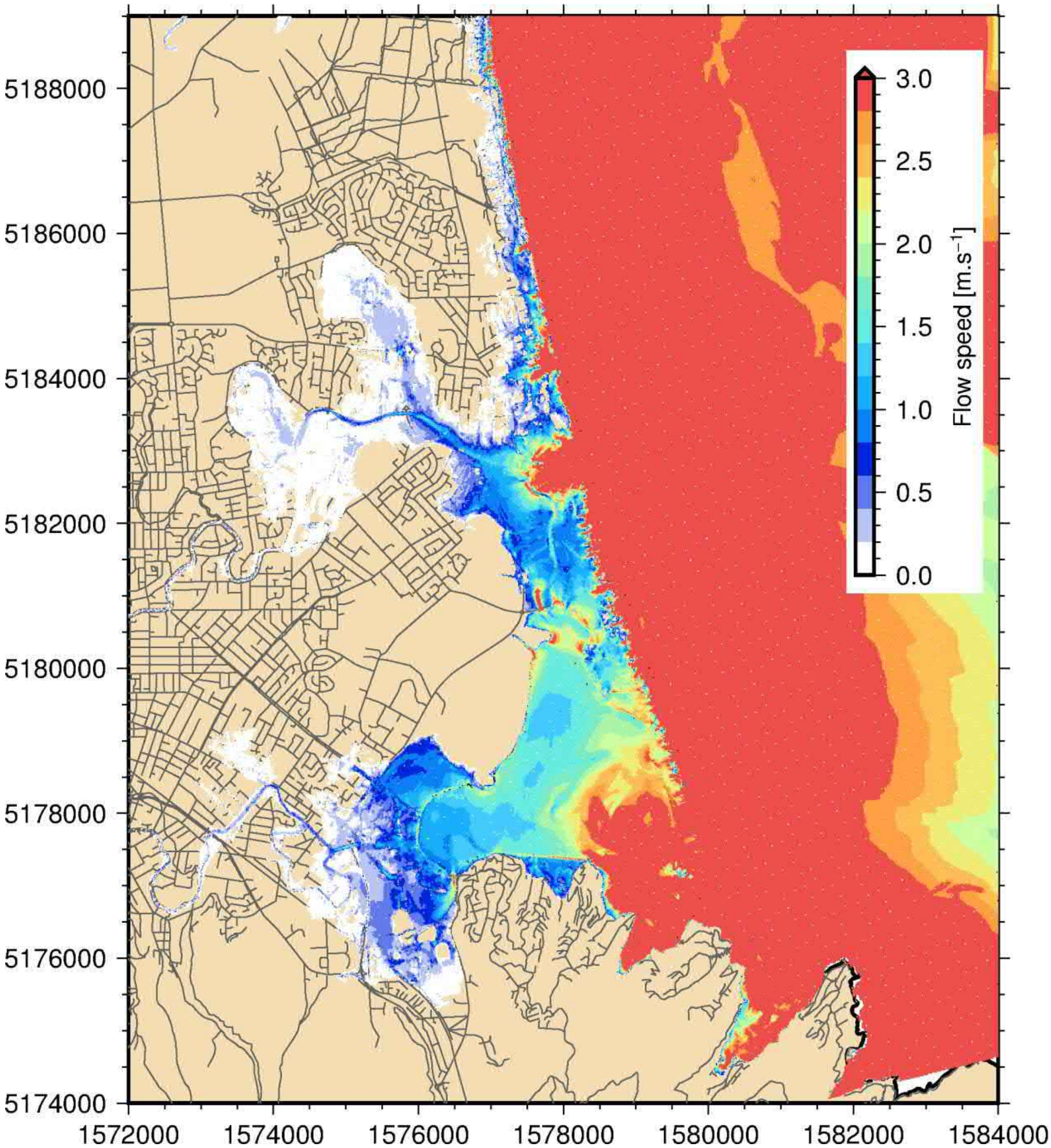

Figure 3-48: Maximum flow velocity for 1:2500-year return period - 2065 Sea Level Scenario – 0.41 m Sea Level Rise - Southern Section.

3.3.8 1:2500-year return period - 2120 Sea Level Scenario – 1.06 m Sea Level Rise

Inundation extent for the 1:2500-year return period tsunami at 1.06 m sea-level rise covers an area of 73 km^2 and reaches a maximum depth of 9.5 m near the Waimakariri River mouth. As expected this scenario shows the worst inundation and largest flow velocities. However, the inundation extent is only slightly larger than the 1:500-year scenario at the 1.06 m sea level rise but with significantly larger maximum inundation depth and flow velocity (for the 1:2500-year return period scenario), especially along the coastal strip. The inundation reaches as far as the Waltham suburb on the Heathcote River and the Avonside suburb on the Avon River and covers the entire coastal strip (Figure 3-49 and Figure 3-51). Simulated flow velocities in the Avon-Heathcote Estuary exceed 12 m/s near the entrance and 8 m/s where the dunes are overtopped (Figure 3-50 and Figure 3-52). This overtopping would likely erode the dunes and could cause increased inundation, but this is not captured in this model.

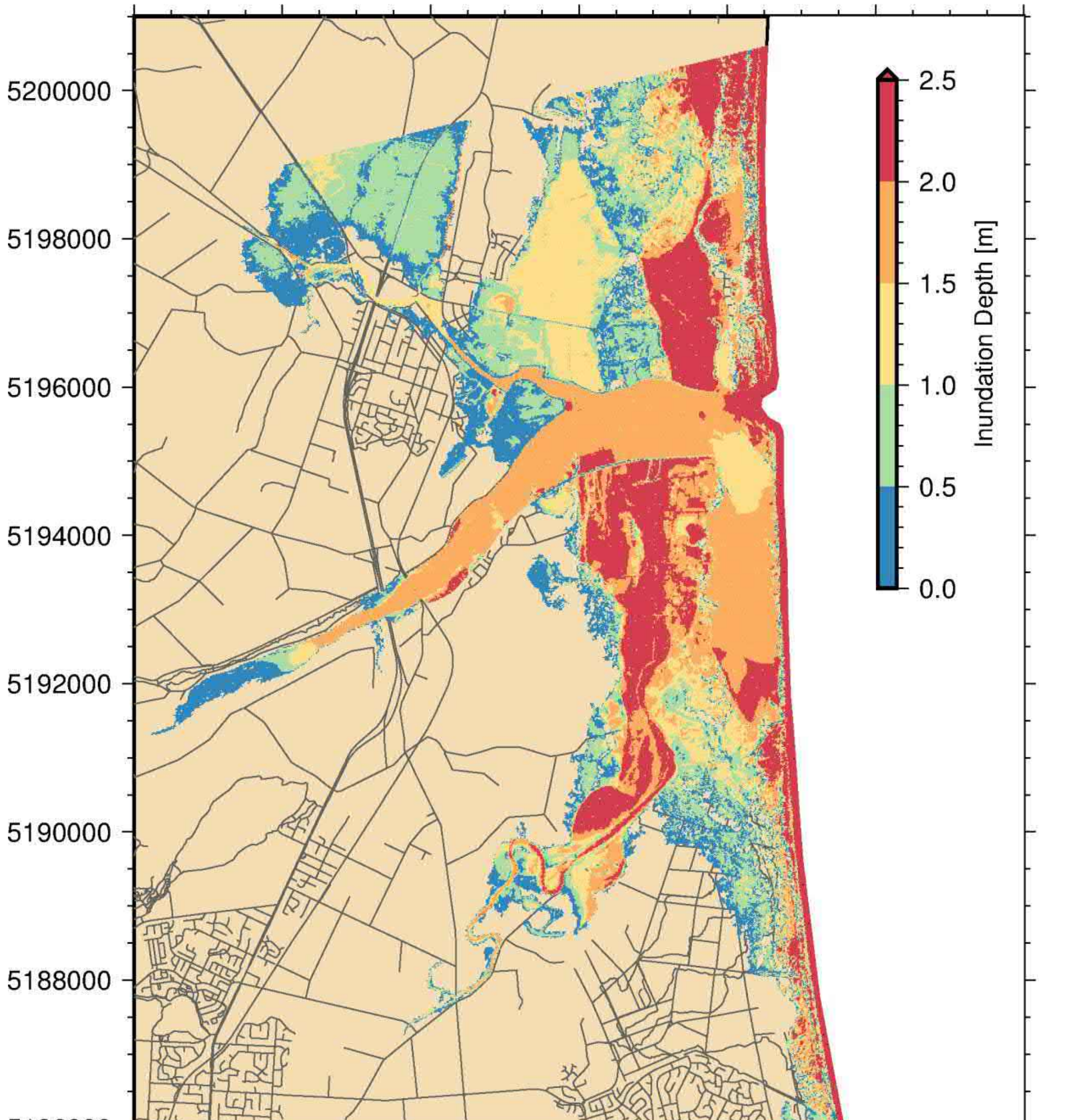

Figure 3-49: Maximum inundation depth (i.e., height above ground) for 1:2500-year return period - 2120 Sea Level Scenario – 1.06 m Sea Level Rise - Northern Section. Note that for the river channels the value given is the height above the pre-tsunami water level.

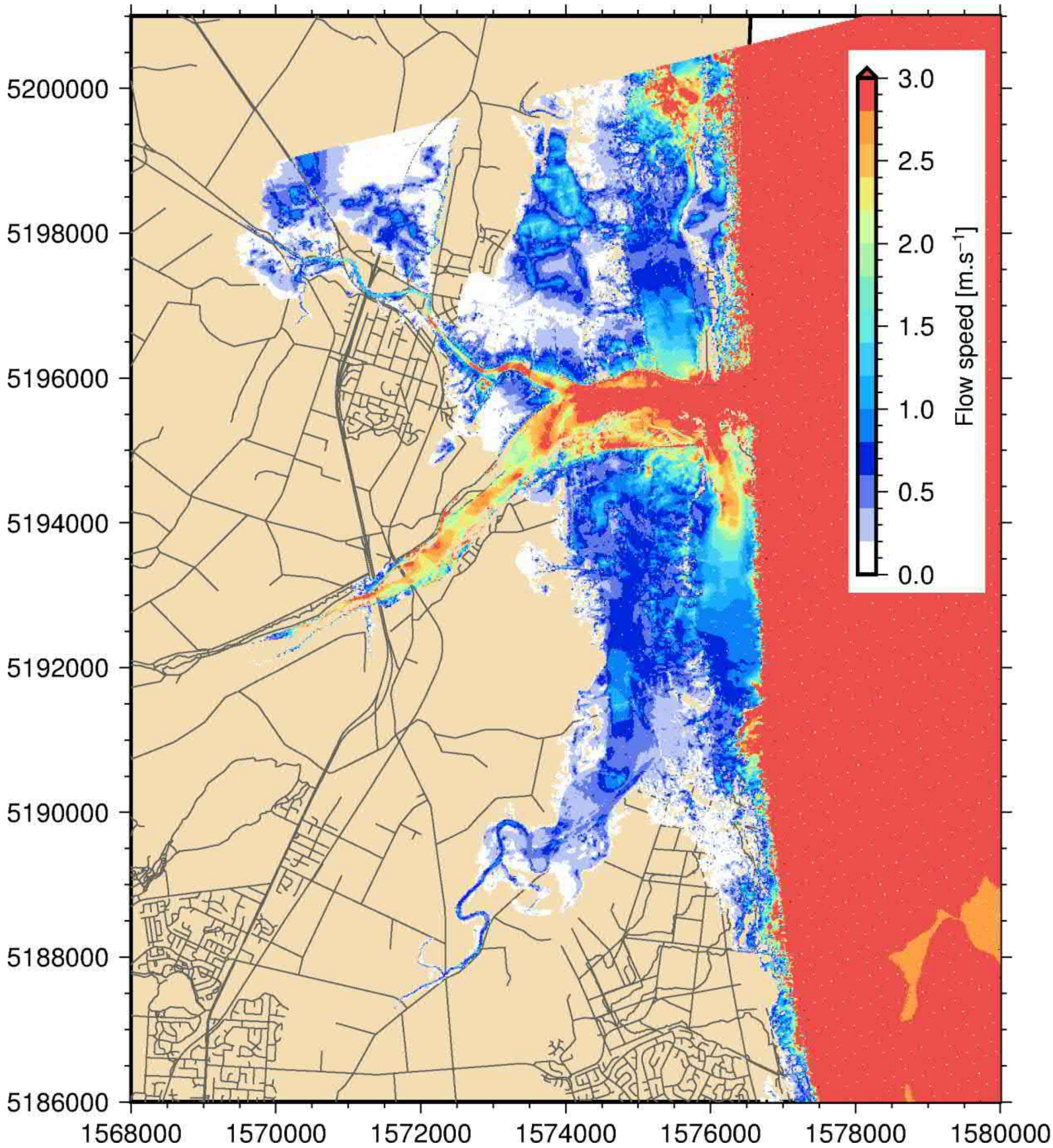

Figure 3-50: Maximum flow velocity for 1:2500-year return period - 2120 Sea Level Scenario – 1.06 m Sea Level Rise - Northern Section.

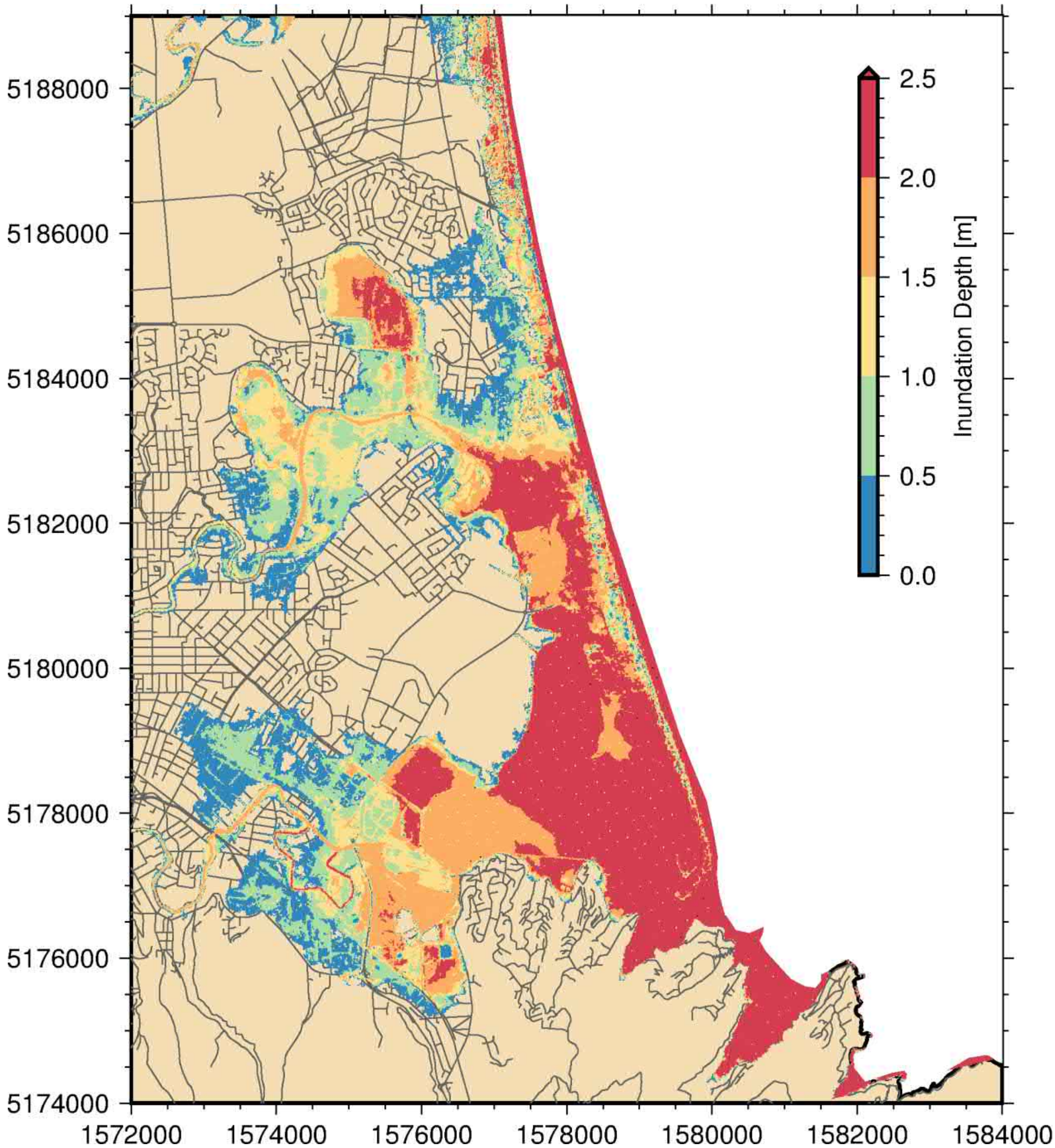

Figure 3-51: Maximum inundation depth (i.e., height above ground) for 1:2500-year return period - 2120 Sea Level Scenario – 1.06 m Sea Level Rise - Southern Section. Note that for the river channels the value given is the height above the pre-tsunami water level.

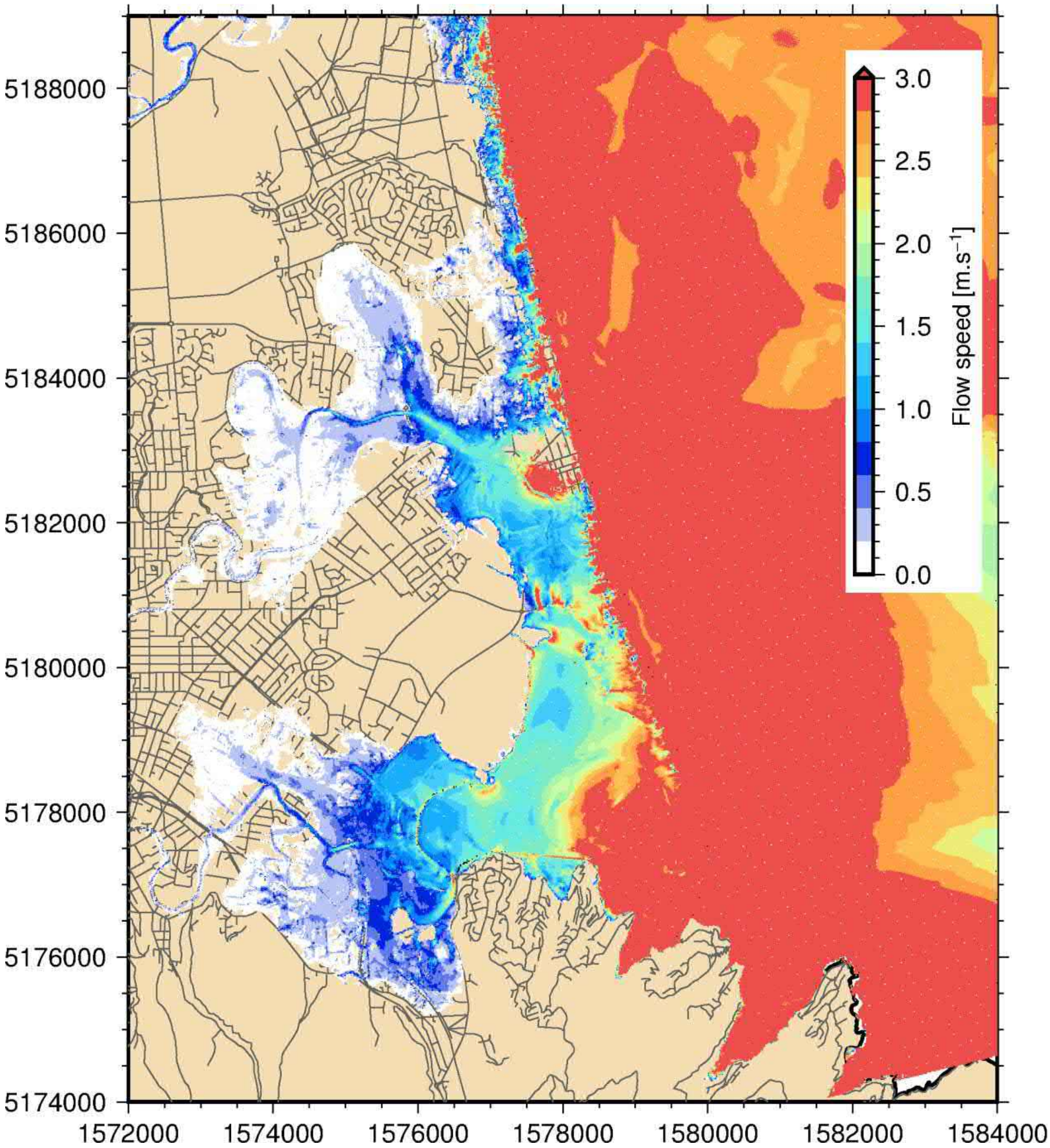

Figure 3-52: Maximum flow velocity for 1:2500-year return period - 2120 Sea Level Scenario – 1.06 m Sea Level Rise - Southern Section.

3.4 Erosion

Tsunami waves can cause strong currents capable of transporting large amount of non-cohesive sediment. These high velocities predominantly occur at (but are not restricted to) the mouth of rivers and below bridges where the flow is constricted. When high flow velocities are sustained, they can cause scouring and severe erosion. The extent and depth of the erosion depends on the type of scouring, the bed sediment and other flow characteristics. Qualitatively, scouring and severe erosion is likely to occur:

- Around channel bend (Bend scour).

- Where flow is constricted (by debris or structures) (constriction scour).
- Near weirs and drops in the topography (weir scour).
- Near piers, abutments and near buildings (local scour).

Erosion potential can be evaluated using empirical relationships specific to each scour type but are designed for specific bed type with specific geometric parameters that are not directly applicable in the case of tsunami inundation. In particular, many empirical equations are available to assess the constriction scour but most of these relationships assumes that the flow upstream is restricted to a channel. These types of empirical relationships are not applicable for dune overtopping or scouring around buildings. The effect of flow constriction is calculated in the model for features that are larger than the model finest resolution (13.2 m) and the sediment transport potential is described by the flow bottom shear stress. This allow for a qualitative assessment of the locations where scouring is most likely to occur for each scenario using information of maximum bottom shear-stress, and results presented above (maximum flow velocity and maximum inundation depth). This is done on a broad scale and does not capture smaller scale scouring that may occur around buildings, small-scale structures or small-scale channels.

The critical shear stress is the minimum shear stress necessary to mobilise a particle of sediment of a given size (Table 3-3). Near Christchurch, the dunes are composed of fine sand, but coarser material is present near the rivers.

Table 3-3: Critical shear stress by particle-size classification for determining approximate condition for sediment. Note that critical shear stress only indicates mobility rather than transport. This table was calculated using a fixed sediment density. From Berenbrock and Tranmer (2008).

Particle classification name	Ranges of particle diameters	Critical bed shear stress (τ_c) (N/m²)
Coarse cobble	128 – 256	112 – 223
Fine cobble	64 – 128	53.8 – 112
Very coarse gravel	32 – 64	25.9 – 53.8
Coarse gravel	16 – 32	12.2 – 25.9
Medium gravel	8 – 16	5.7 – 12.2
Fine gravel	4 – 8	2.7 – 5.7
Very fine gravel	2 – 4	1.3 – 2.7
Very coarse sand	1 – 2	0.47 – 1.3
Coarse sand	0.5 – 1	0.27 – 0.47
Medium sand	0.25 – 0.5	0.194 – 0.27
Fine sand	0.125 – 0.25	0.145 – 0.194
Very fine sand	0.0625 – 0.125	0.110 – 0.145
Coarse silt	0.0310 – 0.0625	0.0826 – 0.110
Medium silt	0.0156 – 0.0310	0.0630 – 0.0826
Fine silt	0.0078 – 0.0156	0.0378 – 0.0630

In all the scenario presented here, the shear-stress exceeds 30 N.m^{-2} at the mouth of the Waimakariri River and at the mouth of the Avon-Heathcote Estuary (Figure 3-53 – Figure 3-68). These values far exceed the critical shear stress necessary to transport fine sand (0.14 – 0.20 N.m^{-2}) present there. The duration where the flow exceeds the critical shear stress for sand was not recorded in the model, but major scour can be expected there.

3.4.1 1:500-year return period tsunami scenarios

For the 1:500-year return period tsunami scenario, the bottom shear-stress is also high in the area where the dune is overtopped (New Brighton, North New Brighton, South Sumner) (10-15 N.m^{-2}) (Figure 3-54, Figure 3-56 and Figure 3-58). This is likely to cause localised dune overwash causing significant erosion and locally worsen the inundation. The shear stress further in the Estuary is high on the Avon at the Bridge Street bridge (5-10 N.m^{-2}) and on the Heathcote River at the Ferry Road bridge (5-10 N.m^{-2}). There, significant scouring can be expected. At higher sea level rise scenarios, the shear-stress near these bridges is somewhat reduced as the inundation extends around the structures so the flow can go around the structure. This is likely to cause erosion around the structure, but this is not captured in the model and difficult to assess. Large areas of inundation show a shear-stress lower than 1 $N.m^{-2}$ (Figure 3-53, Figure 3-55, Figure 3-57, Figure 3-59), in these areas erosion could still occur but may be localised or limited.

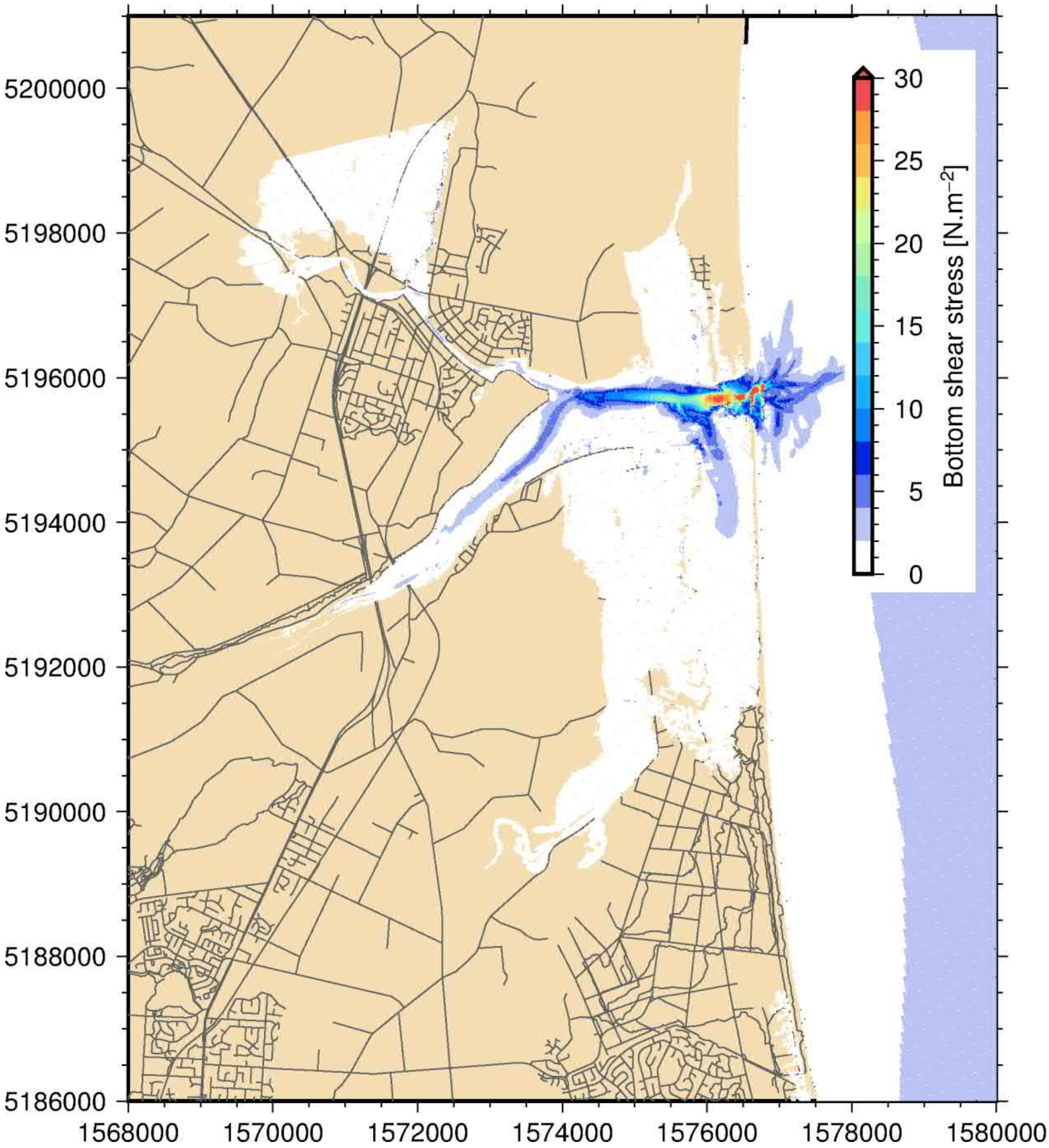

Figure 3-53: Maximum bottom shear stress for 1:500-year return period event Current Sea Level - Northern Section.

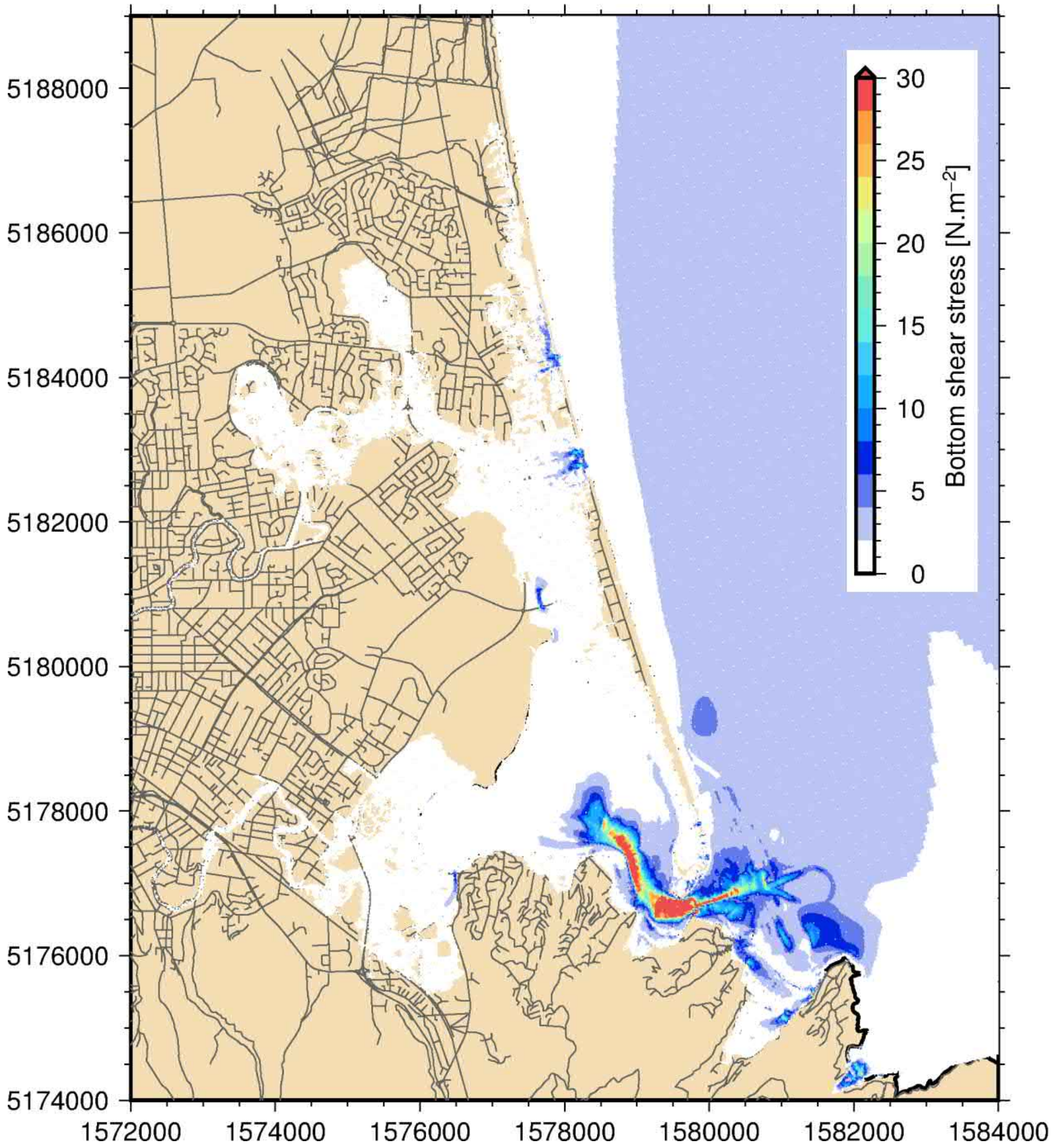

Figure 3-54: Maximum bottom shear stress for 1:500-year return period event Current Sea Level - Southern Section.

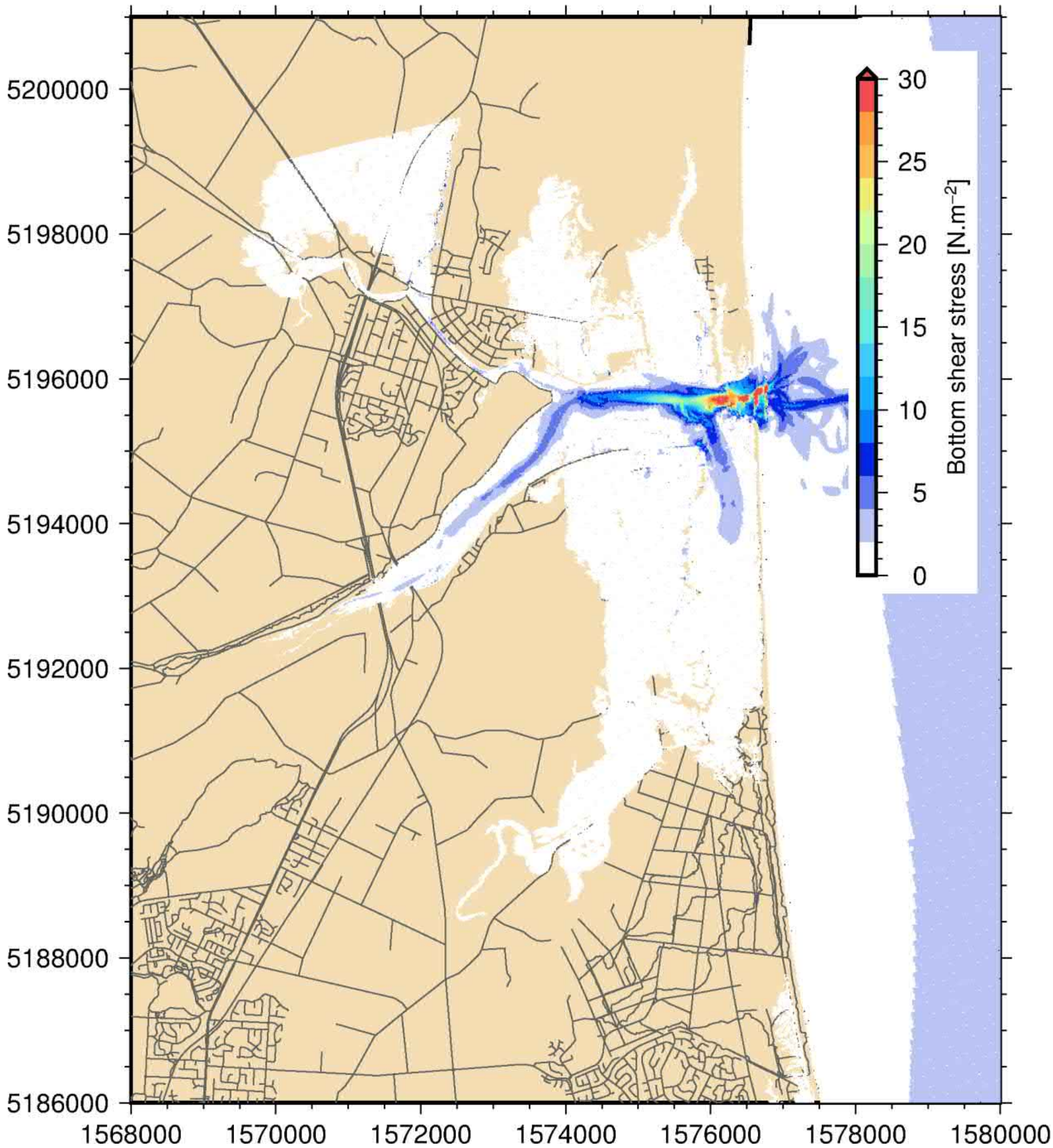

Figure 3-55: Maximum bottom shear stress for 1:500-year return period event 2040 Sea Level Scenario – 0.19 m Sea Level Rise - Northern Section.

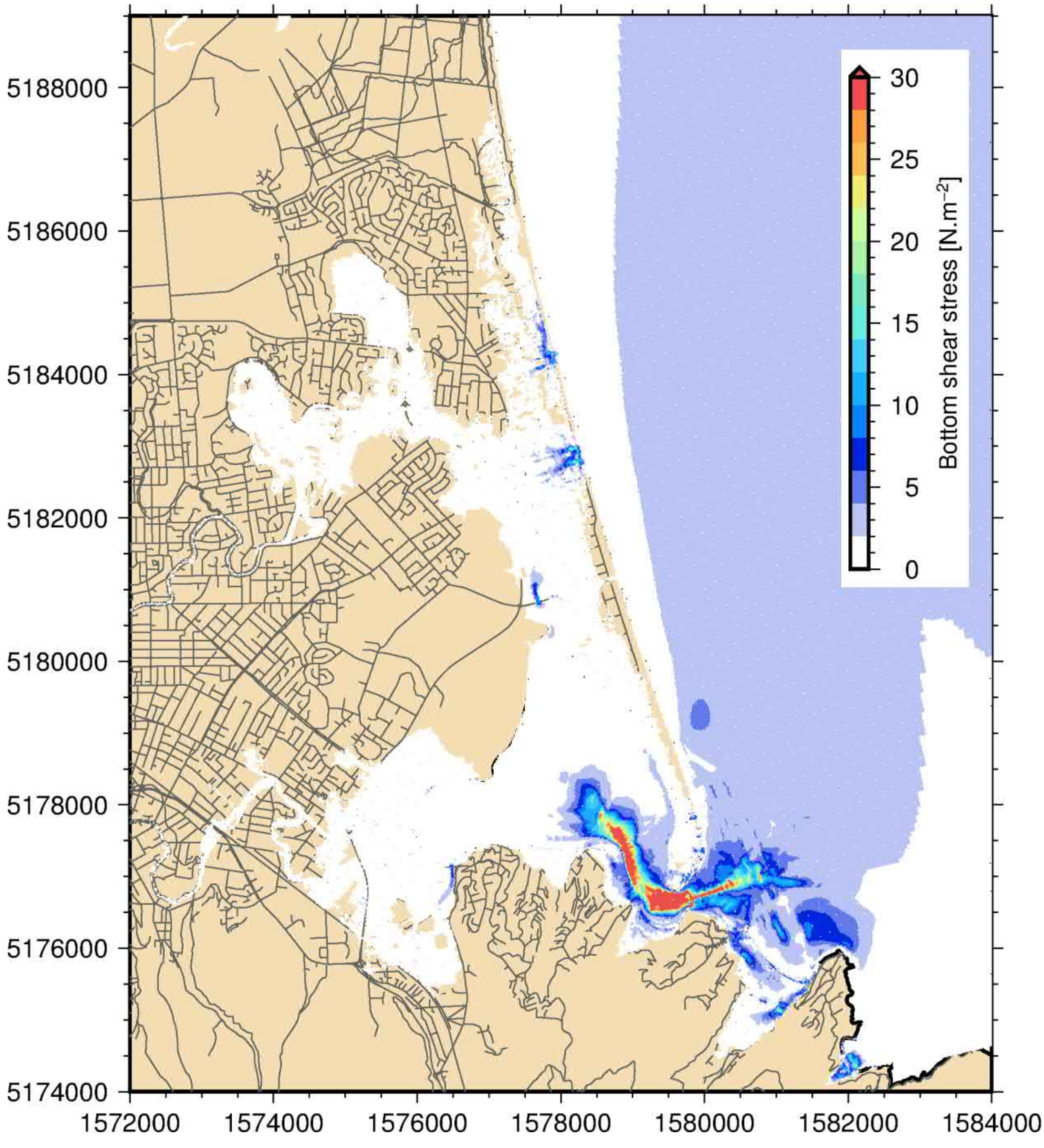

Figure 3-56: Maximum bottom shear stress for 1:500-year return period event 2040 Sea Level Scenario – 0.19 m Sea Level Rise - Southern Section.

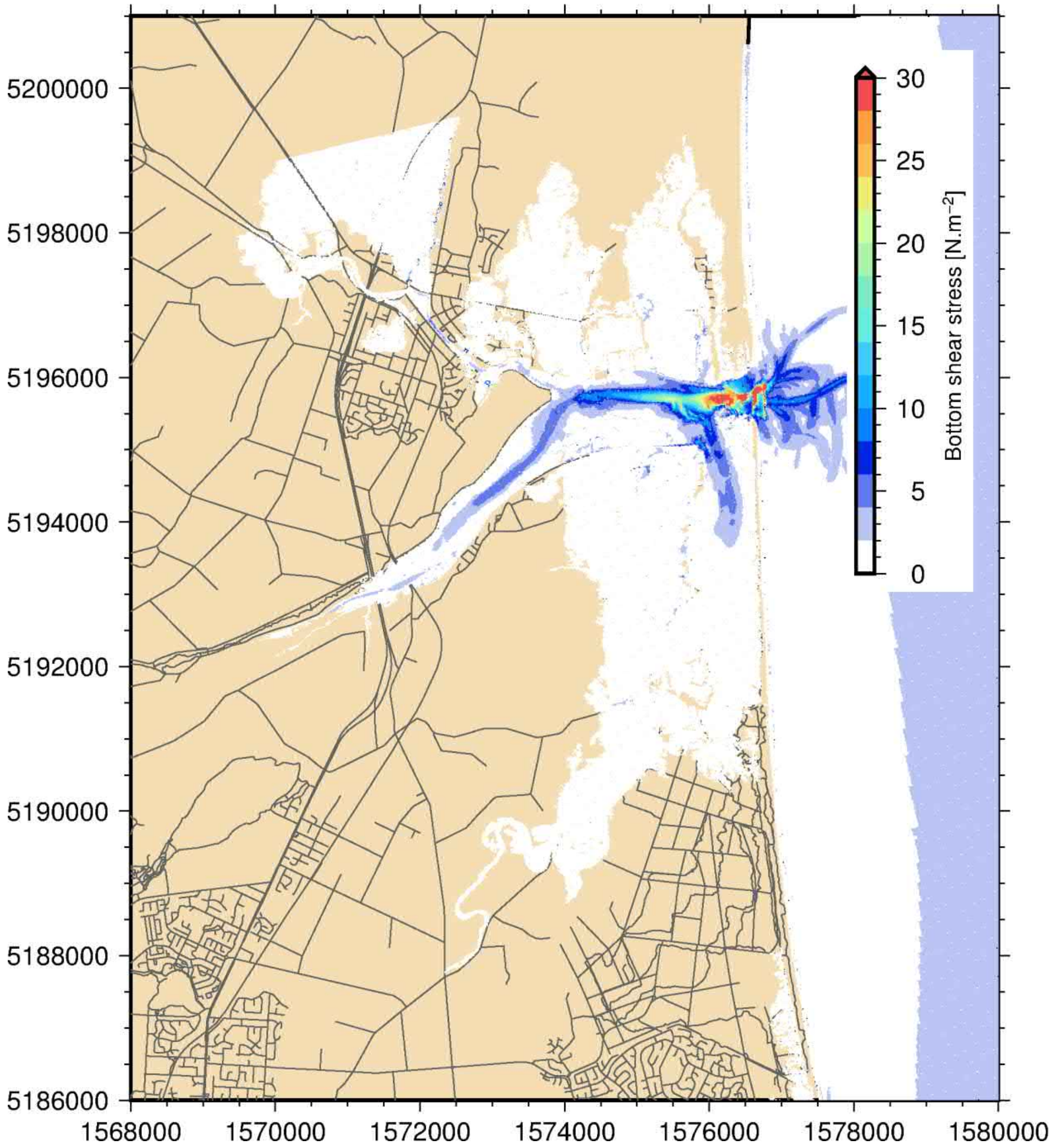

Figure 3-57: Maximum bottom shear stress for 1:500-year return period 2065 Sea Level Scenario – 0.41 m Sea Level Rise - Northern Section.

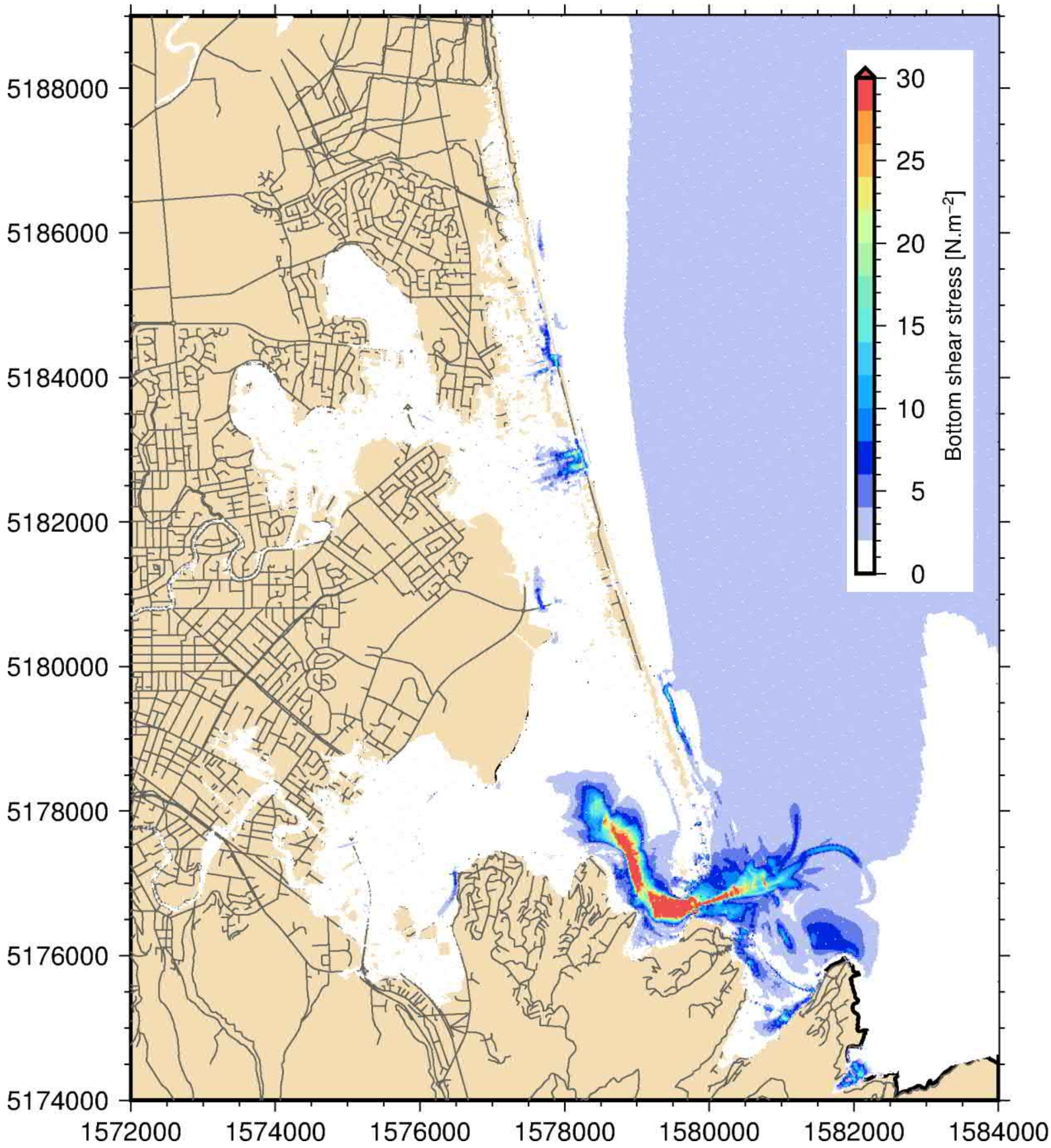

Figure 3-58: Maximum bottom shear stress for 1:500-year return period 2065 Sea Level Scenario – 0.41 m Sea Level Rise - Southern Section.

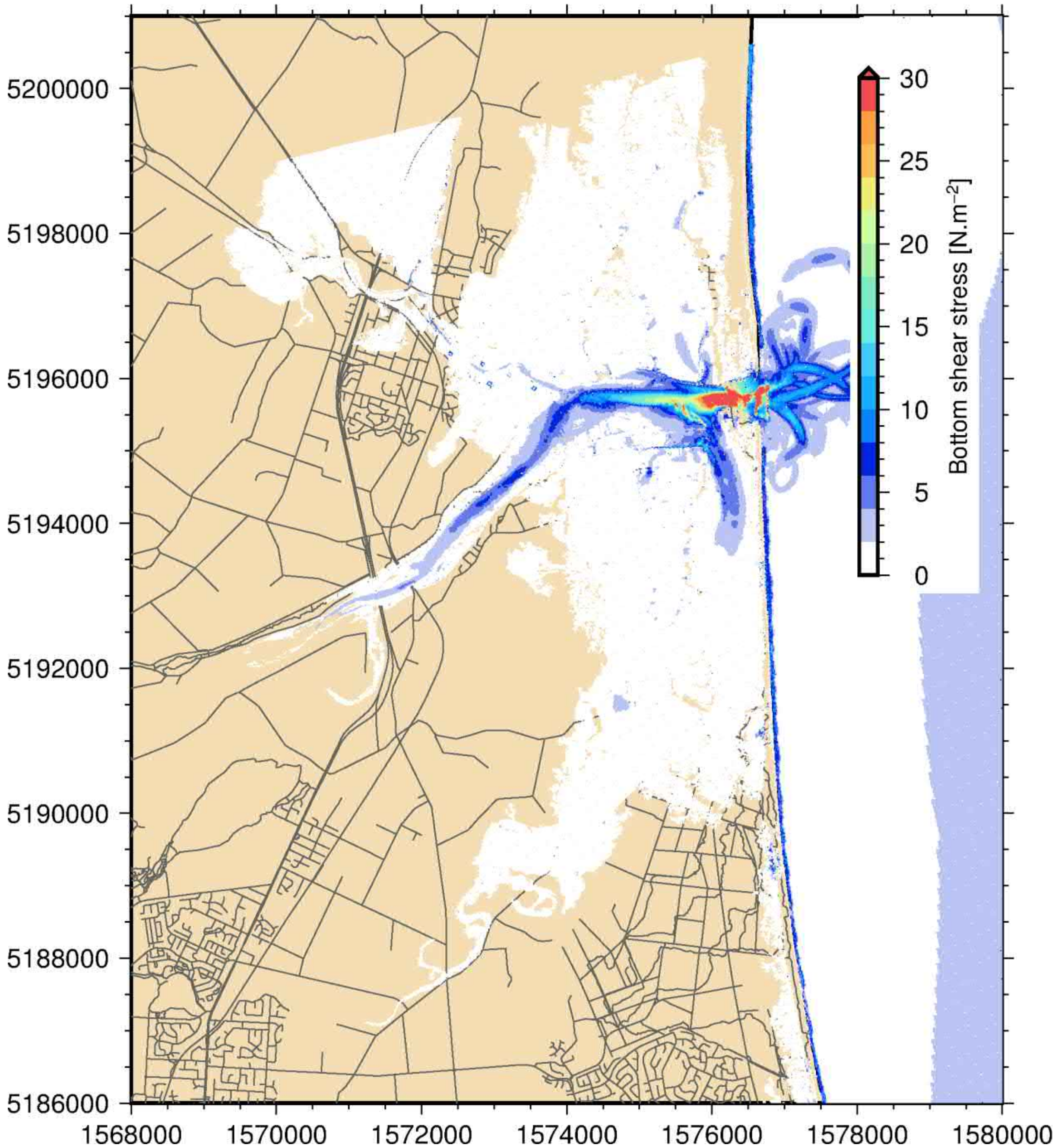

Figure 3-59: Maximum bottom shear stress for 1:500-year return period event 2120 Sea Level Scenario – 1.06 m Sea Level Rise - Northern Section.

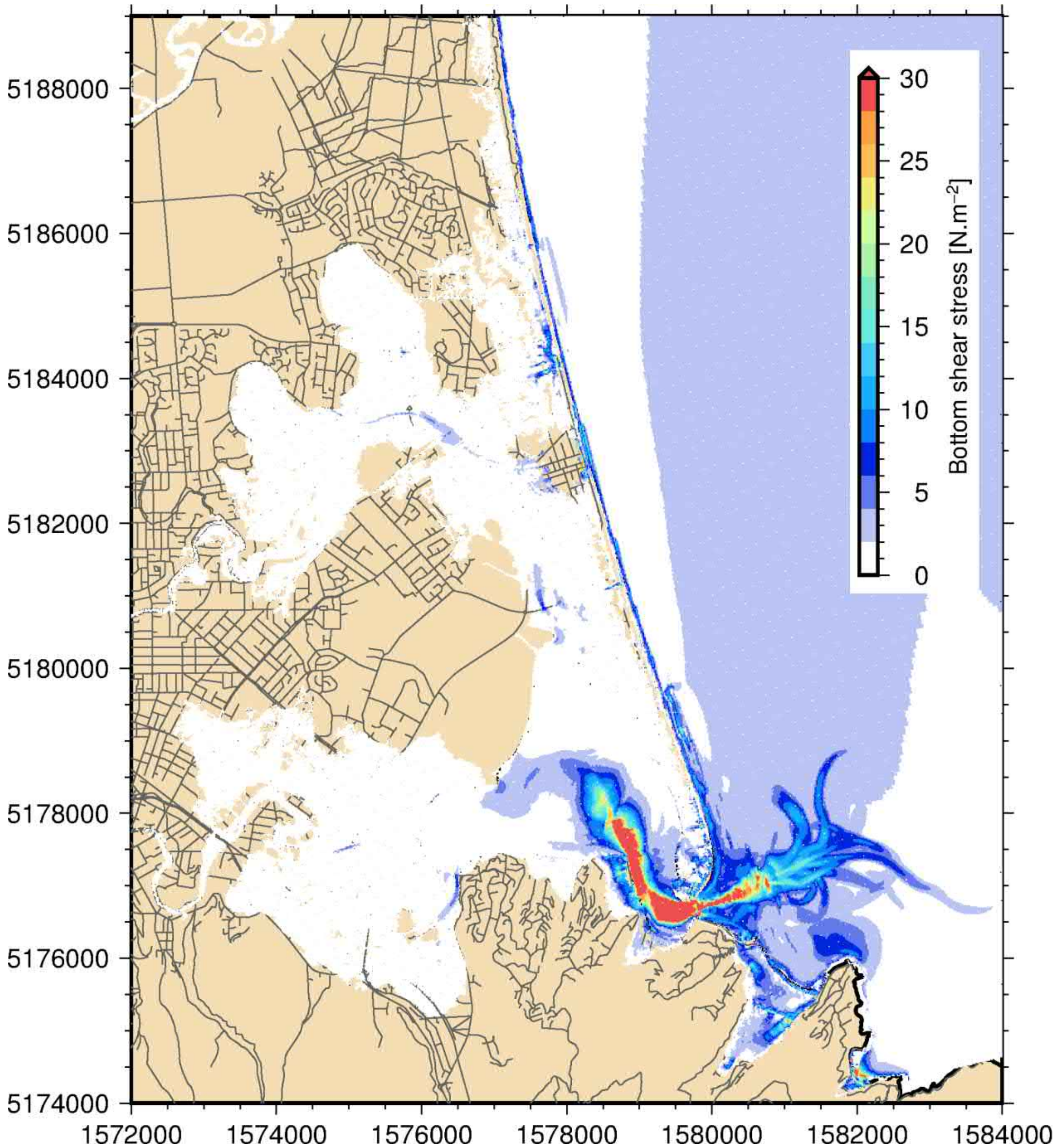

Figure 3-60: Maximum bottom shear stress for 1:500-year return period event 2120 Sea Level Scenario – 1.06 m Sea Level Rise - Southern Section.

3.4.2 1:2,500-year return period tsunami scenarios

For the 1:2,500-year return period tsunami scenario, the dunes are consistently overtopped with flows at high shear-stress (>30 $N.m^{-2}$) likely to cause severe dune overwash along the entire coastal strip (Figure 3-61, Figure 3-63 – Figure 3-68). Dune overwash is likely to severely worsen the inundation depth in the coastal strip, a process not included in this modelling. The maximum shear-stress in the lower part of the Waimakariri River channel (downstream of the Kaiapoi confluence) and in the lower part of the Avon-Heathcote Estuary exceeds 20 $N.m^{-2}$ which implies that major scouring and sediment transport is likely. In all the sea-level scenario, a high shear stress also occurs (5-15 $N.m^{-2}$) on the shore of the Avon-Heathcote Estuary. Although vegetation is likely to limit the extent of the scouring there, significant erosion can be expected. In this tsunami scenario, high shear-stress in the nearshore is likely to cause significant erosion.

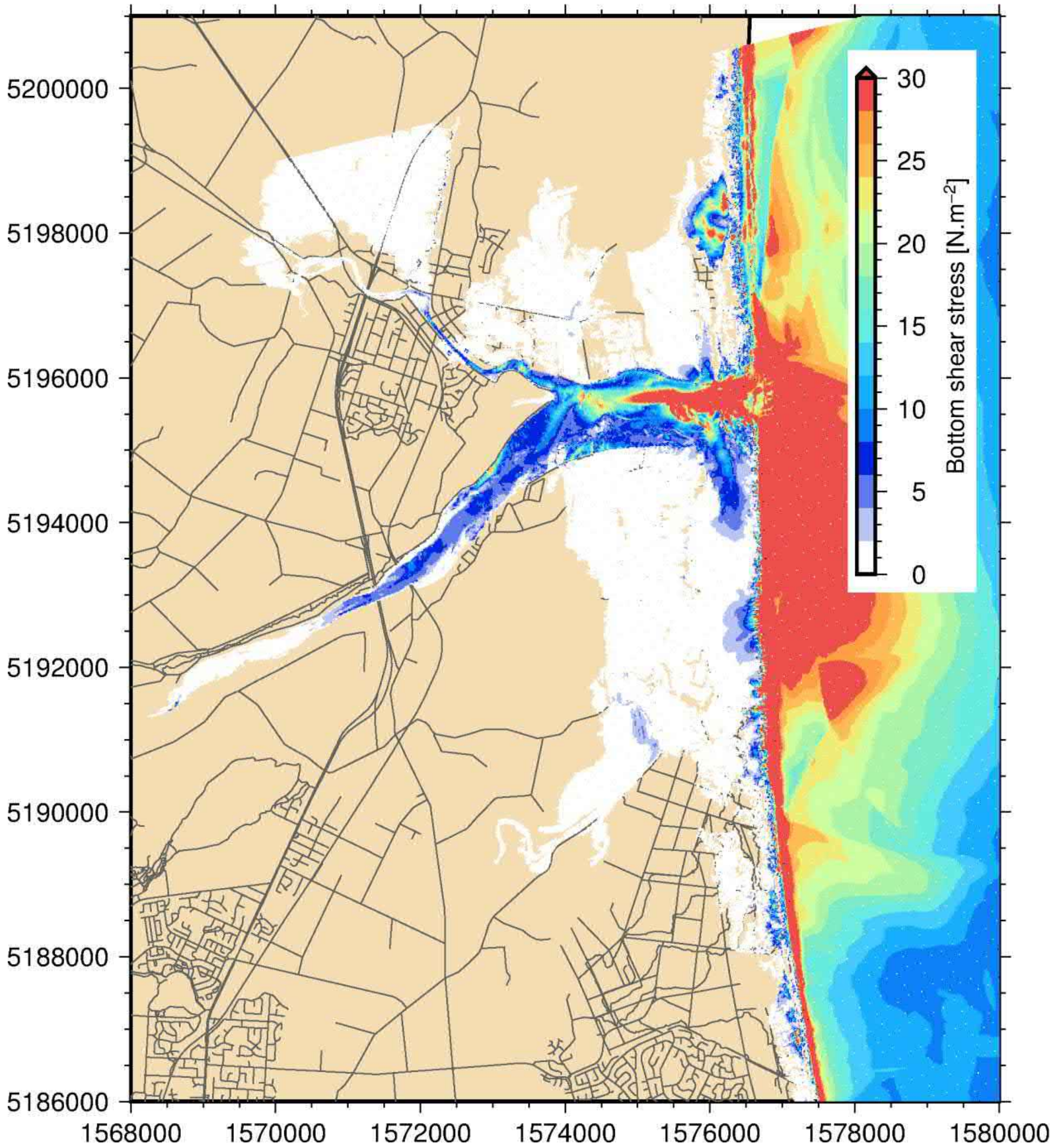

Figure 3-61: Maximum bottom shear stress for 1:2500-year return period event Current Sea Level - Northern Section.

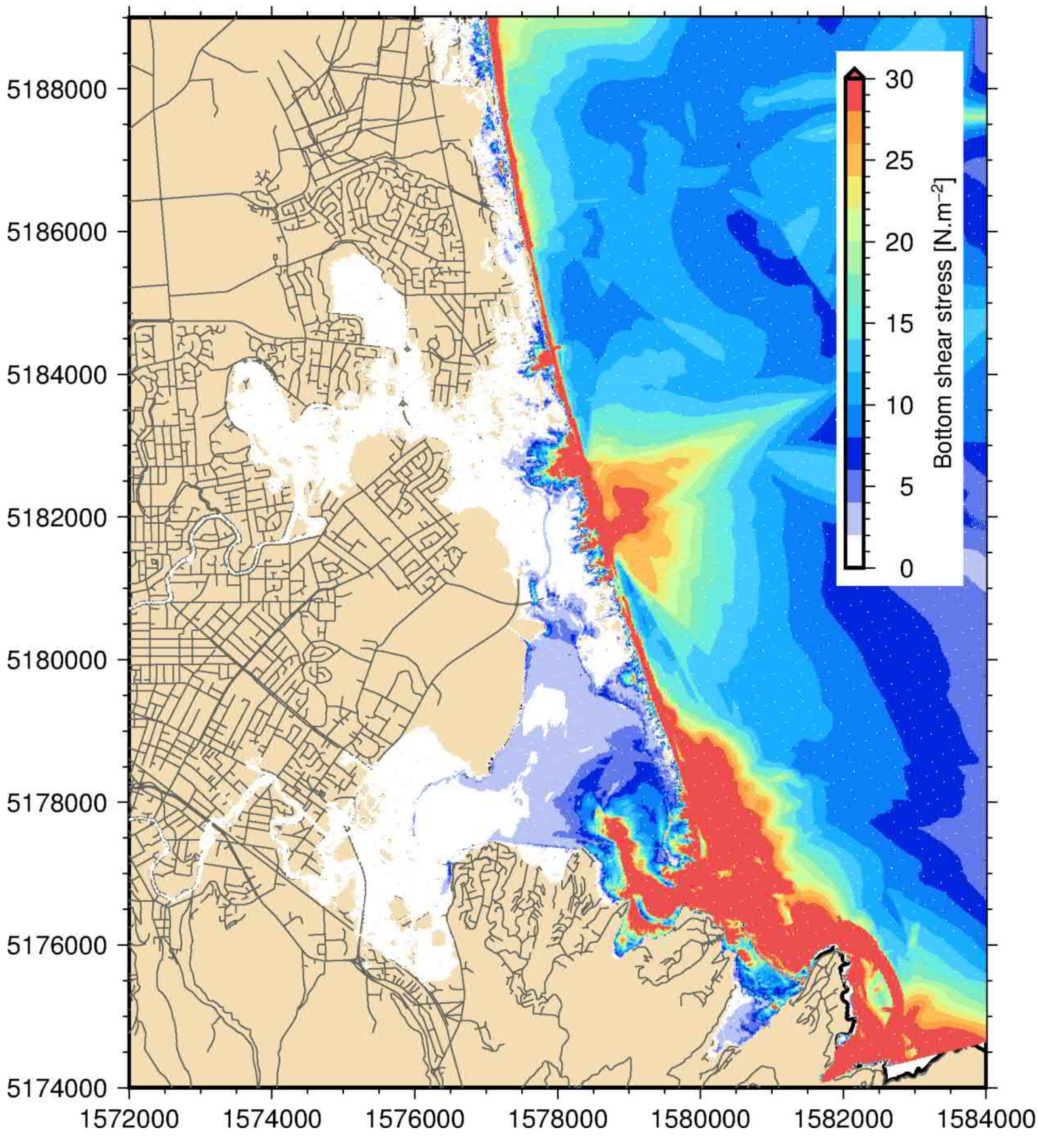

Figure 3-62: Maximum bottom shear stress for 1:2500-year return period event Current Sea Level - Southern Section.

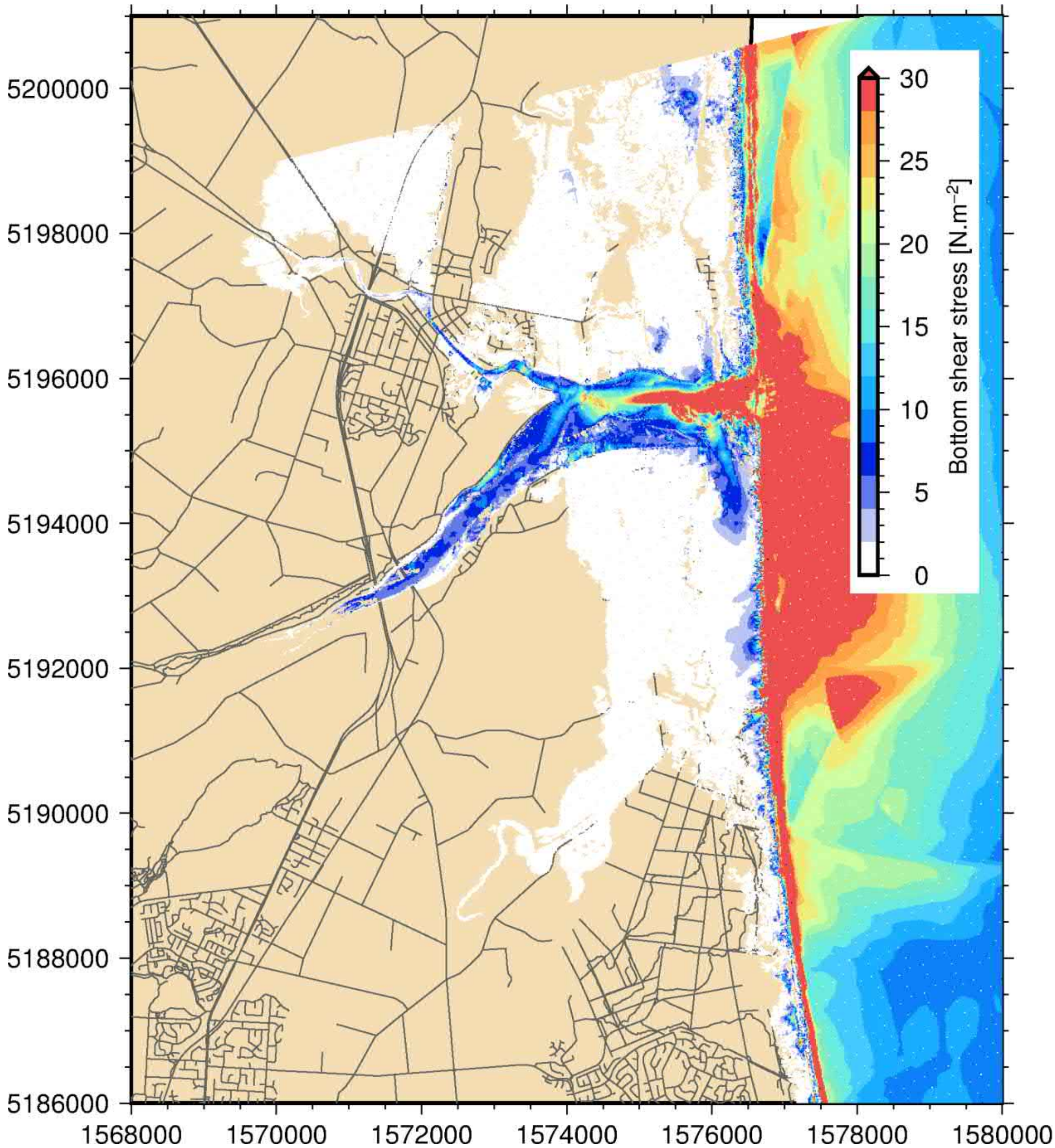

Figure 3-63: Maximum bottom shear stress for 1:2500-year return period - 2040 Sea Level Scenario – 0.19 m Sea Level Rise - Northern Section.

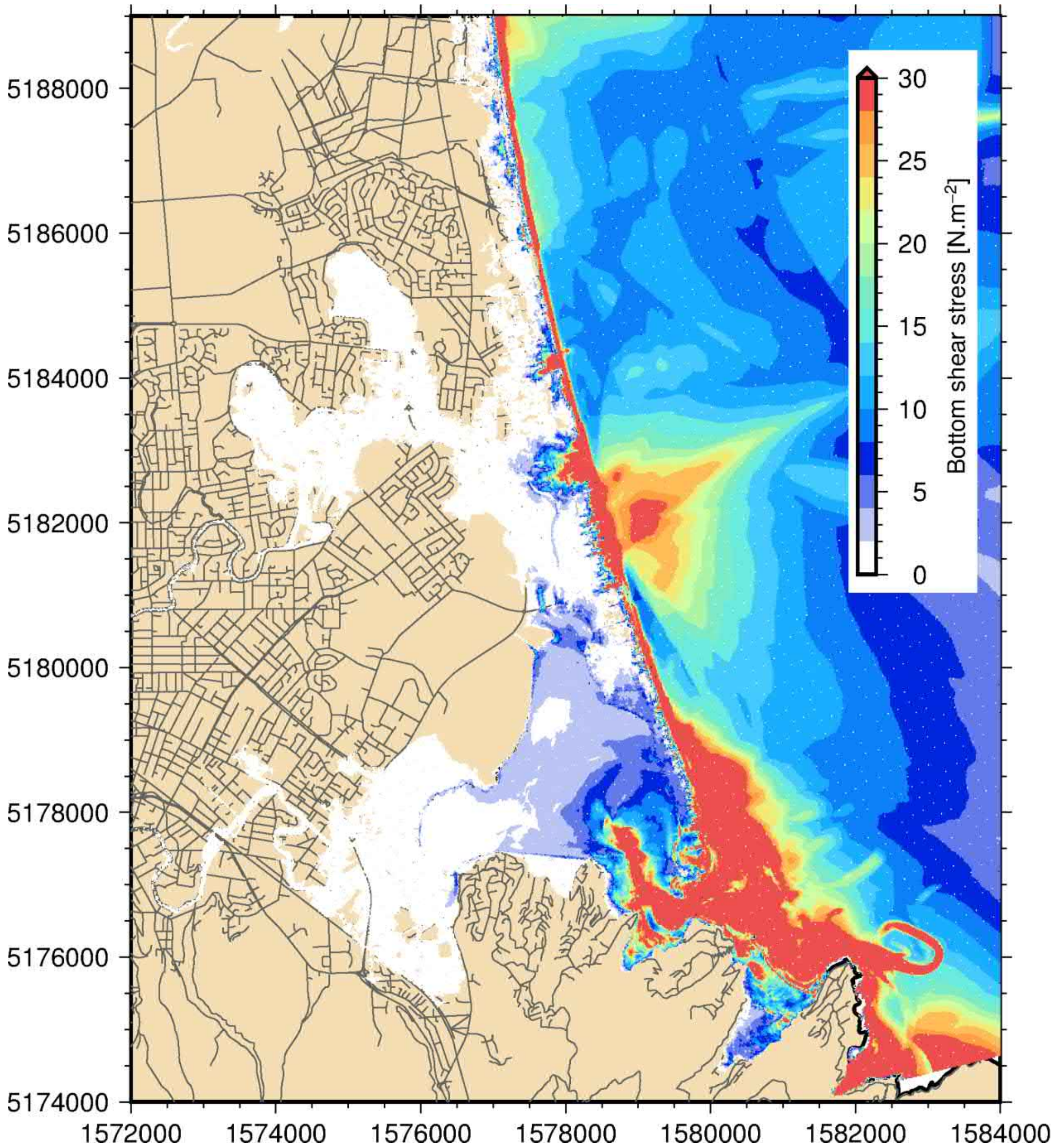

Figure 3-64: Maximum bottom shear stress for 1:2500-year return period - 2040 Sea Level Scenario – 0.19 m Sea Level Rise - Southern Section.

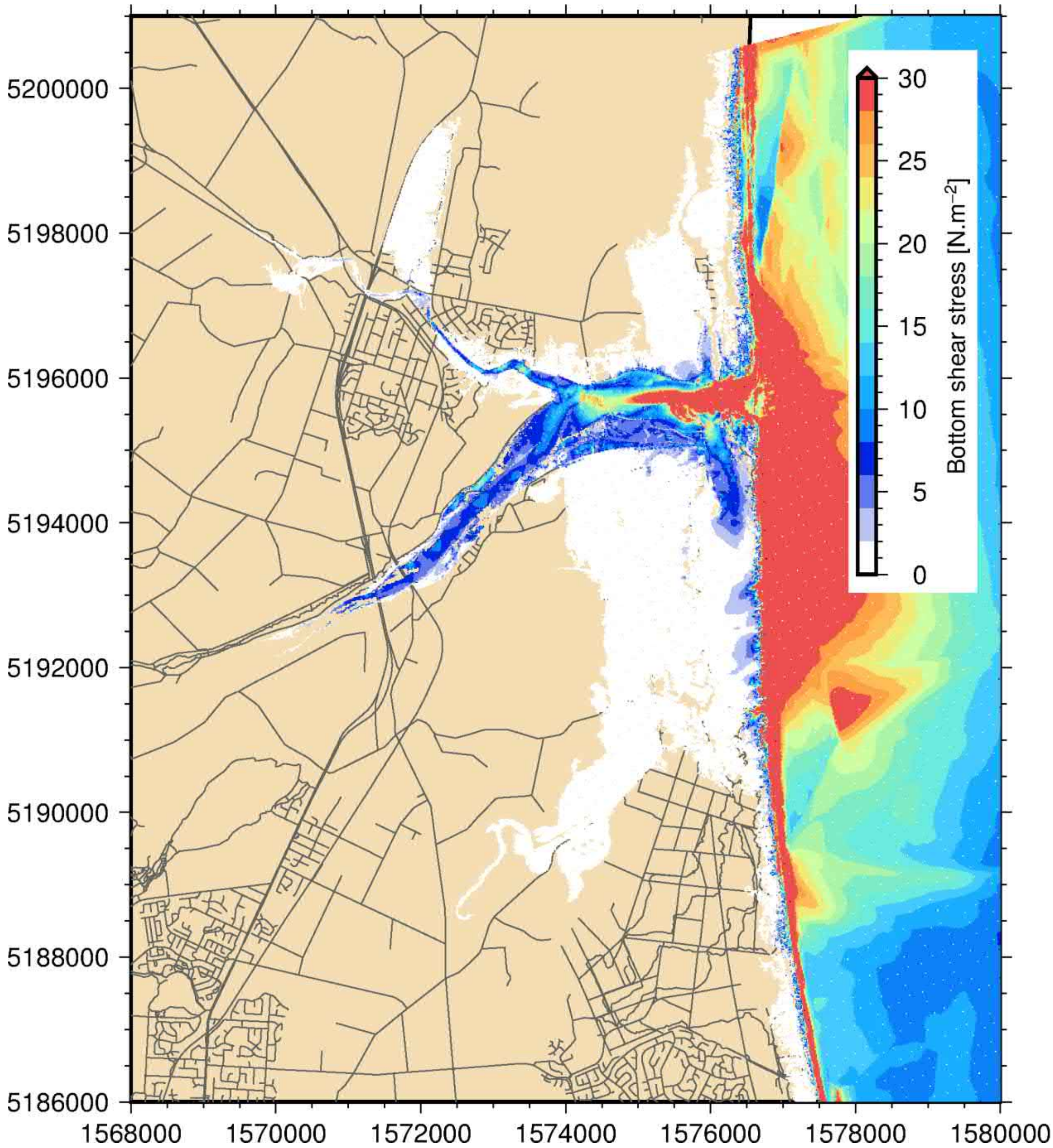

Figure 3-65: Maximum bottom shear stress for 1:2500-year return period - 2065 Sea Level Scenario – 0.41 m Sea Level Rise - Northern Section.

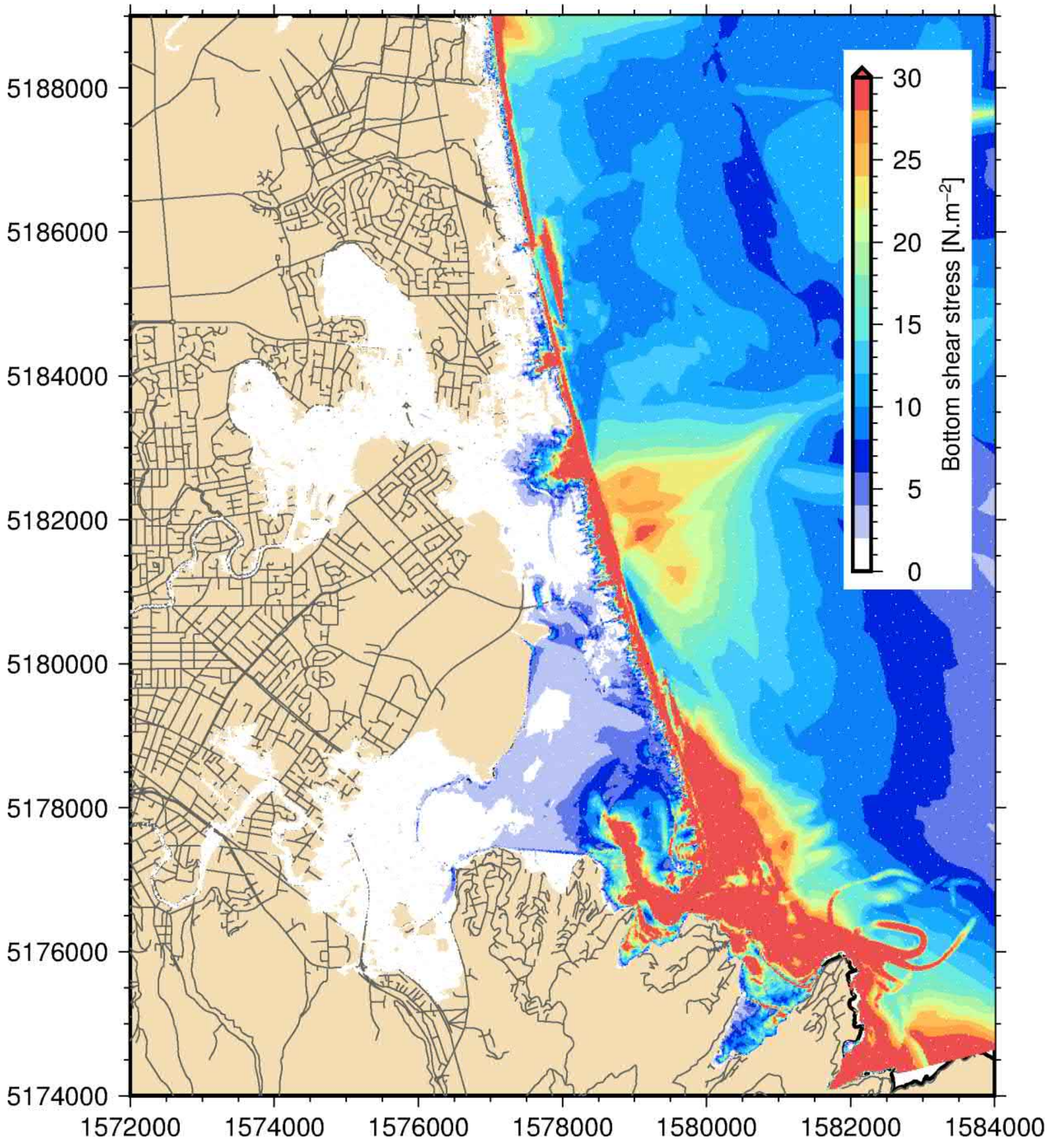

Figure 3-66: Maximum bottom shear stress for 1:2500-year return period - 2065 Sea Level Scenario – 0.41 m Sea Level Rise - Southern Section.

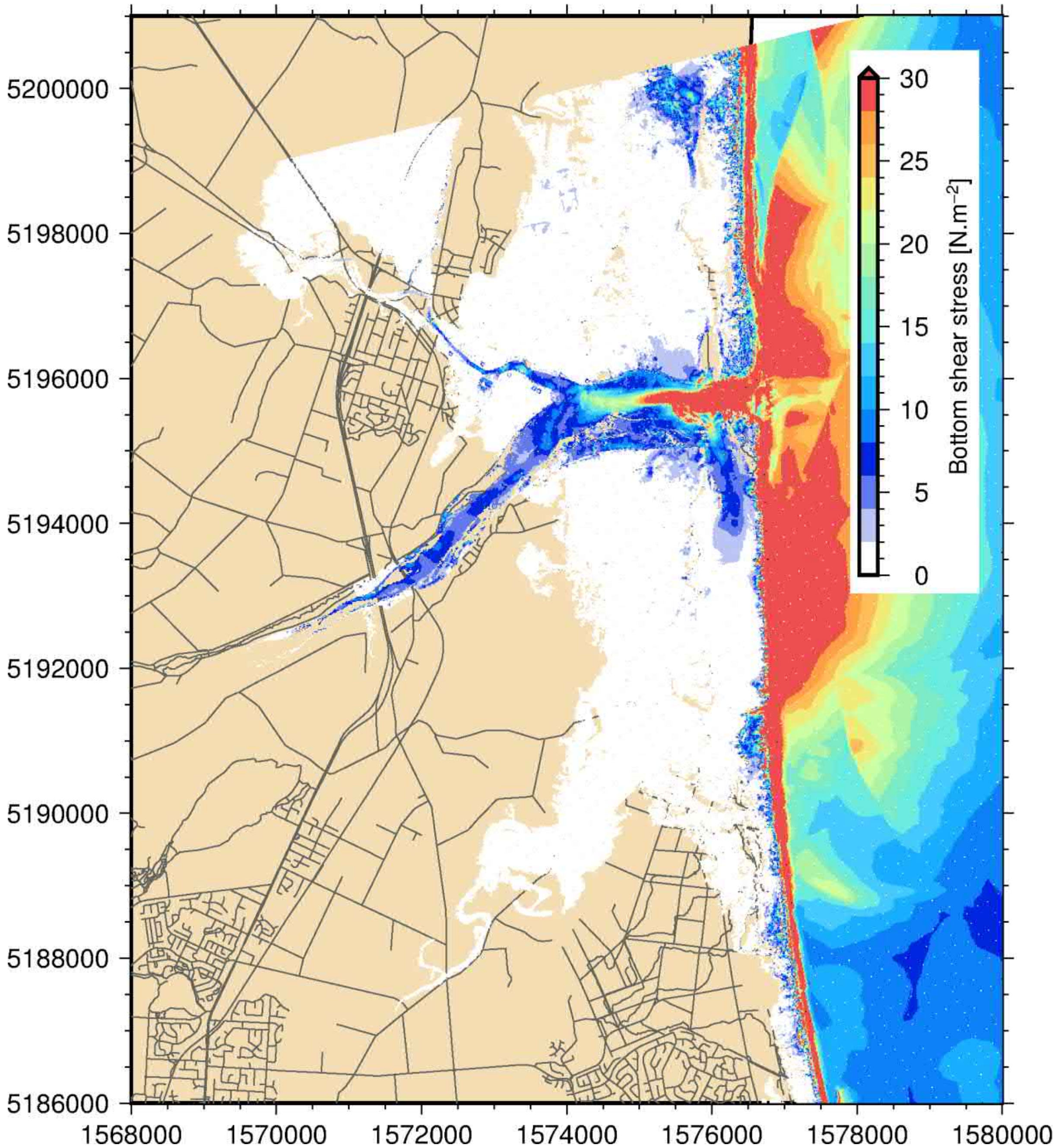

Figure 3-67: Maximum bottom shear stress for 1:2500-year return period - 2120 Sea Level Scenario – 1.06 m Sea Level Rise - Northern Section.

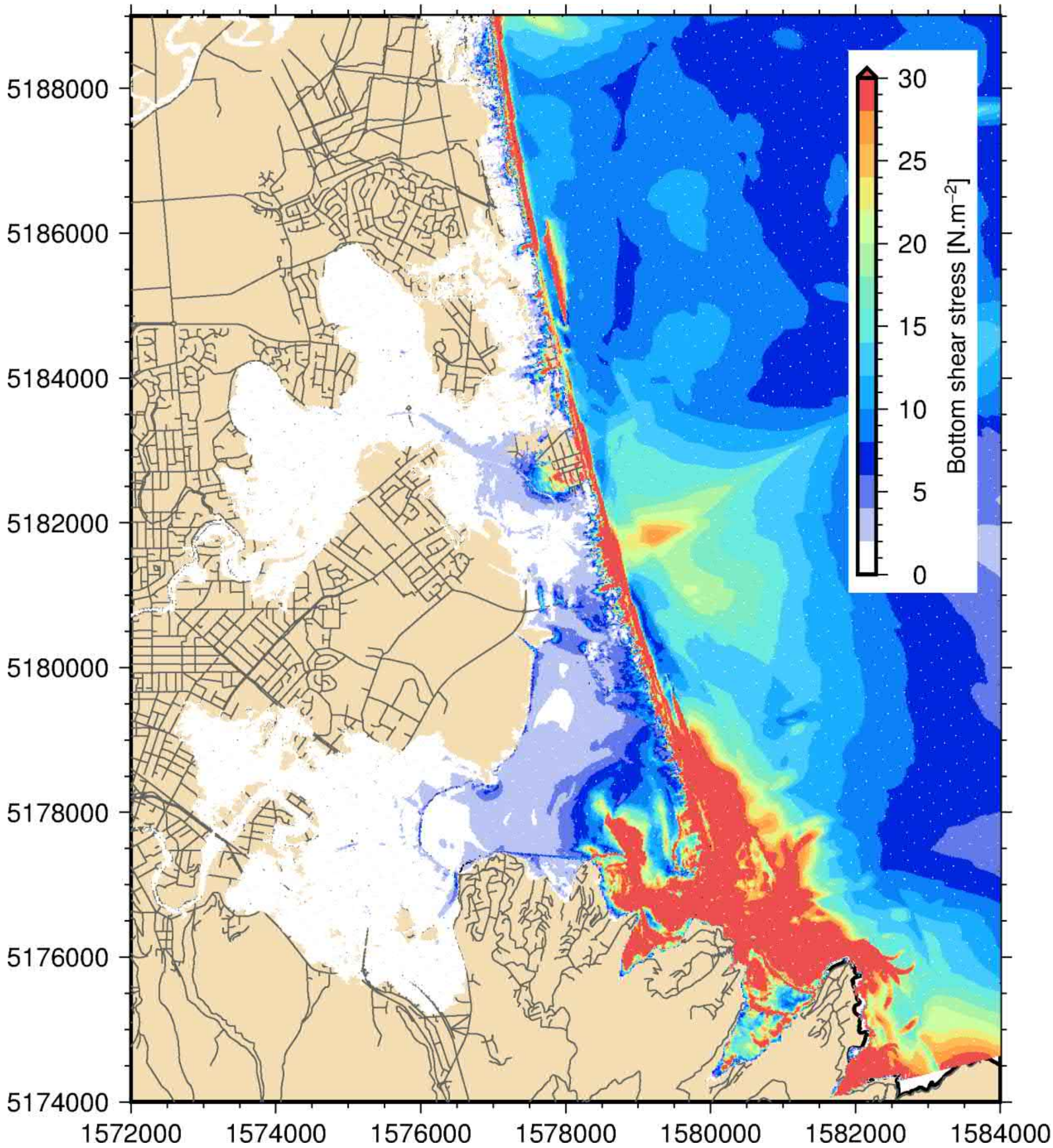

Figure 3-68: Maximum bottom shear stress for 1:2500-year return period - 2120 Sea Level Scenario – 1.06 m Sea Level Rise - Southern Section.

3.4.3 Flow velocity at bridges

Bridges are often associated with a flow constriction and subject to constriction scour during tsunami events. Depth-averaged flow velocity is presented here to qualitatively assess the scour at bridges. The tsunami simulation here does not take into account the flow under the bridge as the water level reaches the soffit of the bridge. It is also important to consider that tsunami transport large quantities of debris that can get caught by the bridge structure and further restrict the flow under a bridge.

Bridges that experience the highest flow velocity (Table 3-4 Table 3-5) are the Avon River Bridge Street bridge (e.g., Figure 3-69 and Figure 3-70), the Heathcote River Ferry Road bridge (e.g., Figure 3-71 and Figure 3-72), Heathcote River Tunnel Road bridge (e.g., Figure 3-73 and Figure 3-74) and bridges on the Waimakariri River (e.g., Figure 3-75 and Figure 3-76)

Table 3-4: Bridges on Waimakariri, Avon and Heathcote rivers with heights above LVD37 and modelled maximum tsunami flow velocity at those locations for the 1:500-year return period scenario.

Bridge	Bridge soffit level	1:500-year return period Tsunami flow speed [m/s]			
	above LVD37 (m)	Current Sea Level	2040 Sea Level 0.19 m Rise	2065 Sea Level 0.41 m Rise	2120 Sea Level 1.06 m Rise
Waimakariri River Main North Rd	7.8	1.47	1.58	1.65	1.76
Waimakariri River SH1		1.34	1.46	1.56	1.62
Avon River Bridge Street	6.2	3.08	3.17	3.00	2.75
Avon River Pages Road	4.2	0.47	0.42	0.51	0.44
Avon River Anzac Drive	4.2	0.68	0.94	1.24	2.00
Avon River Avondale Road	3.8	0.63	0.79	1.05	1.66
Heathcote River Ferry Road	4.6	2.77	2.91	2.98	2.99
Heathcote River Tunnel Road	4.3	0.86	1.15	1.52	1.91
Heathcote River Bamford Street	2.1	0.56	0.65	0.75	0.99
Heathcote River SH 74A		0.61	0.71	0.81	1.19
Heathcote River Connal Street		0.49	0.54	0.60	1.00
Heathcote River Radley Street		0.27	0.30	0.27	0.39

Table 3-5: Bridges on Waimakariri, Avon and Heathcote rivers with heights above LVD37 and modelled maximum tsunami height at those locations for the 1:2,500-year return period scenario.

Bridge	Bridge soffit level above LVD37 (m)	1:2,500-year return period Tsunami flow speed [m/s]		
		2040 Sea Level 0.19 m Rise	2065 Sea Level 0.41 m Rise	2120 Sea Level 1.06 m Rise
Waimakariri River Main North Rd	7.8	2.34	2.45	2.53
Waimakariri River SH1		2.26	2.45	2.67
Avon River Bridge Street	6.2	3.91	3.67	3.67
Avon River Pages Road	4.2	0.97	<u>1.22</u>	<u>1.19</u>
Avon River Anzac Drive	4.2	0.91	1.16	1.69
Avon River Avondale Road	3.8	0.74	0.91	<u>1.30</u>
Heathcote River Ferry Road	4.6	2.90	3.03	3.10
Heathcote River Tunnel Road	4.3	1.06	1.39	<u>1.73</u>
Heathcote River Bamford Street	2.1	0.58	<u>0.62</u>	<u>0.86</u>
Heathcote River SH 74A		0.62	0.66	0.96
Heathcote River Connal Street		0.45	0.50	0.73
Heathcote River Radley Street		0.23	0.28	0.29

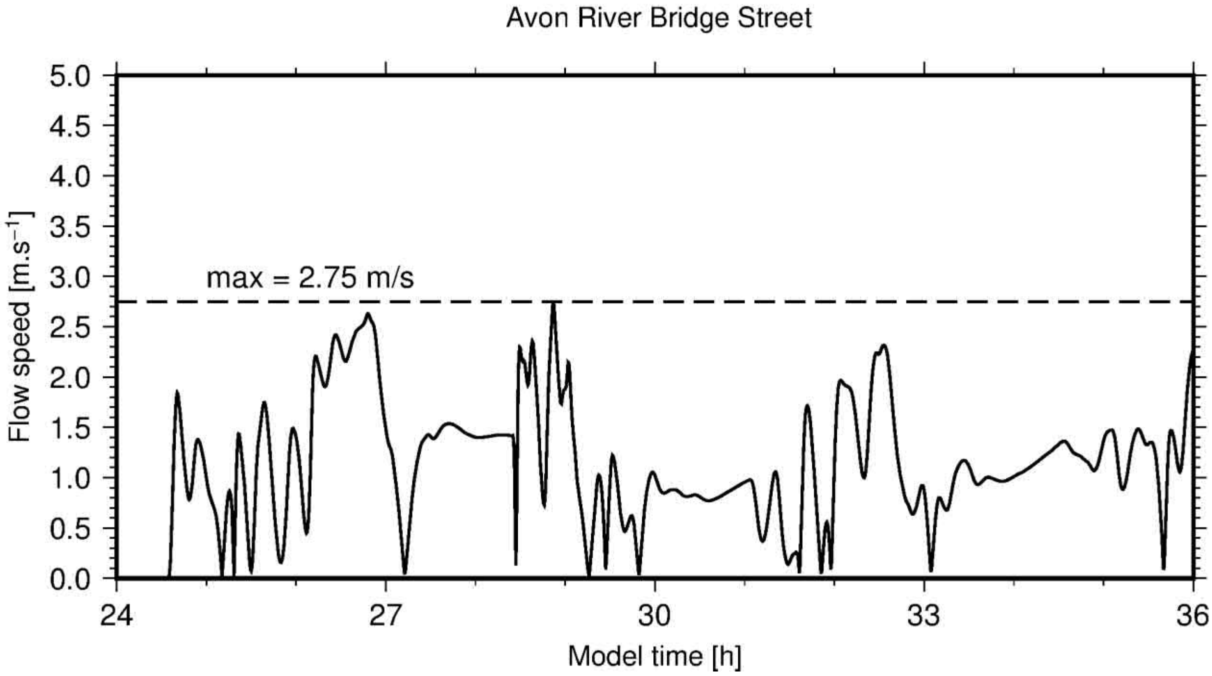

Figure 3-69: Flow velocity timeseries for 1:500-year return period – 2120 Sea Level Scenario – 1.06 m Sea Level Rise at Avon River Bridge Street bridge.

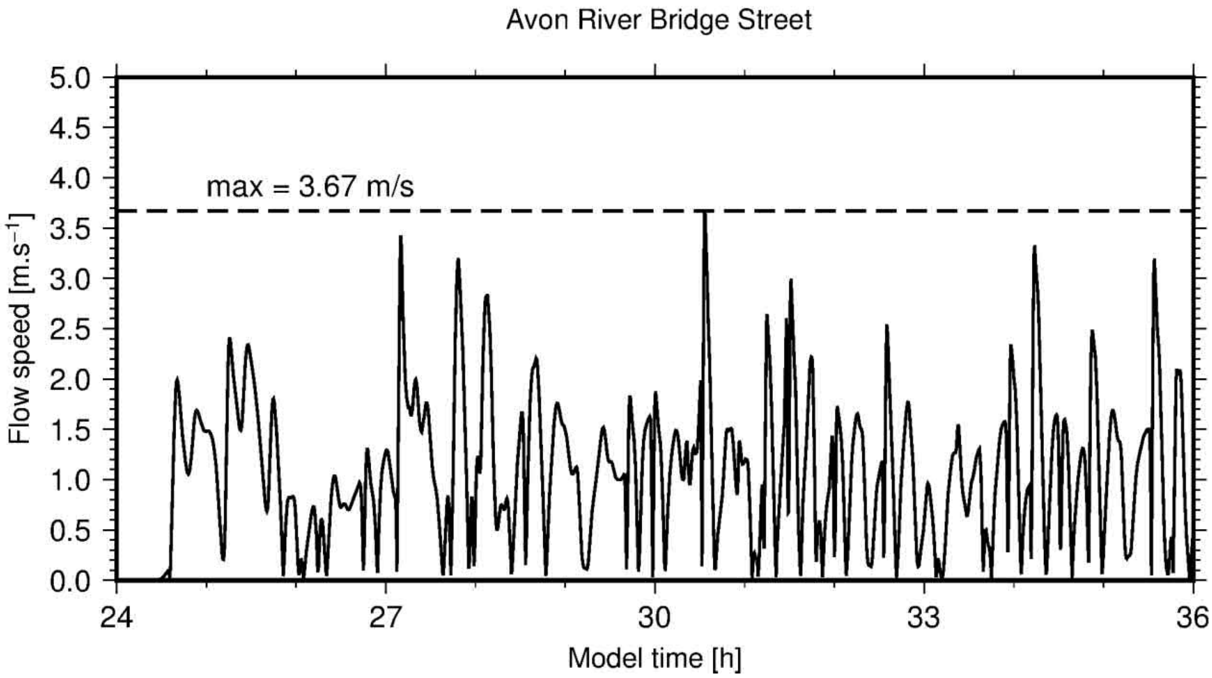

Figure 3-70: Flow velocity timeseries for 1:2,500-year return period – 2120 Sea Level Scenario – 1.06 m Sea Level Rise at Avon River Bridge Street bridge.

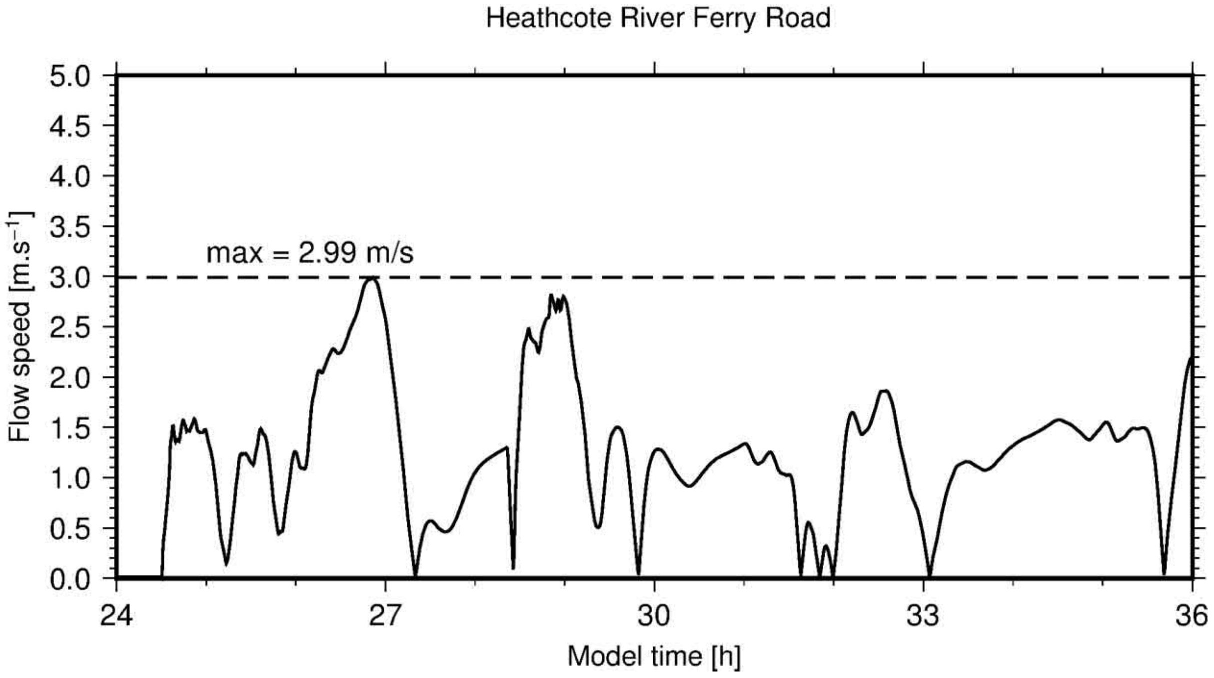

Figure 3-71: Flow velocity timeseries for 1:500-year return period – 2120 Sea Level Scenario – 1.06 m Sea Level Rise at Heathcote River Ferry Road bridge.

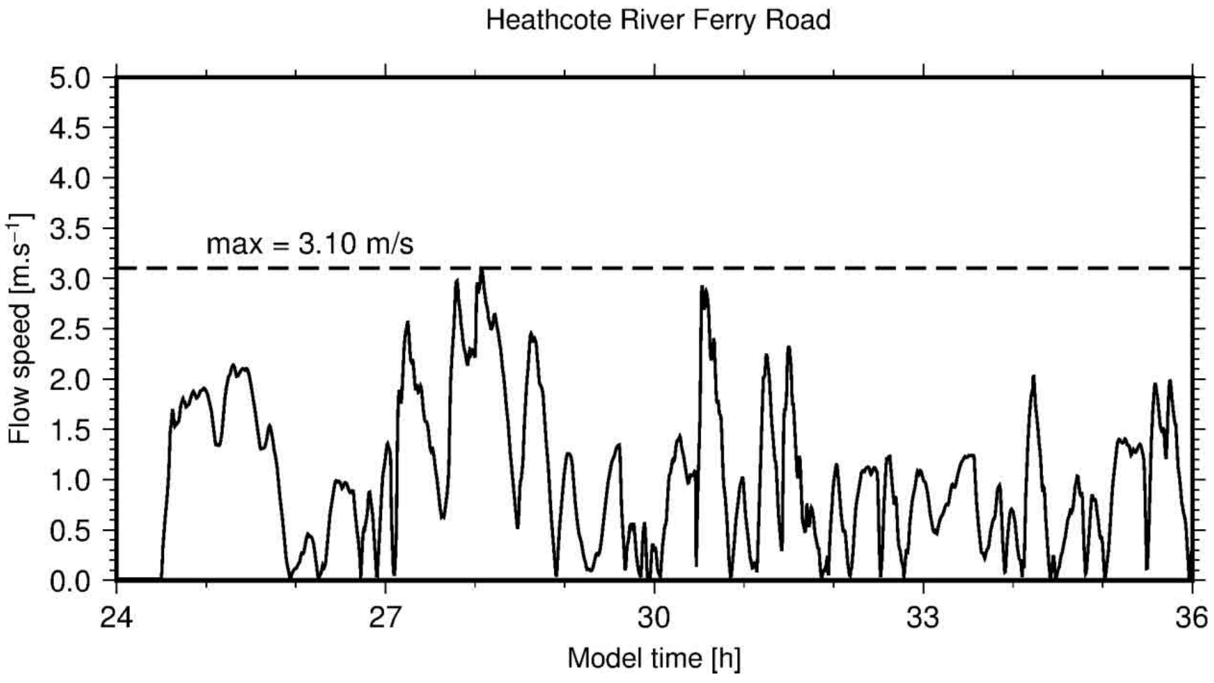

Figure 3-72: Flow velocity timeseries for 1:2,500-year return period – 2120 Sea Level Scenario – 1.06 m Sea Level Rise at Heathcote River Ferry Road bridge.

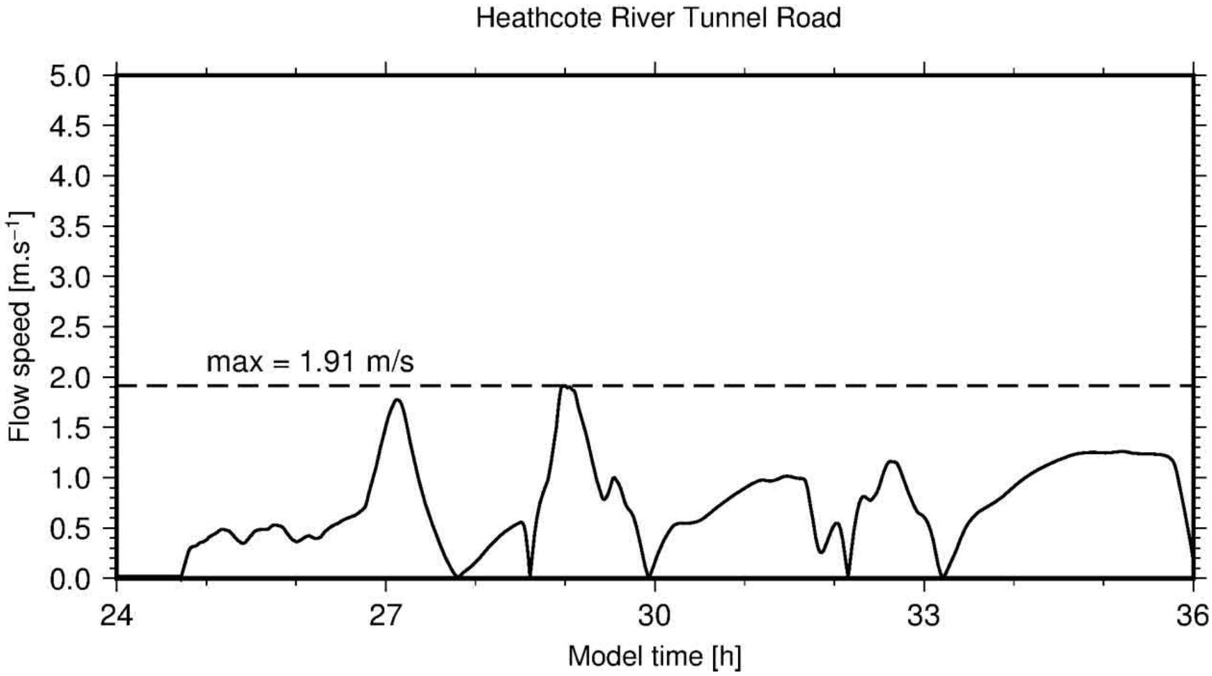

Figure 3-73: Flow velocity timeseries for 1:500-year return period – 2120 Sea Level Scenario – 1.06 m Sea Level Rise at Heathcote River Tunnel Road bridge.

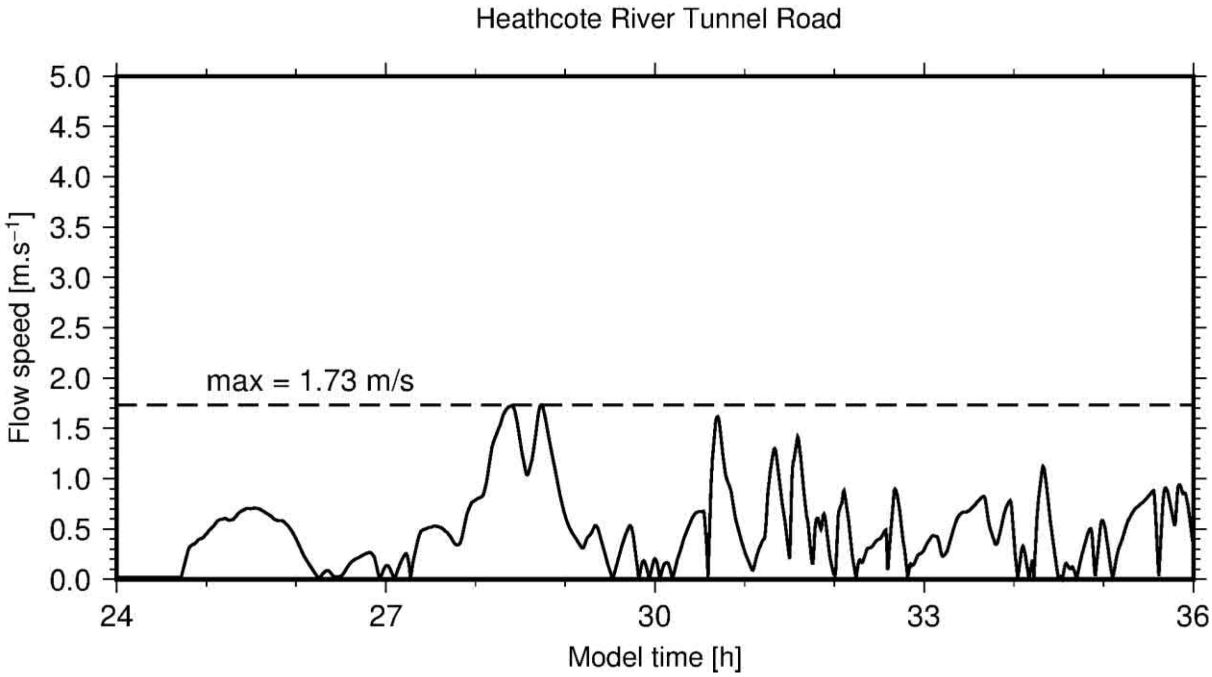

Figure 3-74: Flow velocity timeseries for 1:2,500-year return period – 2120 Sea Level Scenario – 1.06 m Sea Level Rise at Heathcote River Tunnel Road bridge.

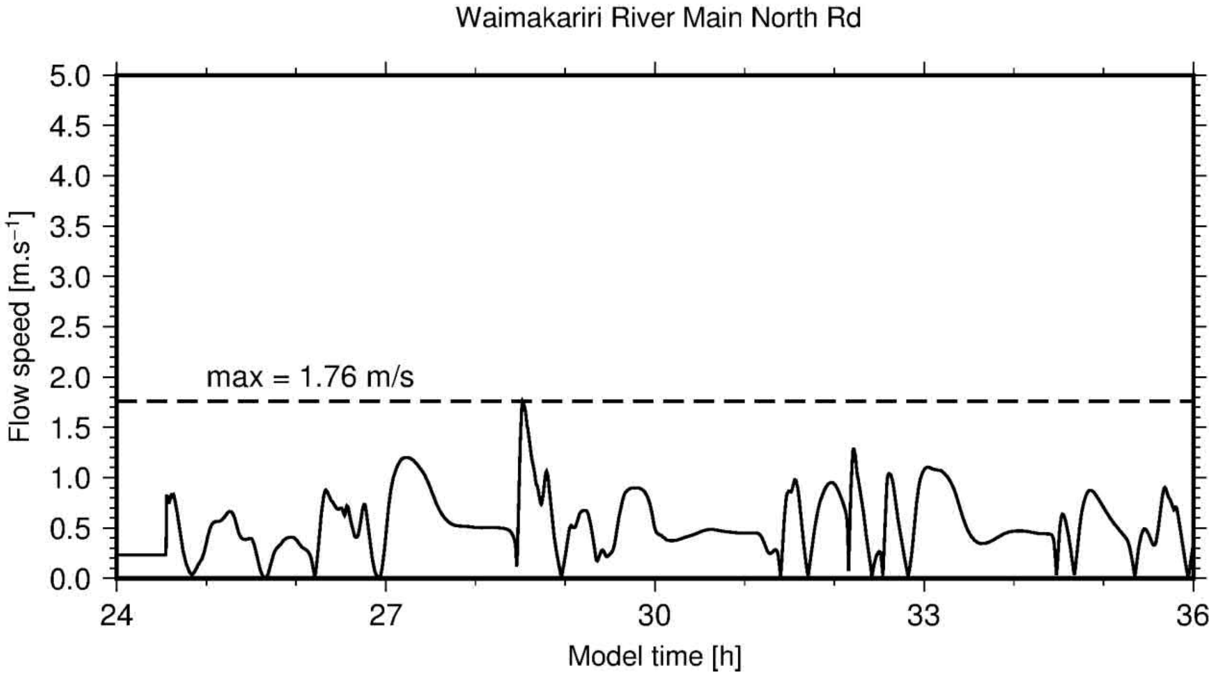

Figure 3-75: Flow velocity timeseries for 1:500-year return period – 2120 Sea Level Scenario – 1.06 m Sea Level Rise at the Waimakariri River Main North Road bridge.

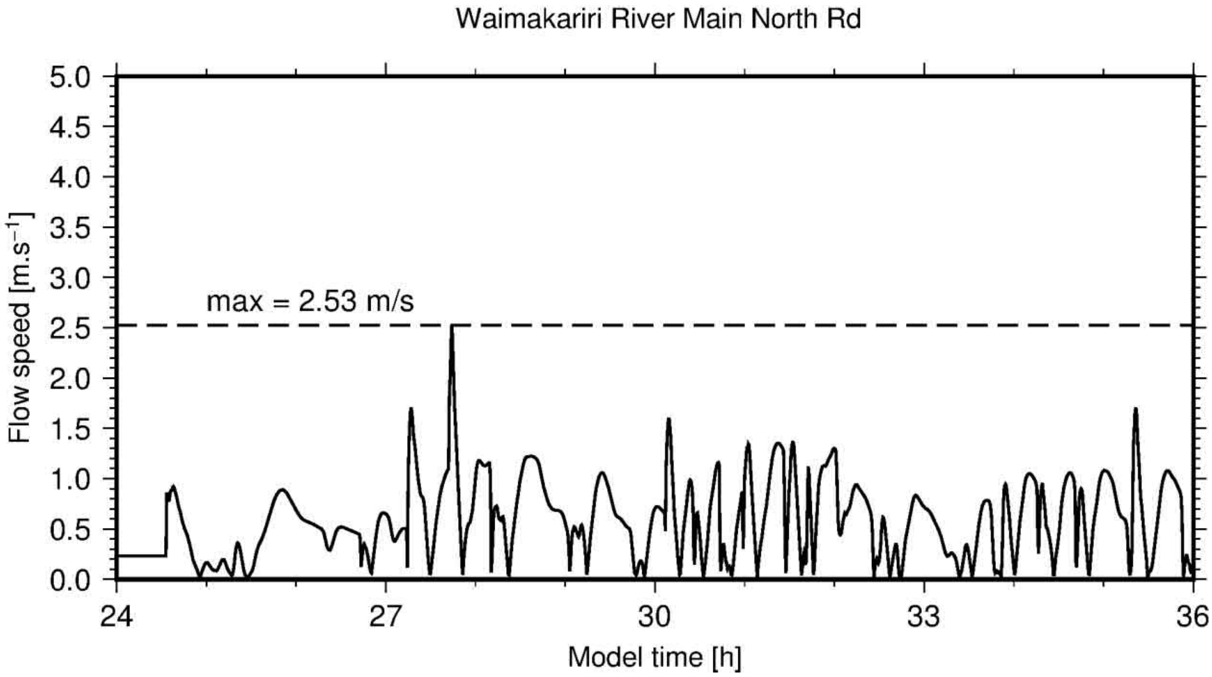

Figure 3-76: Flow velocity timeseries for 1:2,500-year return period – 2120 Sea Level Scenario – 1.06 m Sea Level Rise at the Waimakariri River Main North Road bridge.

4 Conclusion

NIWA was commissioned by Christchurch City Council (CCC) to carry out a numerical modelling study of tsunami inundation in Christchurch caused by two tsunamis originating from distant sources. The selected tsunami sources were a 1:500-year return period event cause by a magnitude 9.28 earthquake and a 1:2,500-year return period event caused by a magnitude M_w 9.485 earthquake both at the Peru subduction zone. The simulations were completed for different sea-level rise scenario (present day, 0.19 m, 0.41 m and 1.06 m) taking into account predicted shoreline changes predicted for 2065 and 2120. Note that the magnitude M_w 9.485 scenario at current sea-level was produced in a previous study (Lane et al. 2017) and not replicated here.

The simulations were completed at MHWS (1.2 m above the Lyttelton Vertical Datum 1937) adjusted according each sea level rise scenario. The flow of the Waimakariri River, Avon River and Heathcote River was also included in the model.

Both tsunami scenarios result in major inundation in Christchurch which, as expected, worsen with the higher sea-level scenarios. The model captures the complexity of the flow over the dunes and inland. The attenuation of the tsunami wave leads to a similar inundation extent for both tsunami scenarios but the inundation depth and flow velocity along the coastal strip was much larger for the worst-case tsunami (1:2,500-year scenario). The total inundation extent for the higher sea level rise scenario (1.06 m above present sea level) was 70 km^2 for the 1:500-year return period tsunami event, 79 per cent more than for the same tsunami occurring at present day sea level.

Such large tsunami events are expected to cause severe erosion to the dunes on the coastal strip and at the mouth of the Waimakariri River and the Avon-Heathcote Estuary. Severe erosion can also be expected at the Avon Bridge Street bridge and the Heathcote Ferry Road bridge.

5 References

Berenbrock C., Tranmer A.W., (2008) Simulation of Flow, Sediment Transport, and Sediment Mobility of the Lower Coeur d'Alene River, Idaho. U.S. Geological Survey Scientific Investigations Report 2008–5093.

Bind, J., Smart, G.M. (2010) Post-Tsunami damage assessment, Samoa, 9-21 October 2009. Current: newsletter of the New Zealand Hydrological Society. no. 37 (May 2010): 49-50.

Cameron, A.G. (1992) *A Hydrogeological Study of the Interaction between Avon River Baseflow and Shallow Groundwater*, Christchurch, New Zealand. Engineering Geology, University of Canterbury. Master of Science.

Kohout, A., Lane, E.M., Arnold, J. R., Sykes, J. (2015) Hikurangi Subduction Zone and Wairarapa Fault tsunami modelling for the Canterbury coast. *NIWA Client Report* Christchurch: 125.

Lane, E.M., Arnold, J.R. (2013) Tsunami inundation modelling for Kaikoura and North Canterbury. *NIWA Client Report*, Environment Canterbury: 31.

Lane, E.M., Bosserelle, C. (2017) Progress report on the tsunami project for LDRP. NIWA Client Report. Christchurch: 14.

Lane, E.M., Kohout, A., Chiaverini, A., Arnold, J.R. (2014) Updated inundation modelling in Canterbury from a South American tsunami. *NIWA Client Report* Christchurch, NIWA: 54.

Lane, E.M., Kohout, A., Sykes, J., Bind, J., Williams, S.P. (2017) Distant tsunami inundation modelling incorporating dune failures and river flow in Christchurch. *NIWA Client Report* Environment Canterbury: 51.

Lee, H.S., Shimoyama, T., Popinet, S. (2015) Impacts of tides on tsunami propagation due to potential Nankai Trough earthquakes in the Seto Inland Sea, Japan. *Journal of Geophysical Research-Oceans* 120(10): 6865-6883.

Measures, R., Bind, J. (2013) Hydrodynamic model of the Avon Heathcote Estuary: Model build and calibration. *NIWA Client Report* Christchurch.

Okada, Y. (1985) Surface deformation due to shear and tensile faults in a half-space. *Bulletin of the Seismological Society of America* 75(4): 1135-1154.

Orchard, S., Measures, R. (2016) Development of a fine-scale salinity model for the Avon Heathcote Estuary Ihutai. Technical Report developed for the Brian Mason Scientific and Technical Trust: 25.

Popinet, S. (2003) Gerris: a tree-based adaptive solver for the incompressible Euler equations in complex geometries. *Journal of Computational Physics* 190(2): 572-600.

Popinet, S. (2011) Quadtree-adaptive tsunami modelling. *Ocean Dynamics.* Vol. 61, no. 9.: 1261-1285.

Popinet, S. (2012) Adaptive modelling of long-distance wave propagation and fine-scale flooding during the Tohoku tsunami. *Natural Hazards and Earth System Sciences* 12(4): 1213-1227.

Popinet, S. (2015) Basilisk. from basilisk.fr.

Power, W.L. (2013) Review of Tsunami Hazard in New Zealand (2013 Update). GNS Science Consultancy Report 2013/131: 222.

Power, W.L. (2014) 84th Percentile/2500-year Peruvian quake for Canterbury. M. Gadsby, E. M. Lane and H. Brackley.

Power, W.L. (2014) Tsunami hazard curves and deaggregation plots for 20 km coastal sections, derived from the 2013 Nation Tsunami Hazard Model. GNS Science Report

Smart, G.M. (2017) Faster efficient flood forecasting. National Hazard Research Platform Final Report. Christchurch: 20.

Tang, L., Titov, V. V., Chamberlin, C.D. (2010) PMEL Tsunami Forecast Series: Vol. 1, A Tsunami forecast Model for Hilo, Hawaii. NOAA OAR Special Report, NOAA: 108.

Tonkin & Taylor Ltd (2017) Coastal Hazard Assessment for Christchurch and Banks Peninsula (2017). Client Report prepared for Christchurch City Council. Christchurch, Tonkin & Taylor Ltd: 86.

6 Appendix A Future Topography

Future sea level rise is associated with shoreline retreat for the coast south of Christchurch (Tonkin & Taylor Ltd 2017). This shoreline retreat was applied to the topography of the shore, for the scenario with sea level rise for 2065 (0.41 m) and the scenario for 2120 (1.06 m), by shifting, landward, the present shore topography based on the shoreline retreat estimated by Tonkin & Taylor Ltd (2017). Below are figure showing the present topography (Figure A-1) and the future topography (Figure A-2 and Figure A-3). The comparison of the different topography is is illustrated in (Figure A-4).

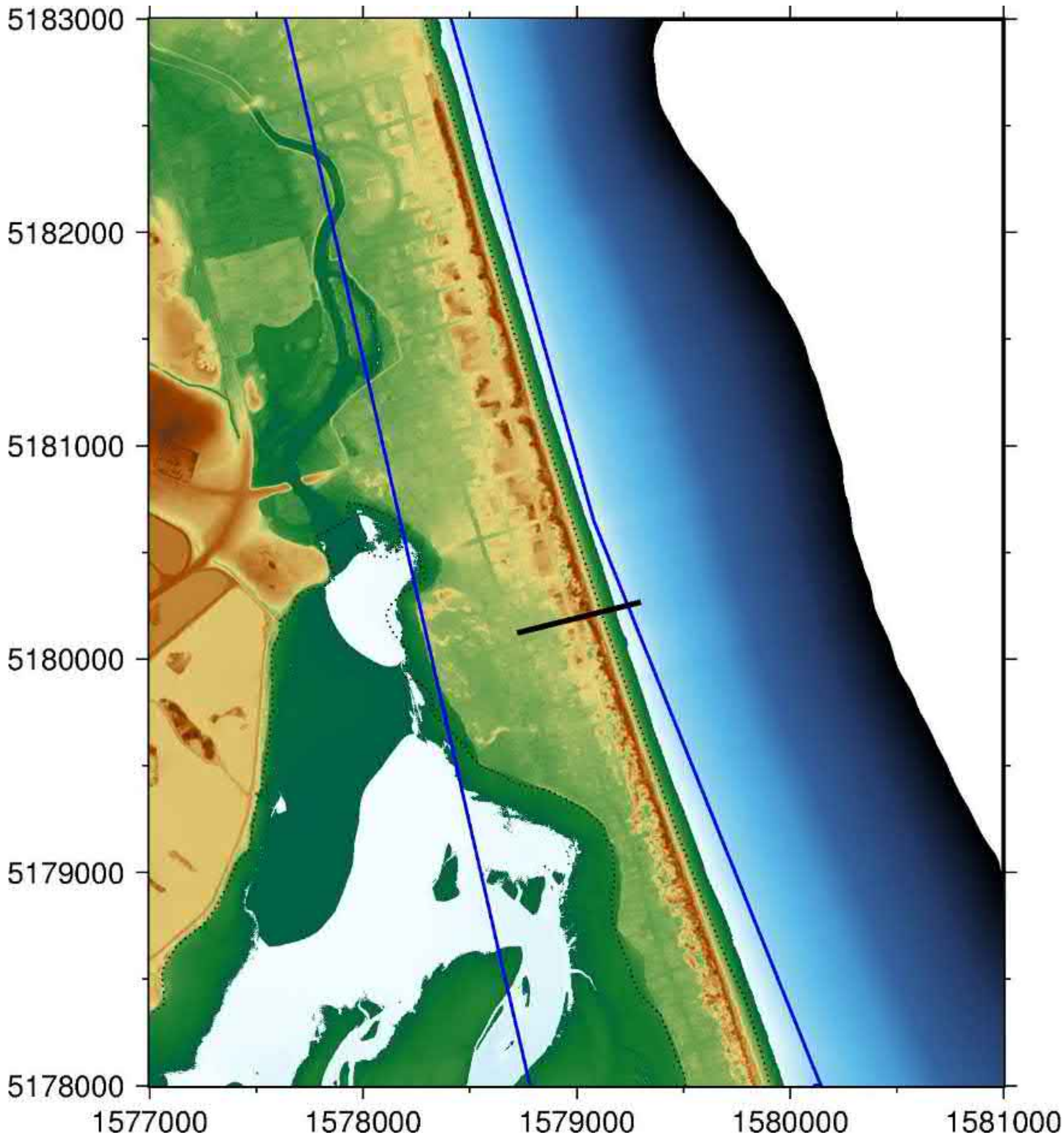

Figure 6-1: Topography and bathymetry of the Brighton shore – Present. The dotted line shows the present shoreline, as defined by LINZ datasets at MHWS; the blue plain line shows the extent of the domain change in the tsunami simulations; the thick black line shows the location of the 600 m long cross-shore profile presented in Figure 6-4. The estuarine/marine edge of the green shading is defined by mean level of sea. Colour shading is indicative.

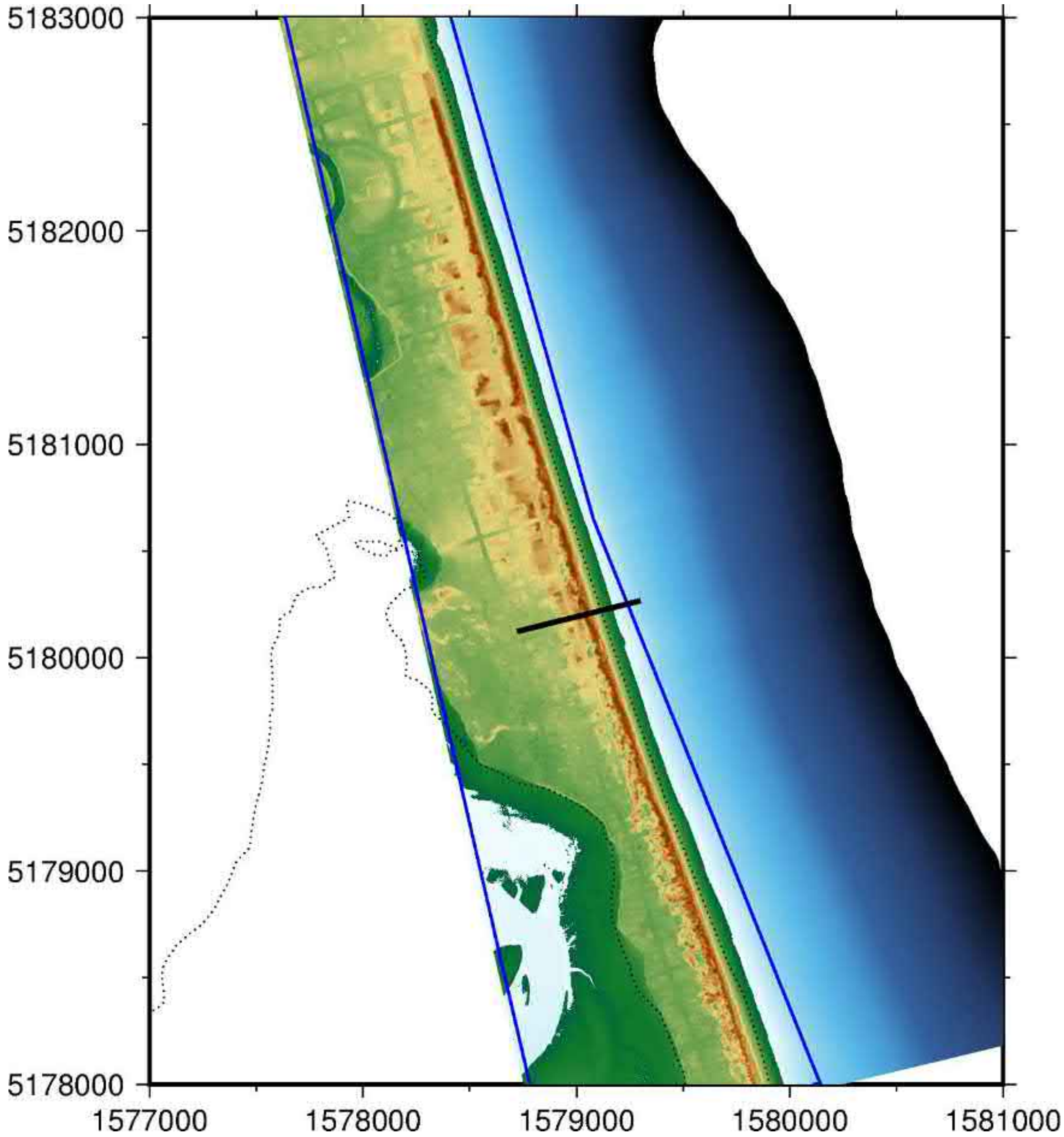

Figure 6-2: Topography and bathymetry of the Brighton shore – 2065. The dotted line shows the present shoreline, as defined by LINZ datasets at MHWS; the blue plain line shows the extent of the domain change in the tsunami simulations; the thick black line shows the location of the 600 m long cross-shore profile presented in Figure 6-4. The estuarine/marine edge of the green shading is defined by mean level of sea. Colour shading is indicative.

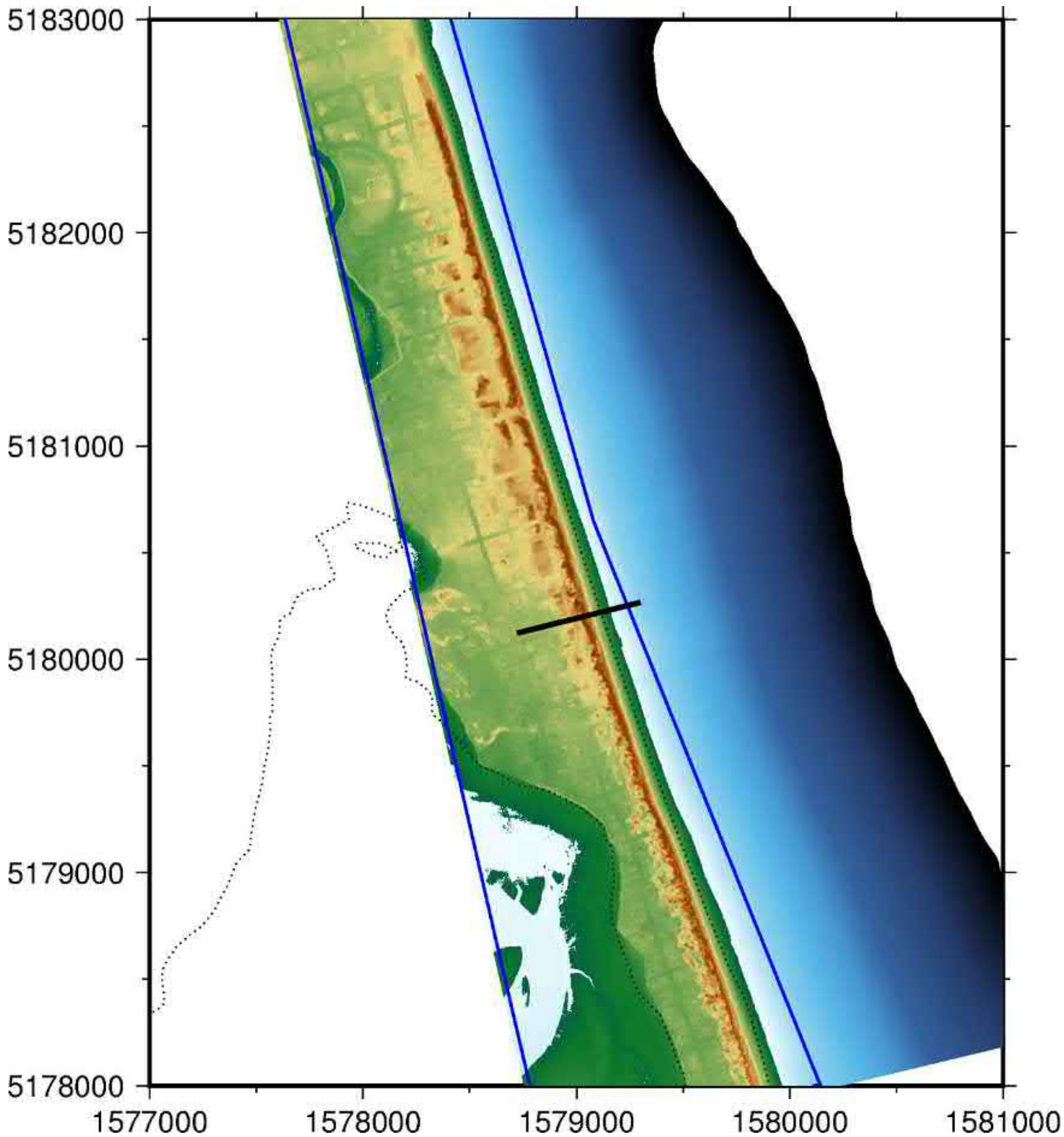

Figure 6-3: Topography and bathymetry of the Brighton shore – 2120. The dotted line shows the present shoreline, as defined by LINZ datasets at MHWS; the blue plain line shows the extent of the domain change in the tsunami simulations; the thick black line shore shows the location of the 600m long cross-shore profile presented in Figure 6-4. The estuarine/marine edge of the green shading is defined by mean level of sea. Colour shading is indicative.

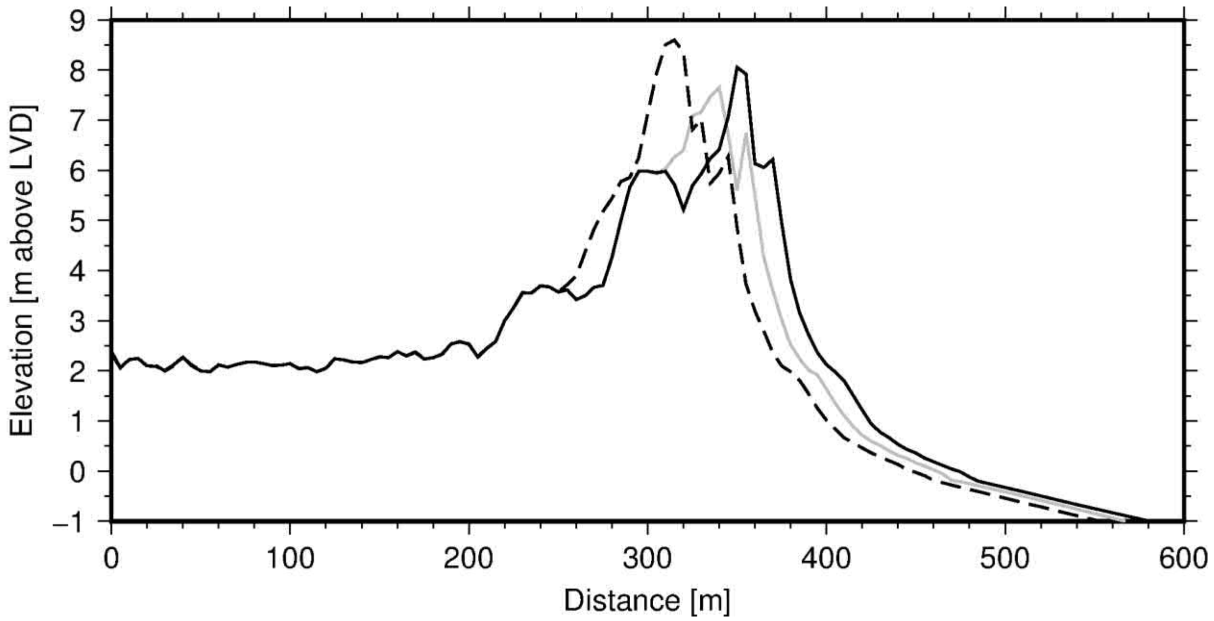

Figure 6-4: Topography along a cross-shore profile. The black line is the present topography (along the cross-section shown in Figure 6-1), the grey line is the 2065 topography (along the cross-section shown in Figure 6-2), the dashed line is the 2120 topography (along the cross-section shown in Figure 6-3). Where only the black line is visible, the three lines are on top of each other.

7 Appendix B Progress Report

7.1 Local Source

Local faults with a high likelihood of causing a significant tsunami in Christchurch between Sumner and Waimakariri River mouth were identified in consultation with Dr Phil Barnes based on data in Barnes et al. (2016). Faults rupture parameters are taken from Barnes (personal communication). Figure 7-1 shows the locations of the faults used and Table 7-1 give some of their parameters. The maximum values for rupture parameters were used to test the worst-case scenarios for local faults. The four scenarios modelled were two single fault ruptures and two multiple fault ruptures, viz.:

- LeithfieldNC1137.
- Pegasus1nw.
- LeithfieldNC1137 and NorthCant8.
- Pegasus1nw and NorthCant4.

Figure 7-1: Faults used in local tsunami modelling. Single fault rupture scenarios of LeithfieldNC1137 and Pegasus1nw are modelled as well as combined fault of LeithfieldNC1137 and NortCant8 and Pegasus1nw and NorthCant4.

Table 7-1: Faults used in local tsunami scenarios. Maximum length, slip, magnitude and associated recurrence interval.

Fault Name	Length (km)	Slip (cm)	Mw	Recurrence interval (years)
Leithfield1137	45.1	236	7.4	12,500
Pegasus1nw	40.7	213	7.3	22,500
NorthCant4	25.3	132	7.0	35,000
NorthCant8	37.4	195	7.3	21,000

The magnitude of the combined LeithfieldNC1137 and NorthCant8 faults rupturing is M_w 7.7, and for Pegasus1nw and NorthCant4 combined it is M_w 7.6.

Figure 7-2 to Figure 7-5 show the maximum water level over four hours of simulation from the four scenarios and Figure 7-6 to Figure 7-9 show close-ups for the region of interest. Note that the baseline water level for these runs is set to mean sea level. In all four scenarios, the northern portion of Pegasus Bay and the northern facing bays on Banks Peninsula are considerably more affected than the area of Christchurch City between Sumner and the Waimakariri River mouth. The scenario that most affects that region is the combined LeithfieldNC1137 and NorthCant8, where maximum wave height at coast exceed 3 m in some parts of that region and run-up can be up to 6 m. The combined Pegasus1nw and NorthCant4 scenario has maximum wave heights at coast of up to 2 m, with run-ups potentially higher. The single faults scenarios (LeithfieldNC1137 fault and Pegasus1nw fault) give maximum wave heights at coast around Christchurch of up to 1.5 m. Figure 7-10 shows time series of the water levels at locations approximately 500 m off-shore New Brighton, Sumner and Lyttelton for the four scenarios. Based on this modelling we recommend inundation modelling of the combined LeithfieldNC1137 and NorthCant8 scenario and the combined Pegasus1nw and NorthCant4 rupture scenario.

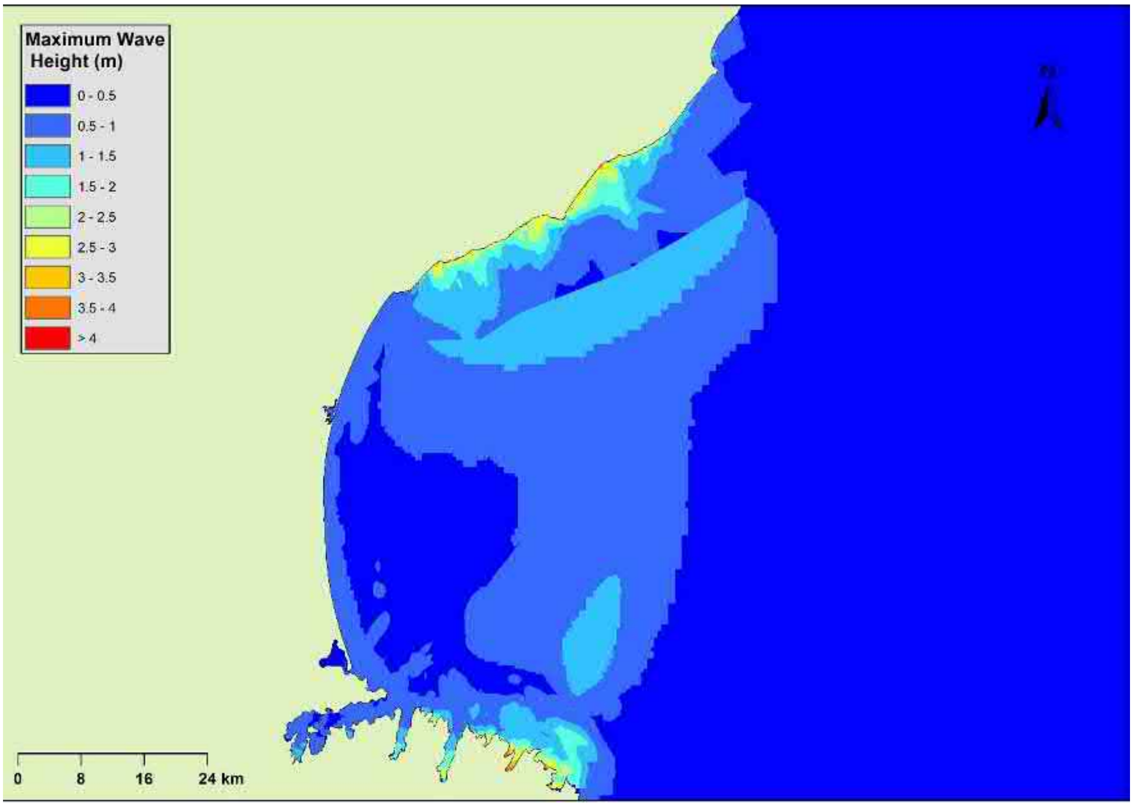

Figure 7-2: Maximum water level over entire simulation for rupture of LeithfieldNC1137 fault.

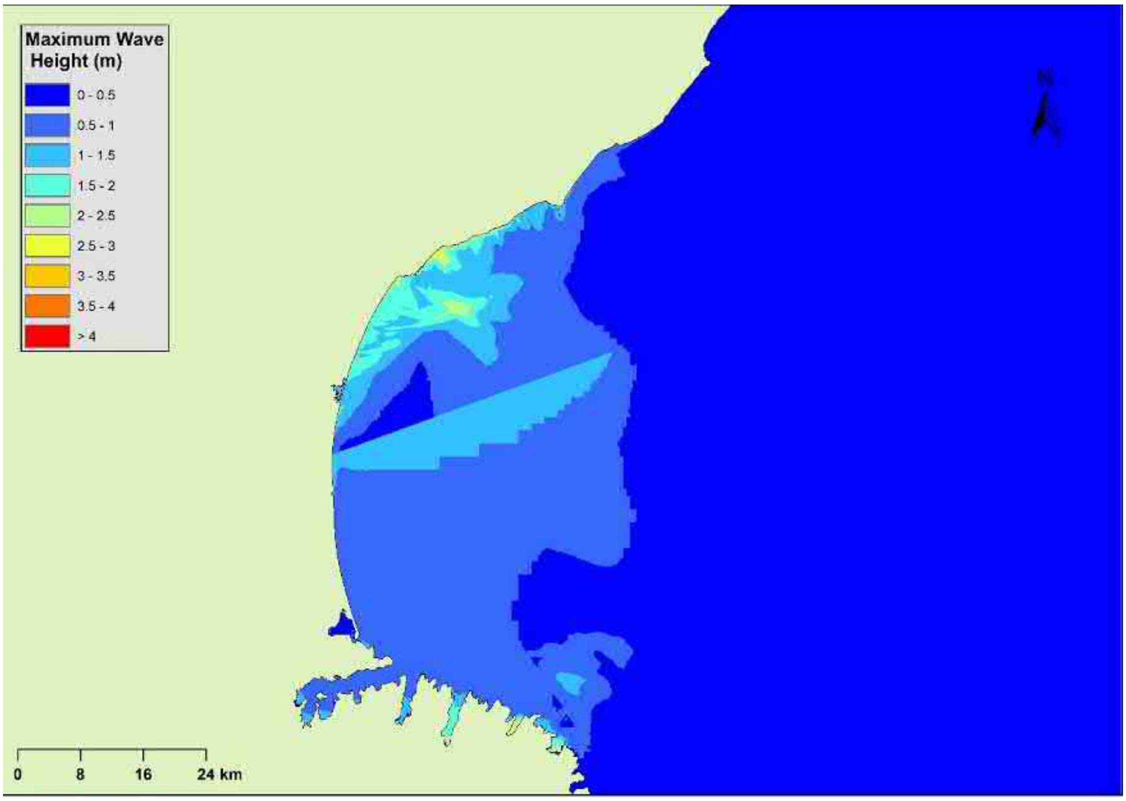

Figure 7-3: Maximum water level over entire simulation for rupture of Pegasus1nw fault.

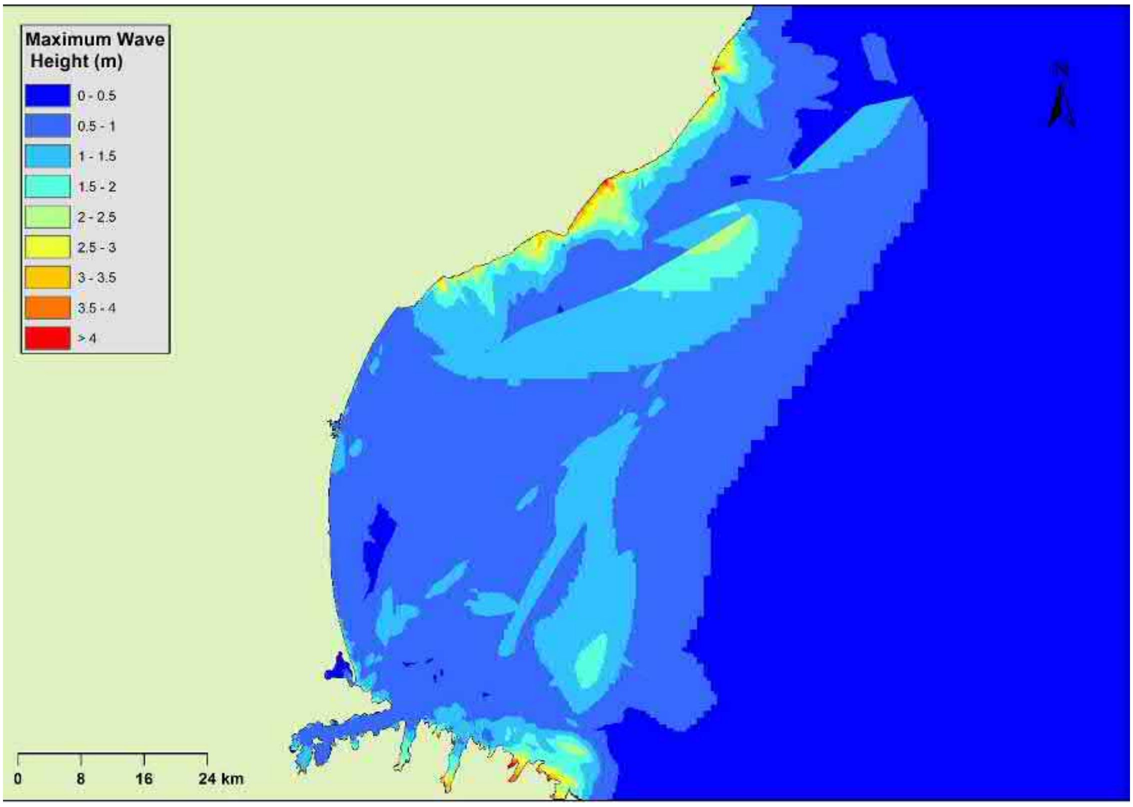

Figure 7-4: Maximum water level over entire simulation for rupture of LeithfieldNC1137 and NorthCant8 faults.

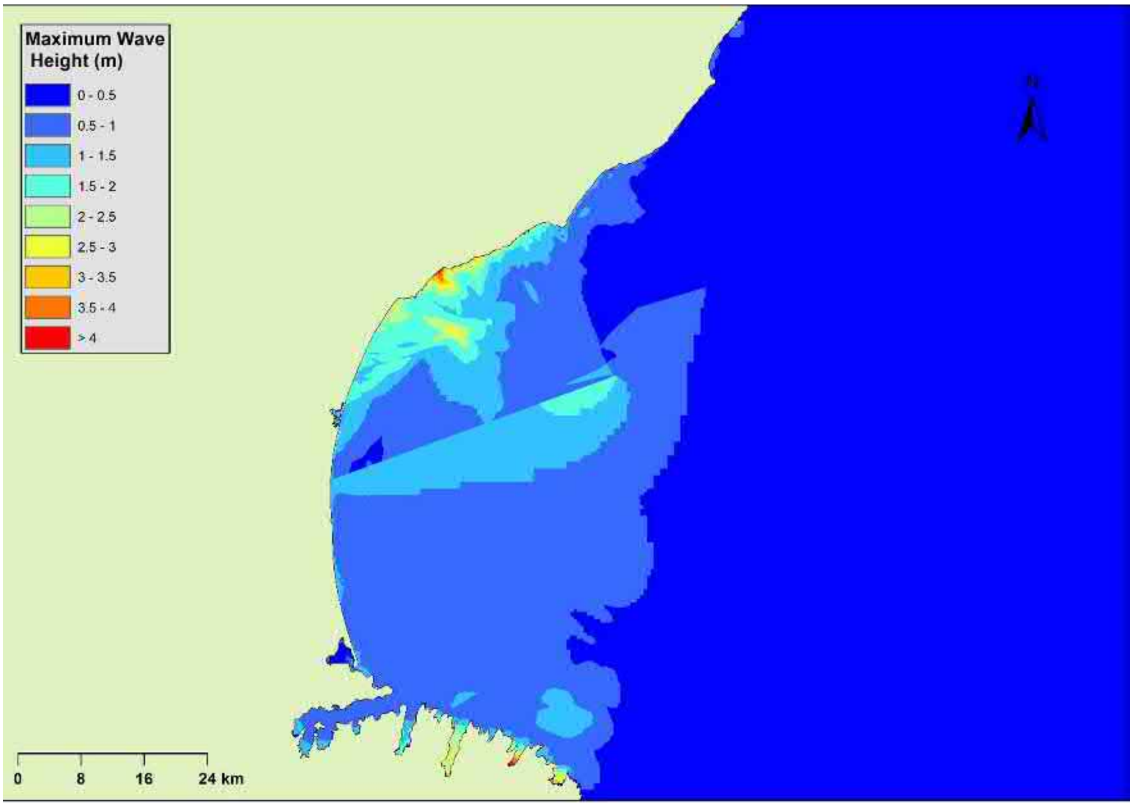

Figure 7-5: Maximum water level over entire simulation for rupture of Pegasus1nw and NorthCant4 faults.

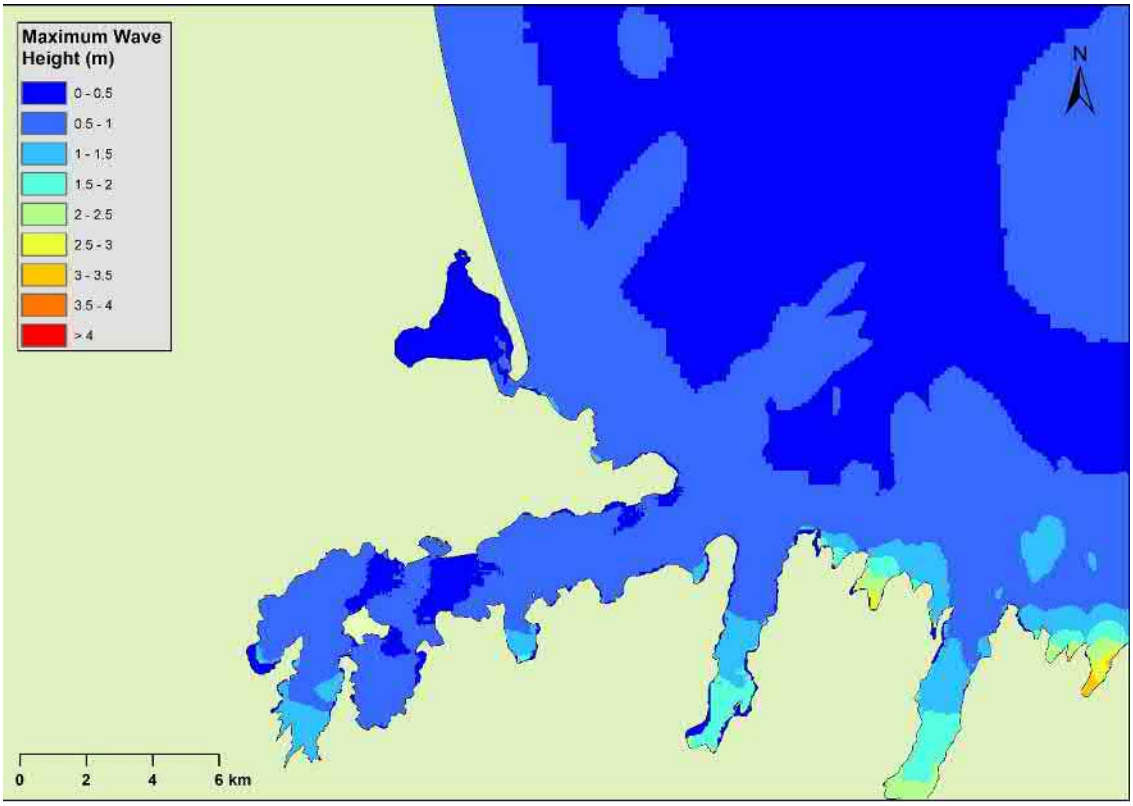

Figure 7-6: Close-up of Christchurch City: Maximum water level over entire simulation for rupture of LeithfieldNC1137 fault.

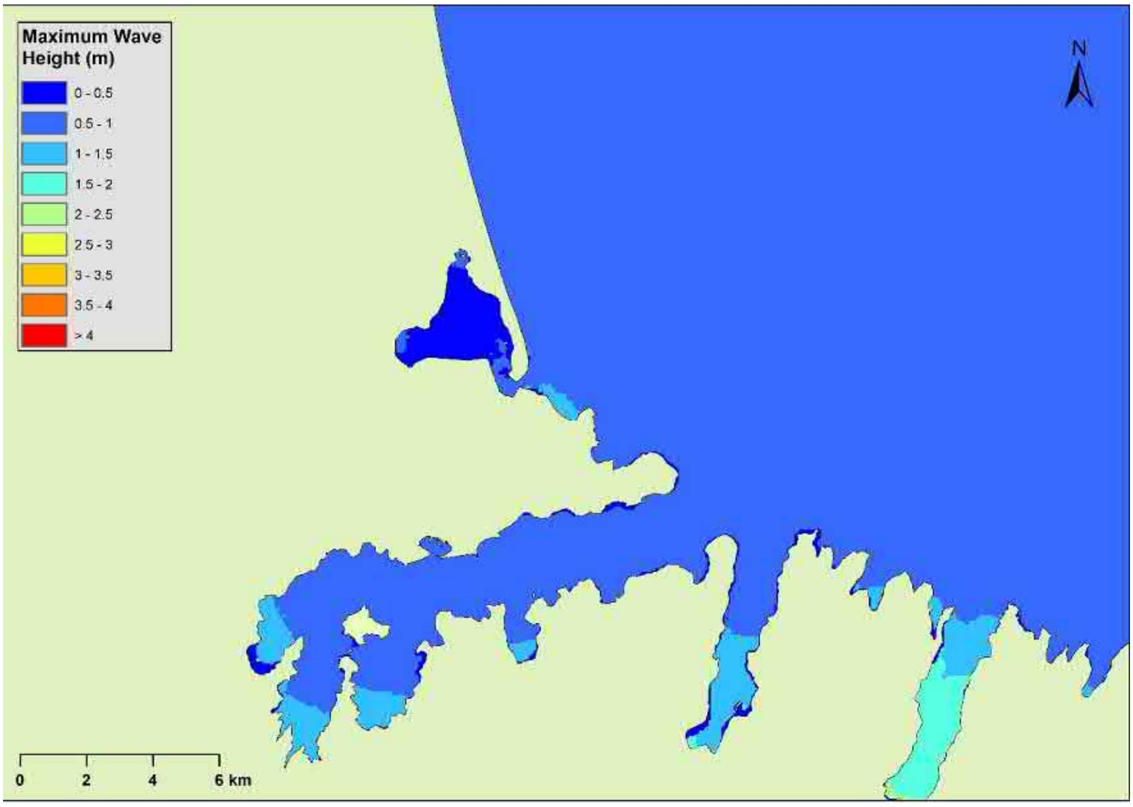

Figure 7-7: Close-up of Christchurch City: Maximum water level over entire simulation for rupture of Pegasus1nw fault.

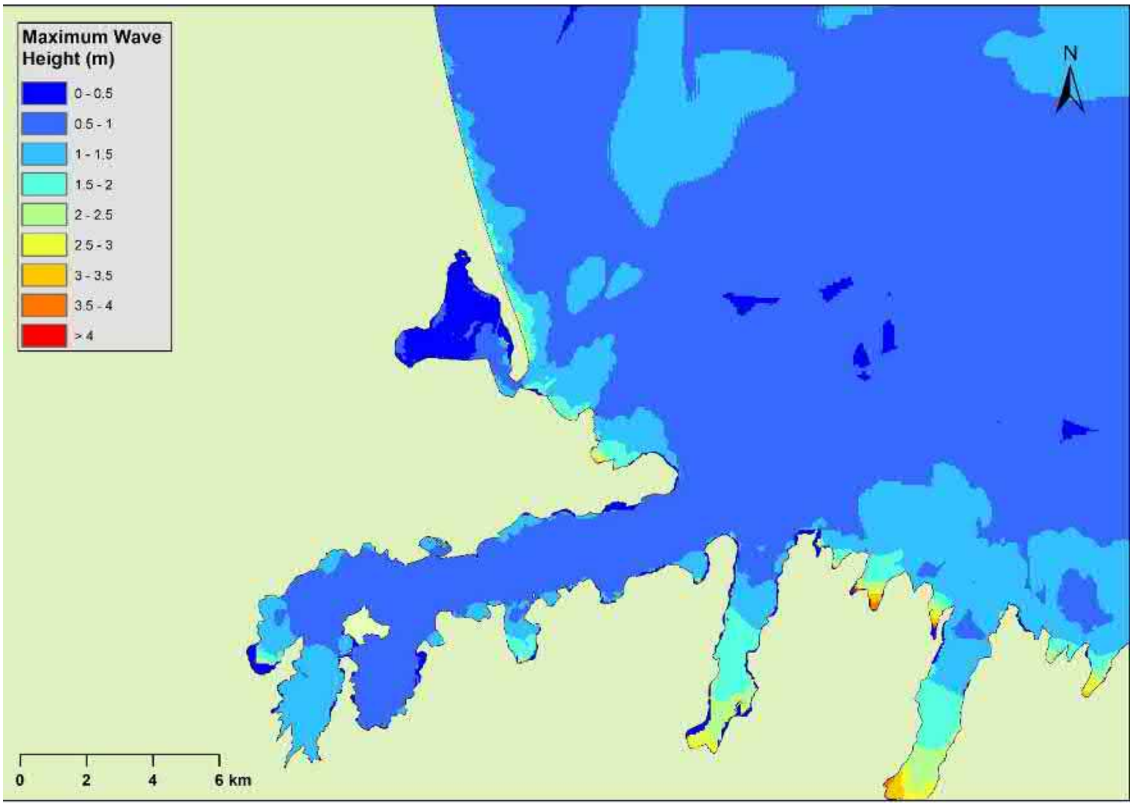

Figure 7-8: Close-up of Christchurch City: Maximum water level over entire simulation for rupture of LeithfieldNC1137 and NorthCant8 faults.

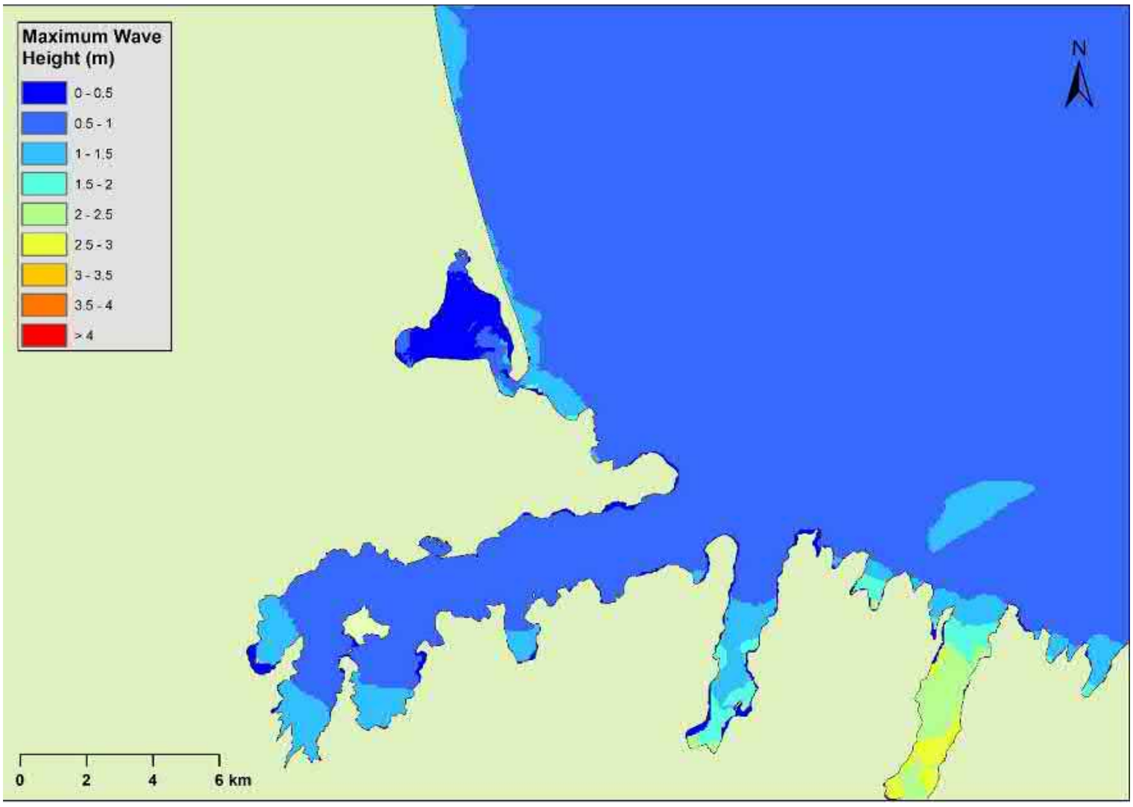

Figure 7-9: Close-up of Christchurch City: Maximum water level over entire simulation for rupture of Pegasus1nw and NorthCant4 faults.

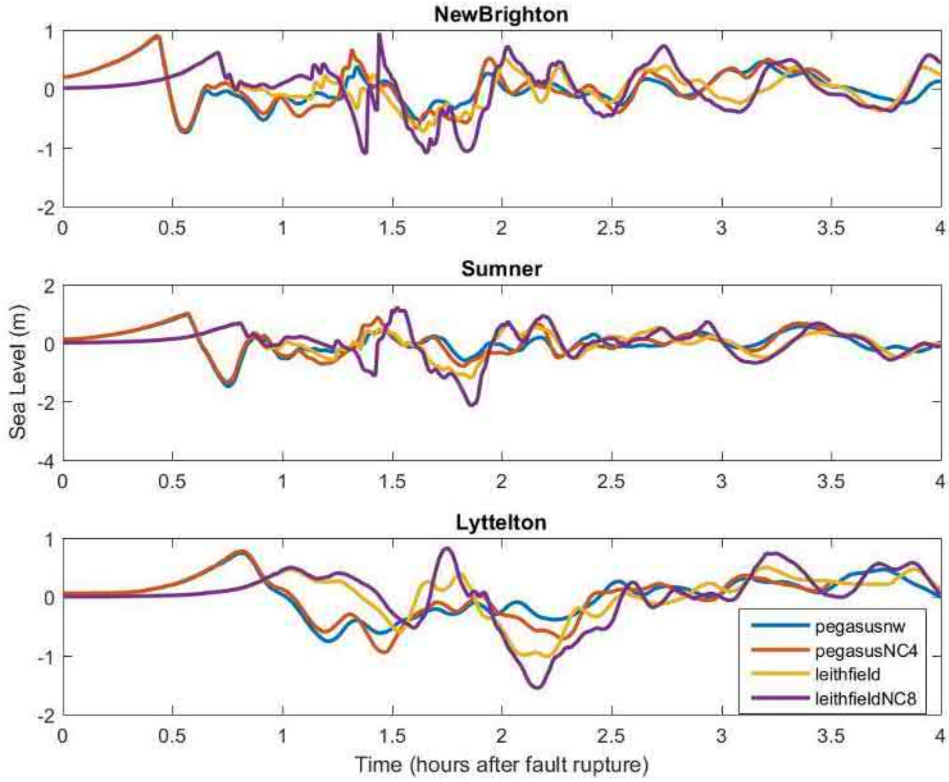

Figure 7-10: Time series for tsunamis off-shore New Brighton, Sumner and Lyttelton.

7.2 Far field tsunami

The following scenarios were chosen for far-field tsunami inundation modelling based on the disaggregation analysis of Power (2013,2014):

- 1:500-year tsunami inundation in Christchurch City due to a M_w 9.28 subduction earthquake occurring off the coast of Peru (the most likely source for a 1:500-year tsunami for Christchurch City at 50th percentile as identified by Power 2013; 2014).
- 1:2,500-year tsunami inundation (maximum credible tsunami) in Christchurch City due to a M_w 9.485 subduction earthquake originating off the coast of Peru (the most likely source for a 1:2,500-year tsunami for Christchurch City at 84th percentile as identified by Power 2013; 2014).

7.2.1 Source

Tsunami propagation of the 1:2500-year tsunami event was previously completed by Lane et al. (2017) and will be reused here. However, a rupture scenario had not been selected for the 1:500-year tsunami originating off the coast of Peru. The de-aggregation analysis (Power 2013) does not provide the fault segments involved nor the amount of slip to be expected for each segment. To determine the fault segments involved for each scenario, a sensitivity analysis was completed using the SIFT (Short-term Inundation Forecast for Tsunamis) database (Gica et al. 2008) and the ComMIT interface (Titov et al. 2011).

The SIFT database is a collection of Pacific-wide tsunami propagation results modelled from unit sources (1 m slip on fault segments 100 km long by 50 km wide, each with its own fault parameters, covering all the major Pacific subduction zones). Approximations of trans-Pacific tsunamis can be quickly estimated using super-position of the unit sources.

To establish the most suitable fault units for a M_w 9.28 in south Peru, the SFIT databased was downloaded for fault segments on the coast of South America from 5º S to 25º S. A 20 m slip was applied to each segment of the database and the resulting wave height in the center of Pegasus Bay was extracted.

The segments that produced the largest waves for Pegasus Bay (Figure 7-11) are located just North of the border between Peru and Chile. The segment producing the largest waves in Pegasus Bay are:

- cs68z.
- cs69z.
- cs70z.

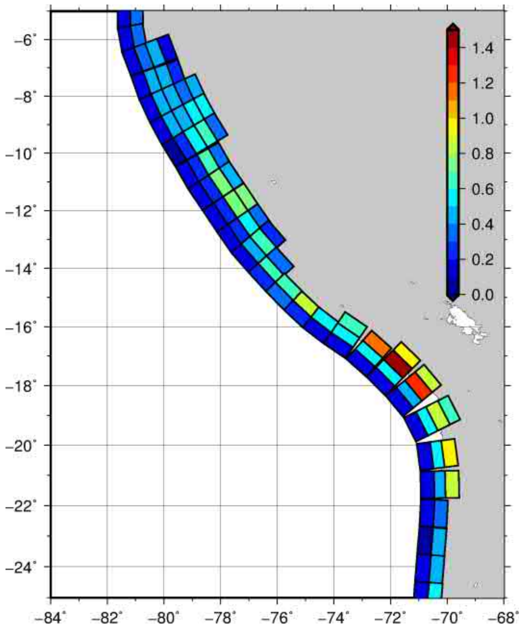

Figure 7-11: Maximum wave height in Pegasus Bay resulting from a 20 m slip earthquake applied at each fault unit in the SIFT database for South America. A scenario producing a M_w 9.28 earthquake would involve more faults segments than the three segments identified. The scenarios (Table 7-2) were designed to produce the desired moment magnitude earthquake and a continuous fault rupture.

Table 7-2: Earthquake scenario for 1:500-year tsunami inundation.

Scenario A	Scenario B
Segments: cs67z, cs68z, cs69y, cs69z, cs70y, cs70z, cs71y, cs71z, cs72z, cs73z Slip: 46.66m	Segments: cs67a, cs67z, cs68a, cs68z, cs69a, cs69y, cs69z, cs70a, cs70y, cs70z, cs71a, cs71y, cs71z Slip: 35.89m
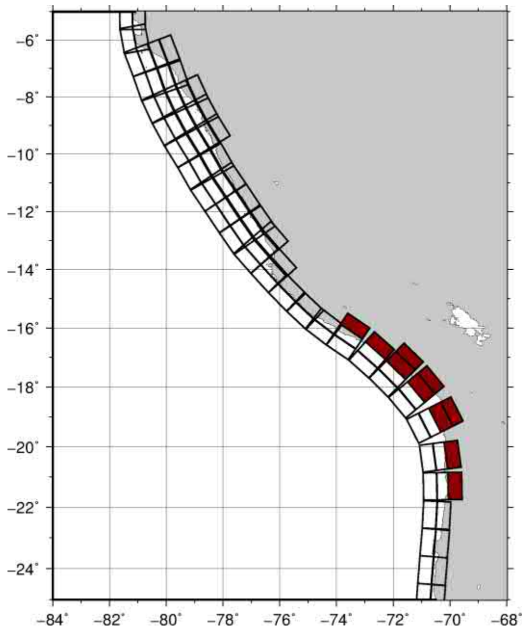	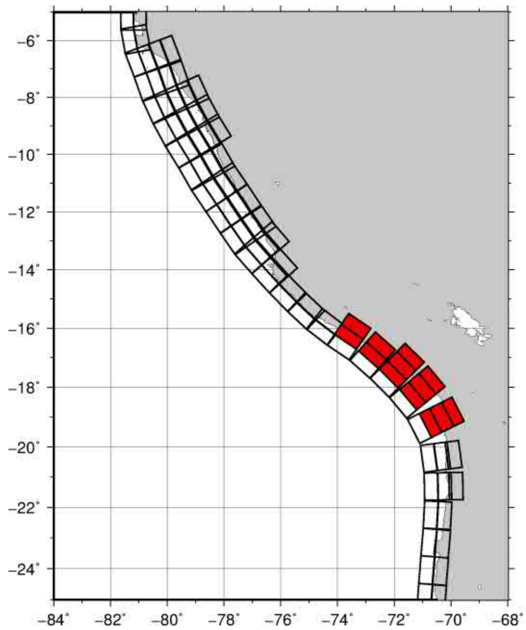

7.2.2 Transpacific propagation

Both scenario show waves between 1 and 3 m propagating across the South Pacific with scenario B generating smaller waves

Figure 7-12 and Figure 7-13). These waves are greatly amplified in Pegasus Bay with maximum wave amplitudes exceeding 4.0 m. Off the coast of Christchurch (3 km offshore), the two scenario produces similar waves with wave amplitude exceeding 4.5 m in scenario A and 3.5 m in scenario B (Figure 7-14).

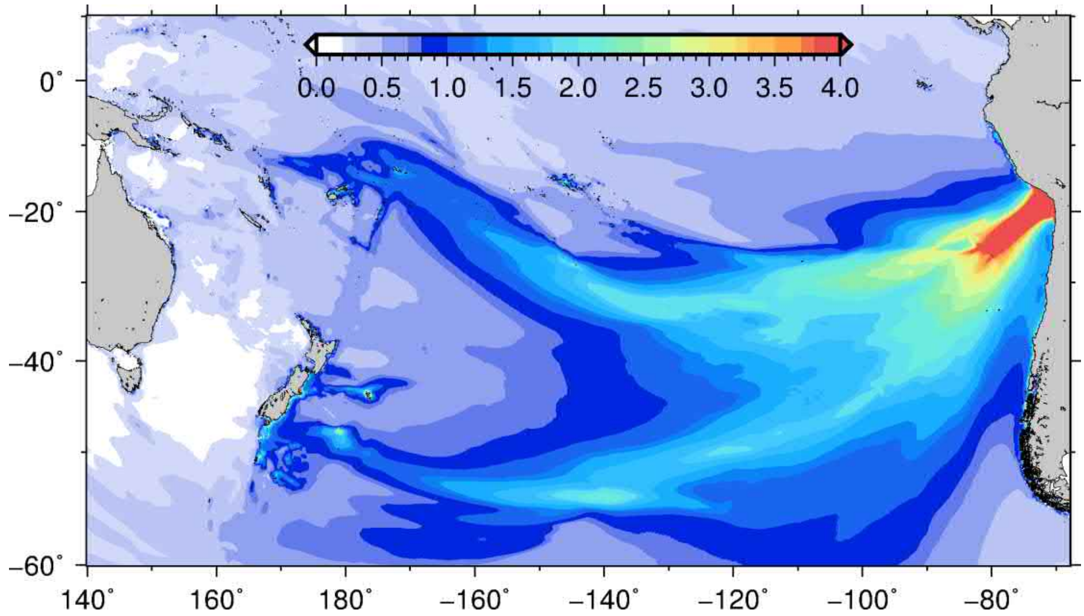

Figure 7-12: Maximum wave amplitude [m] across the South Pacific produced by Scenario A.

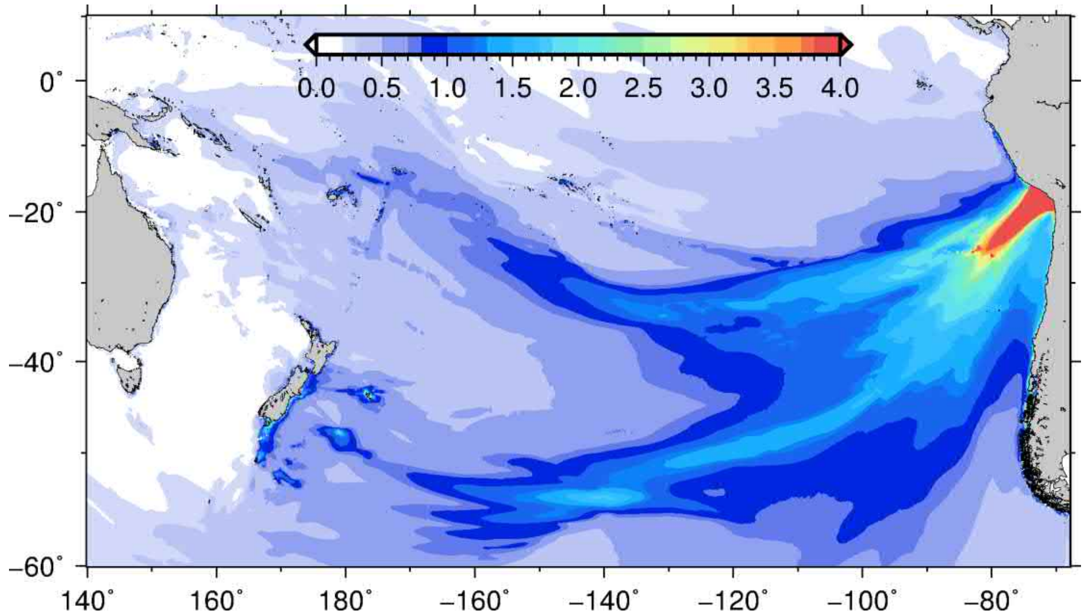

Figure 7-13: Maximum wave amplitude [m] across the South Pacific produced by Scenario B.

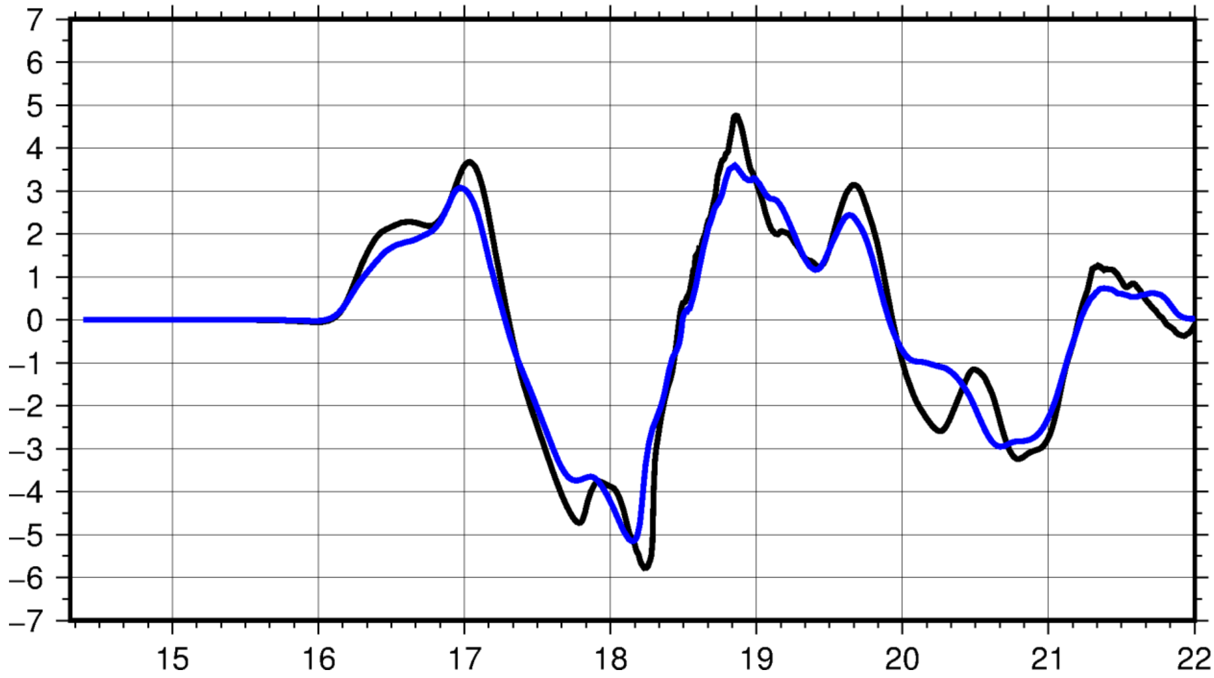

Figure 7-14: Tsunami wave off the coast (3 km offshore) of Christchurch. Black: scenario A; Blue: Scenario B.

7.3 References

Barnes, P. M., Ghisetti, F.C., Gorman, A.R. (2016) New insights into the tectonic inversion of North Canterbury and the regional structural context of the 2010–2011 Canterbury earthquake sequence, New Zealand, Geochem. Geophys. Geosyst., 17, 324–345, doi:10.1002/2015GC006069.

Gica, E., Spillane, M., Titov, V.V., Chamberlin, C., Newman, J.C. (2008) Development of the forecast propagation database for NOAA's Short-term Inundation Forecast for Tsunamis (SIFT). NOAA Tech. Memo. OAR PMEL-139, 89 pp.

Lane, E.M., Kohout, A., Bind, J., Williams, S.P. (2017) Distant tsunami inundation modelling incorporating dune failures and river flow in Christchurch. *Draft NIWA Client Report* 2016148CH.

Power, W.L. (2013) Review of Tsunami Hazard in New Zealand (2013 Update). GNS Science Consultancy Report 2013/131: 222.

Power, W.L. (2014) Tsunami hazard curves and de-aggregation plots for 20km coastal sections, derived from the 2013 National Tsunami Hazard Model. GNS Science Report GNS Science Report 2013/59.

Titov, V.V., Moore, C.W., Greenslade, D.J.M. et al. Pure Appl. Geophys. (2011) A New Tool for Inundation Modeling: Community Modeling Interface for Tsunamis (ComMIT). 168: 2121. https://doi.org/10.1007/s00024-011-0292-4.

Tonkin & Taylor (2017) Coastal Hazard Assessment - Stage Two. Report for the Christchurch City Council.